



UNIVERSITÀ
DEGLI STUDI
FIRENZE

PhD in Forest economics, planning and wood science
CYCLE XXV

COORDINATOR Prof. Erminio Monteleone

Hygro-Mechanical Behaviour of Wooden Panel Paintings

Academic Discipline (SSD) AGR/06

Doctoral Candidate

Dr. Riparbelli Lorenzo

Supervisor

Prof. Marco Fioravanti

Supervisor

Prof. Joseph Gril

Coordinator

Prof. Erminio Monteleone

Years 2019/2023

*to my three Amazons
Valentina, Cora, Patrizia*

Table of contents

Introduction.....pag. 1

First Article.....pag. 9

A method to assess the hygro-mechanical behaviour of original panel paintings, through in situ non-invasive continuous monitoring, to improve their conservation: a long-term study on the Mona Lisa

Second Article.....pag. 27

Hygromechanical behaviour of wooden panel paintings: Classification of their deformation tendencies based on numerical modelling and experimental results

Third Article.....pag. 55

Modelling of Hygro-mechanical deformations of wooden panel paintings: model calibration and artworks characterization

Fourth Article.....pag. 84

Coupling numerical and experimental methods to characterise the mechanical behaviour of the Mona Lisa: a method to enhance the conservation of panel paintings

Conclusions.....pag.113

Acknowledgements.....pag.120

Introduction

Wooden Panel Paintings (WPP) represent one of the most significant components of our Cultural Heritage and are generally characterized by an high level of complexity due to their constituent materials, to the construction and production techniques, the interaction with the environment, and their history of conservation and ageing [1]. They were mainly spread over a period of time between the 12th and 16th centuries, when wood represented the main support for painting, later gradually replaced by canvas.

They present, schematically, a multi-layered structure [2] consisting of the wooden support, usually made up of several boards, covered with paint layers; they are made up of preparatory layers, consisting main of gesso and glue and sometimes canvas, and of tempera or oil pigments and dyes, and often a varnish on top.

In most of them, there is a containment system for the wooden support, consisting of crossbars or frames, or sometimes a combination of both [3], [4]; these devices have the two main functions of (i) to control the distortions that a painted panel may present and (ii) to facilitate its handling and transport.

As far as warping are concerned, we can affirm that their main cause is variations in the relative humidity (RH) of the environment in which the work of art is immersed and that they can be of a transitory or permanent nature ; it should be remembered that wood is a highly hygroscopic material and therefore tends to exchange moisture with the surrounding environment in order to equilibrate with it and that this exchange of moisture leads to changes in shape.

Deformations of a transitory nature are generally caused by fluctuations in humidity and environmental temperature, which generates variations in the equilibrium moisture content of the wood, which develops internal moisture gradients, exacerbated by the hygroscopic asymmetry between the painted front and the bare back of the support. The transient deformation tends to stabilize when the wood becomes completely balanced with the surrounding environment. In practice, however, except in exceptional cases of climate-conditioned showcases, there are always fluctuations, albeit small, of the environmental thermo-hygrometric conditions, and the paintings are, therefore, constantly affected by transient deformations that result in continuous variations in their cupping.

Permanent deformations can be divided into the following macro-categories:

1. The cutting of the boards and the resulting orientation of the annual rings. The cause is due to the anisotropy [5] of the shrinkage and swelling of the wood, especially in relation to the tangential and radial directions, the ratio of which is not negligible, approximately 2 [6]. This type of cupping remains even when the board is in perfect equilibrium with its environment, is reversible and does not represent damage, but rather the physical behavior of a wooden board [7]; it does not occur in the case of radial cut boards.
2. Compression set. This is a permanent cupping [8] caused by repeated cycles of environmental humidity [9], which induces tension-compression within the thickness of the board, and is associated with a possible plasticization of the material [10]. In combination with mechanosorption phenomena, i.e. the combination of load and variations in humidity at the same time as viscoelastic deformations, they confer a non-recoverable and non-reversible curvature, that invalidates the shape and enjoyability of the work.
3. Ageing of the wood. The loss of hemicellulose over time, particularly in the superficial layers of the bare back of the wood [11], [12], causes a reduction in their hygroscopicity, which translates into an additional fictitious moisture gradient at the deformation level
4. The mechanical asymmetry of the panel. The paint layers, present on one side only, constitute an asymmetry of stiffness [13] for the board [14] and, with shrinkage/swelling

coefficients orders of magnitude lower than those of wood, also a general asymmetry in the hygroscopic behavior of the whole panel painting.

Until the end of the 19th century, the preservation of the supports of paintings on boards was entrusted to the sensitivity and expertise of cabinetmakers, whose skill, experience and intuition sometimes allowed them to develop ingenious and effective solutions in particular cases. In general, however, such solutions ran the risk of being imitated and slavishly reproduced, sometimes in completely different contexts, often with very negative long-term results.

Gradually, studies of construction techniques were separated from the description of restoration interventions, although they remained closely intertwined [15].

At the same time, extensive and in depth studies were published on the hygro-mechanical properties of the constituent materials of WPPs [16]–[20], the influence of environmental variations on the conservation of works of art [21]–[23], and these studies have led to the drafting of important guidelines and standards [24], [25].

More recently, in-depth studies have been carried out on physical-mathematical models [26] to represent the complex deformation phenomena of WPP [27]–[31] and on laboratory tests on copies and simplified models [32]–[34].

However, the above mentioned works have shown, on the one hand, the extreme complexity of the hygro-mechanical and deformation behaviors of WPPs, and on the other hand the extreme diversity from one case to another in terms of construction techniques, construction and materials used [35]; this has highlighted the need for direct measurements in order to be able to understand the dynamics of each individual work [36] and to support its conservation [37].

It is precisely in response to this need that this work aims to synthesize the state of the art of the studies carried out to date in this field and to combine them with direct measurements in order to assist conservators and restorers in assessing the actions to be taken for the correct conservation of the artworks.

This work was carried out in collaboration with two world-leading organizations for the conservation and restoration of works of art, the Opificio delle Pietre Dure in Florence and the Louvre Museum in Paris, in both cases for the evaluation and characterization of original paintings.

The Opificio delle Pietre Dure has for decades, and especially during the direction and guidance of Dr. Marco Ciatti, adopted a far-sight multidisciplinary approach to restoration, in which the technical component is always backed up by scientific support. This approach has resulted in a collaboration that has led us together to question the profound nature and implications of painting deformations in relation to environmental variations. It must be emphasized that the nature of the OPD is not only that of a Restoration Laboratory but also that of a School; this always implies the systematization of concepts and procedures into methods and has allowed us to collaborate with great effectiveness in the application of scientific procedures and advanced experimentation. This synchronization of intentions and thoughts made it possible for the OPD to give us the opportunity to carry out an experiment on 6 original paintings, the first documented case in literature of such large-scale experiment on original paintings.

It is indispensable to mention here some concepts explicitly expressed by Ciatti [38]–[39], which assess the importance of the study of the materials of Cultural Heritage that, limited to wood science and technology applied to WPP, we present in this study. Ciatti emphasizes the importance of conceiving restoration not as a series of more or less refined technical operations to be applied to the work to be treated but rather as a project that must be re-

formulated in each case of application according to the characteristics and requirements of the individual work. The first part of this design must consist of research into the constituent materials and the intangible meaning they carry within themselves; once this knowledge has been acquired, it is possible to define the theoretical objectives and thus the priorities that will guide of the entire operation, including the work on the wooden support. Following Ciatti, we must also consider that the correct conservation of works of art has a strategic value for society, but there is also an ethical duty to give an account of one's work, the reasons for restoration work and its results in technical and scientific terms.

In the case of the Louvre Museum, its curators who are extremely sensitive to the scientific approach to conservation, asked a team of experts in wood science and technology to study the wooden support of the Mona Lisa, painted by Leonardo da Vinci, in close collaboration with associate scientists, restorers and the curators themselves, in order to answer the following practical conservation questions

1. Assessment of the display case specifications
2. Assessing the risk of propagation of a fracture in the painting
3. Suggestion of possible improvements in the painting's framing system
4. To improve the technological aspects of the method of monitoring the work.

Once again, the foresight of the Louvre's curators allowed, under their supervision and responsibility, the implementation of a totally innovative non-invasive techniques for inspecting and characterizing the work.

The emerging questions addressed to wood scientists were to devise a methodological approach that would allow us to answer the basic problem needed to support both OPD and Louvre, i.e. how to experimentally characterize a work in a non-invasive manner and then how to use this characterization to extract useful information for the conservation of the work.

Obviously, from an experimental point of view, because each work is different from the other, different methods are needed each time, tailored to the individual work; and these methods must be designed to provide information that can then be effectively processed. It is clear that, normally, material characterization takes place with destructive or highly stressful tests, often standardized and produced under simplified standard conditions, neither of which are acceptable or feasible here. The solution we have designed and introduced within this research project was the use of extremely advanced numerical analysis and modelling techniques coupled with correspondingly advanced experimental procedures and methods; the parallel and equal dialogue between experiments and numerical simulations allowed us to approach the problem in a comprehensive manner and to answer the questions of conservators and curators. To use an allegory, we have decided to 'listen' to the needs and desires of works of art with a mathematical 'ear' that will allow us, on the one hand, to understand them more deeply and, on the other, to extend their scope and range of depth to a human ear. The present research should therefore be seen not only as an exercise in numerical simulation techniques, but also as a concrete attempt at dialogue between the experimental and numerical worlds.

This approach has led us to the need to carefully evaluate our working tools, especially with regard to numerical analyses. In fact, being conservation of WPP a strategic issue [38]; this requires us to use tools that are advanced, transparent, repeatable, inspectable, highly documented and with a high level of industrial validation. The choice has been based on the open source software Salome Meca, code_aster [40], mfront [41] and openturns [42]; all of them belong to a family of software developed in the French context of nuclear energy and related to strategic works, and they respond to all the characteristics mentioned above, ensuring

transparency of the procedures and algorithms used, and complementing them with advanced algorithms for resolving both performance and theoretical implementation of complex mechanical phenomena, such as field projection, contacts, ad hoc written constitutive laws, etc. It is necessary to highlight these aspects in relation to the following simulation modes whose solution is neither simple nor obvious, both in terms of convergence and technical feasibility:

1. The construction of a model of a WPP generally implies the construction of a model of extremely high dimensions - in the case of the Mona Lisa we have about two million degrees of freedom-, friction in the panel-frame contact zones, material laws constructed ad hoc to respect the cutting anatomy of the board.
2. A characterization procedure, such as the one we have designed, requires an optimization algorithm that brings the numerical results to coincide with the experimental ones; such procedures involve, invariably, a considerable amount of computation.
3. The Global, variance-based sensitivity analyses (i.e. Sobol method) we used require thousands of computations to express results.

From a computational point of view, therefore, we can see from the outset that the demands are extreme and therefore require appropriate advanced solutions.

In terms of the experimental tools used, a distinction shall be made between the case studies:

1. In the case of the Mona Lisa, the measuring instruments were all ad-hoc designed with the dual purpose of continuously monitoring the behavior of the work closed in the conservation case and simultaneously characterizing its behavior. These methods are therefore generally valid for monitoring WPP, but need to be adapted and differently configured for other specific cases.
2. The Deformometric Kit [43] which has already been used by our research group for decades and has proven to be effective and reliable in many experiments [36], was used for the characterisation of the frameworks granted by the OPD. With the specific knowledge of the instrument and the dynamics of the phenomena it measures, this specific tool can enable a standardisation of the method and the instrument.

Aware of an extraordinary complexity of the field of WPP research, this study aims to lay the methodological and analytical foundations for the conservation of these objects, in relation to some major "decision making" problems of curators and conservators, which we could summarize in the sizing of the containment systems (design of the thickness of the crossbeams for example) during restoration, and the evaluation and optimization of the microclimate for conservation.

This doctoral thesis is organised in this introduction, followed by four journal papers submitted to peer-reviewed journals and a final chapter of conclusions.

The main objective of the first work presented in this research is to use an employ an experimental approach for the characterization of the current state of an iconic artwork, namely the Mona Lisa. The main challenge posed in this investigation is the necessity to maintain the non-intrusive nature of the analysis, which entails the use of sensors to facilitate dedicated measurements and continuous monitoring. The ultimate objective of this research is to evaluate the in situ hygro-mechanical responses of this singular object, which will be leveraged to develop a comprehensive numerical model in subsequent chapters. Although earlier studies have employed experimental devices to gather relevant data, this study employs more sophisticated equipment to enhance the understanding of the artwork. Furthermore, the analysis takes into account not only the present condition of the object but also its existing surroundings, which necessitates a non-traditional mechanical characterization approach.

The second paper of this research delves into a comprehensive investigation of hygroscopic testing performed on six distinct wooden panels. The primary goal of this phase of the study was to arrive at a more general conclusions and guidelines. To achieve this objective, the study

employs numerical simulations, which enable a detailed examination of the panels' behaviors with respect to their past designs and current state. Furthermore, to make well-informed comparisons between the various cases, an innovative experimental testing procedure is conducted. Moreover, developing the models to accurately capture the essential effects while restricting the parameters to fit a minimum, essential set is a crucial aspect of this research. This approach is necessary to enable the models to replicate the various effects significantly, while also being relevant and informative. Furthermore, a critical aspect involves the development of models that precisely capture the essential effects, while limiting the parameters to a minimum, yet indispensable, set.

The third paper of this research delve into the inverse calibration of hygro-mechanical models, which involves determining the model parameters based on the response of a specific object. To achieve accurate and reliable results, advanced numerical tools for data analysis are necessary. The proposed methodology, known as "learning from objects," is specifically designed to address the unique challenges posed by studying one-of-a-kind objects. The result is a non-invasive analytical method that allows for the characterization of the hygro-mechanical behavior of paintings on wooden panels in a completely non-intrusive manner. The fourth paper presents the practical case of the non-invasive characterization of the Mona Lisa and demonstrates how the techniques previously discussed can be used to construct a descriptive model of an artwork, allowing scientists, curators, and conservators to understand its functioning, its response to external actions, and its state of conservation.

REFERENCES

- [1] J. Gril, "Wood science for conservation COST Action IE0601," *Journal of Cultural Heritage*, vol. 13, no. 3S, 2012.
- [2] C. Cennini, *Il libro dell'arte*, Neri Pozza. Frezzato F., 2009.
- [3] L. Uzielli, "Historical overview of panel-making techniques in central Italy," in *Proceedings of a Symposium at the J. Paul Getty Museum 24-28 April 1995*, 1998, pp. 110–135.
- [4] J. Wadum, "Historical overview of panel-making techniques in northern countries," in *Proceedings of a Symposium at the J. Paul Getty Museum 24-28 April 1995*, 1998, pp. 149–177.
- [5] J. Bodig and B. A. Jayne, *Mechanics of Wood and Wood Composites*. Van Nostrand Reinhold, 1982.
- [6] P. Mazzanti, M. Togni, and L. Uzielli, "Drying shrinkage and mechanical properties of Poplar wood (*Populus alba* L.) across the grain," *Journal of Cultural Heritage*, vol. 13, no. 3, pp. S85–S89, 2012.
- [7] D. Guitard, *Mécanique du matériau bois et composites*. Toulouse: Cepadues-Editions, 1987.
- [8] J. Gril, D. Jullien, and D. Hunt, "Compression set and cupping of painted wooden panels," in *Analysis and Characterisation of Wooden Cultural Heritage by Scientific Engineering Methods*, Halle (Saale), Germany, Apr. 2016. Accessed: Dec. 13, 2022. [Online]. Available: <https://hal.archives-ouvertes.fr/hal-01452161>

- [9] P. Mazzanti, J. Colmars, D. Hunt, and L. Uzielli, “A hygro-mechanical analysis of poplar wood along the tangential direction by restrained swelling test,” *Wood Science and Technology volume*, vol. 48, pp. 673–687, 2014, doi: 10.1007/s00226-014-0633-4.
- [10] R. Hoadley, “Chemical and physical properties of wood,” in *The structural conservation of panel paintings: Proceedings of a Symposium at the J. Paul Getty Museum 24-28 April 1995*, US, 1998, vol. 2–20.
- [11] M. Sassoli, “Characterization of Wood Aging by means of Volatile Organic Compounds (VOCs) Analysis,” PhD, University of Florence, 2018.
- [12] L. Esteban, J. Gril, P. De Palacios, and A. Casaus, “Reduction of wood hygroscopicity and associated dimensional response by repeated humidity cycles,” *Annals of Forest Science*, 2005, doi: 10.1051/forest:2005020.
- [13] O. Allegretti, J. Bontadi, and P. Dionisi-Vici, “Climate induced deformation of Panel Paintings: experimental observations on interaction between paint layers and thin wooden supports,” *International Conference Florence Heri-tech: the Future of Heritage Science and Technologies*, vol. 949, Oct. 2020.
- [14] D. Hunt, L. Uzielli, and P. Mazzanti, “Strains in gesso on painted wood panels during humidity changes and cupping,” *Journal of Cultural Heritage*, vol. 25, pp. 163–169, 2017.
- [15] “The structural conservation of panel paintings,” in *Proceedings of a Symposium at the J. Paul Getty Museum 24-28 April 1995*, The Getty Conservation Institute, US, 1998.
- [16] A. Janas *et al.*, “Shrinkage and mechanical properties of drying oil paints,” *Heritage Science*, vol. 10, no. 1, p. 181, Nov. 2022, doi: 10.1186/s40494-022-00814-2.
- [17] M. Mecklenburg, C. Tumosa, and D. Erhardt, “Structural response of painted wood surfaces to changes in ambient relative humidity,” in *Painted Wood: History and Conservation*, The Getty Conservation Institute., US: Dorge V. and Howlett FC, 1998, pp. 464–483.
- [18] B. Rachwał, Ł. Bratasz, L. Krzemień, M. Łukomski, and R. Kozłowski, “Fatigue Damage of the Gesso Layer in Panel Paintings Subjected to Changing Climate Conditions,” *Strain*, vol. 48, no. 6, pp. 474–481, 2012, doi: <https://doi.org/10.1111/j.1475-1305.2012.00844.x>.
- [19] “Response of Wood Supports in Panel Paintings Subjected to Changing Climate Conditions - Rachwał - 2012 - Strain - Wiley Online Library.” <https://onlinelibrary.wiley.com/doi/abs/10.1111/j.1475-1305.2011.00832.x> (accessed Oct. 04, 2022).
- [20] M. Richard, “Factors affecting the Dimensional response of wood” *Studies in Conservation*, vol. 23, no. sup1, pp. 131–135, Sep. 1978, doi: 10.1179/sic.1978.s030.
- [21] D. Camuffo, *Microclimate for cultural heritage*. Amsterdam ; New York: Elsevier, 1998.
- [22] A. Kupczak *et al.*, “HERIE: A Web-Based Decision-Supporting Tool for Assessing Risk of Physical Damage Using Various Failure Criteria,” *Studies in Conservation*, vol. 63, no. sup1, pp. 151–155, Aug. 2018, doi: 10.1080/00393630.2018.1504447.
- [23] J. Wadum, “Microclimate boxes for panel paintings,” 1998.
- [24] ASHRAE, “ASHRAE [American Society of Heating, Refrigerating, and Air-Conditioning Engineers]., Museums, Galleries, Archives, and Libraries. Chap 24 in ASHRAE Handbook—HVAC Applications, vol. 4, 4 voll. Atlanta, USA: ASHRAE [American Society of Heating, Refrigerating, and Air-Conditioning Engineers]., 2019.”
- [25] EN 15757:2010, “«EN 15757:2010 - Conservation of Cultural Property - Specifications for temperature and relative». <https://standards.iteh.ai/catalog/standards/cen/ad03d50b-22dc-4c57-b198-2321863f3870/en-15757-2010>.”
- [26] J. Froidevaux, “Wood and paint layers aging and risk analysis of ancient panel painting,” PhD, Université Montpellier II - Sciences et Techniques du Languedoc, 2012.

- [27] O. Allegretti, M. Fioravanti, P. Dionisi-Vici, and L. Uzielli, “The influence of dovetailed cross beams on the dimensional stability of a panel painting from the Middle Ages,” *Studies in Conservation*, vol. 59, no. 4, pp. 233–240, Jul. 2014, doi: 10.1179/2047058413Y.0000000095.
- [28] Ł. Bratasz and M. R. Vaziri Sereshk, “Crack Saturation as a Mechanism of Acclimatization of Panel Paintings to Unstable Environments,” *Studies in Conservation*, vol. 63, no. sup1, pp. 22–27, Aug. 2018, doi: 10.1080/00393630.2018.1504433.
- [29] C. Gebhardt, D. Konopka, A. Börner, M. Mäder, and M. Kaliske, “Hygro-mechanical numerical investigations of a wooden panel painting from ‘Katharinenaltar’ by Lucas Cranach the Elder,” *Journal of Cultural Heritage*, vol. 29, pp. 1–9, 2018.
- [30] D. Konopka, C. Gebhardt, and M. Kaliske, “Numerical modelling of wooden structures,” *Journal of Cultural Heritage*, vol. 27, pp. S93–S102, Oct. 2017, doi: 10.1016/j.culher.2015.09.008.
- [31] D. Konopka and M. Kaliske, “Transient multi-F ick ian hygro-mechanical analysis of wood,” *Computers & Structures*, vol. 197, pp. 12–27, Feb. 2018, doi: 10.1016/j.compstruc.2017.11.012.
- [32] Ł. Bratasz, “Allowable microclimatic variations for painted wood,” *Studies in Conservation*, vol. 58, no. 2, pp. 65–79, Apr. 2013, doi: 10.1179/2047058412Y.0000000061.
- [33] P. Dionisi-Vici, P. Mazzanti, and L. Uzielli, “Mechanical response of wooden boards subjected to humidity step variations: climatic chamber measurements and fitted mathematical models,” *Journal of Cultural Heritage*, vol. 7, no. 1, pp. 37–48, 2006.
- [34] M. Łukowski, “Painted wood. What makes the paint crack?,” *Journal of Cultural Heritage*, vol. 13, no. 3, pp. S90–S93, Sep. 2012, doi: 10.1016/j.culher.2012.01.007.
- [35] M. Ciatti, Ed., *Panel painting: technique and conservation of wood supports*, Rev. English ed. Firenze: Edifir, 2006.
- [36] J.-C. Dupre *et al.*, “Experimental study of the hygromechanical behaviour of a historic painting on wooden panel : devices and measurement techniques,” *Journal of Cultural Heritage*, vol. 46, pp. 165–175, Nov. 2020, doi: 10.1016/j.culher.2020.09.003.
- [37] B. Marcon, G. Goli, and M. Fioravanti, “Modelling wooden cultural heritage. The need to consider each artefact as unique as illustrated by the Cannone violin,” *Heritage Science*, vol. 8, no. 1, p. 24, Mar. 2020, doi: 10.1186/s40494-020-00368-1.
- [38] M. Ciatti, Ed., *Per la conservazione dei dipinti: esperienze e progetti del Laboratorio dell’OPD (2002 - 2012); atti della Giornata di Studi in occasione degli 80 anni del Laboratorio di restauro dei dipinti mobili (1932 - 2012) del 5 dicembre 2012 (Firenze, Auditorium di Sant’Apollonia)*. Firenze: Edifir, 2013.
- [39] M. Ciatti and C. Frosinini, Eds., *Structural conservation of panel paintings at the Opificio delle Pietre Dure in Florence: method, theory, and practice*. Florence (Italy): Edifir Edizioni Firenze, 2016.
- [40] EDF - Électricité De France, “Finite element Code_Aster: Analyse des Structures et Thermo-mécanique pour des Etudes et des Recherches.” 2022.
- [41] T. Helfer, B. Michel, J.-M. Proix, M. Salvo, J. Sercombe, and M. Casella, “Introducing the open-source mfront code generator: Application to mechanical behaviours and material knowledge management within the PLEIADES fuel element modelling platform,” *Computers & Mathematics with Applications*, vol. 70, no. 5, pp. 994–1023, 2015, doi: <https://doi.org/10.1016/j.camwa.2015.06.027>.
- [42] M. Baudin, A. Dutfoy, B. Iooss, and A.-L. Popelin, “OpenTURNS: An Industrial Software for Uncertainty Quantification in Simulation,” in *Handbook of Uncertainty Quantification*, R. Ghanem, D. Higdon, and H. Owhadi, Eds. Cham: Springer International Publishing, 2017, pp. 2001–2038. doi: 10.1007/978-3-319-12385-1_64.

- [43] L. Uzielli, L. Cocchi, P. Mazzanti, M. Togni, D. Julien, and P. Dionisi-Vici, “The Deformometric Kit: A method and an apparatus for monitoring the deformation of wooden panels,” *Journal of Cultural Heritage*, vol. 13, no. 3, pp. 94–101, 2012.

A method to assess the hygro-mechanical behaviour of historic panel paintings, through *in situ* non-invasive continuous monitoring, to improve their conservation: a long-term study on the *Mona Lisa*

Luca Uzielli^{1*}, Paolo Dionisi-Vici^{1*}, Paola Mazzanti^{1*}, Lorenzo Riparbelli^{1*}, Giacomo Goli¹, Patrick Mandron², Marco Togni¹, Joseph Gril^{3,4}

¹ DAGRI, University of Florence, Florence, Italy

² Independent Restorer, Ateliers d'Enghien, 12 rue d'Enghien 75010 Paris, France

³ Université Clermont Auvergne, CNRS, Clermont Auvergne INP, Institut Pascal, Clermont-Ferrand, France

⁴ Université Clermont Auvergne, INRAE, PIAF, Clermont-Ferrand, France

* These Authors contributed equally

Highlights

- Non-invasive methods and equipment to measure and monitor panel painting's behaviour
- Technological analysis and state of conservation of the *Mona Lisa*'s wooden panel
- Studying mechanical properties and conditions of an artwork painted on wood
- Monitoring mechanical response of panel paintings to environmental fluctuations
- Collecting data to feed and reliably calibrate numerical models

Keywords: *Mona Lisa*, technological analysis, panel paintings, conservation, non-invasive monitoring, hygro-mechanical behaviour.

Declarations of interest: The authors declare the absence of any conflict of interest.

Abstract

This paper describes an innovative method, and related equipment, developed by the authors to monitor non-invasively historic panel paintings under museum display conditions. This method permits in-depth knowledge about such artworks, allowing us to understand their reactions to climatic variations, and provides objective data on which conservation decisions can be confidently based, since the data are directly obtained from the individual artwork. Since 2004, following the invitation from the Louvre Museum and the C2RMF (National Centre for Research and Restoration of French Museums), the wooden panel on which Leonardo da Vinci painted his *Mona Lisa* has been studied by an international research team of wood technologists and engineers, including researchers from French and Italian universities and related scientific institutions (Montpellier, Clermont Auvergne, Poitiers, Florence), to understand its mechanical, hygroscopic and shape characteristics and behaviour, to evaluate its present state, and to provide suggestions for optimizing its conservation

conditions. Non-invasive methods and equipment were therefore devised and implemented to measure (during the annual opening day of its display case) and automatically monitor (during the time the display case remains closed) both the deformations that the panel undergoes (mainly produced by the inevitable small climatic fluctuations within the case) and the constraining forces acting on the panel itself. The method and the related equipment, improved over the years, are based on miniature load cells and displacement transducers, whose outputs are automatically logged at desired time intervals, typically ranging between 30 minutes for monitoring during the whole year, and a few seconds for manual measurements, calibrations, and other selected events; the stored data can be downloaded both through a cable connection and wirelessly, by means of a specially developed connection apparatus. The panel is confined in a climate-controlled display case, which typically is opened only for a few hours once a year. Additionally, close restrictions must be respected, including absolute non-invasiveness, non-interference with the enjoyment of the artwork by the public, and compliance with strict procedures for safe and secure conservation. The implementation of this method has provided significant information about the actual behaviour of the panel during the whole year. Comparing several annual force-deformation curves, their good linearity suggests that no unacceptable stress or deformation has taken place in it, showing that the climatic conditions (air temperature and relative humidity) maintained in the display case can be considered favourable to the conservation of the artwork. Moreover, based on the collected data, reliable Finite Element Method (FEM) models are being developed and calibrated, with the aim of describing the mechanical behaviour of the panel and virtually evaluating the risk of damage (including the propagation of an ancient crack) deriving from external conditions or actions to which it would be unthinkable to submit the original historic artwork.

1. Introduction

The *Mona Lisa* was painted by Leonardo da Vinci during the period 1503-1514 on a poplar (*Populus alba* L.) wooden board. Using wood as a support for paintings was a common practice between the 13th and 16th centuries [1, 2]; however, the hygroscopicity [3-5] and susceptibility to degradation [6] of wood pose problems for conservators, as for all wood users. The study of any individual object belonging to the cultural heritage presents complexities, including individual structure, making, history, conservation conditions, constraints related to the conservation and security, restrictions on access and manipulation, decisions related to the public display, and exposure to microclimatic conditions. When the object is made of wood, the intrinsic variability of the material itself makes the problem even more complex [7]. Panel paintings constitute a category of objects whose conservation is particularly critical, since they are formed by wooden panels on which layers of various materials are applied, featuring quite different chemical, mechanical and hygroscopic properties [8, 9]. Conservation of panel paintings includes maintaining integrity of both the wooden support and the superposed layers, which must remain intimately connected while presenting potential problems of compatibility [10]. When the surrounding environment undergoes any thermo-hygrometric variation, panels painted on one face only, like the *Mona Lisa*, tend to exhibit typical distortions [11], better discussed in Section 3.1. This tendency has often been worsened by the introduction of inappropriate heating or air conditioning of the exhibition or storage rooms, as well as by the controversial interventions such as thinning and cradling (*parquetage*) of panels [10]. In summary, today preventive conservation mainly aims at maintaining the thermo-hygrometric conservation conditions stable, while ensuring that mechanical constraints do not lead to damage of panels or paint layers in case of excessive climatic variations. In addition, the presence of crossbeams opposing the increase of the panel's cupping has a significant influence: while on the one hand it prevents the risk of progressively increasing permanent deformations, on the other it generates additional mechanical stresses in the wood [12]. If the stresses become excessive, they can put the artwork's integrity at risk, regarding both the panel (e.g. cracks, open joints, irreversible deformations) and the paint layers (e.g. flaking,

cleavage or buckling) [3], [5], [10]. To ensure the best conservation, deformations due to inevitable microclimate fluctuations should be prevented, but, at the same time, the forces counteracting the deformations should be maintained at a safe level even in case of unusually high fluctuations. The problems highlighted so far make it necessary to improve the knowledge of the artwork to be conserved in relation to its deformation dynamics, i.e. how environmental variations influence the state of the forces and deformations to which the panel painting is subjected over time. An appropriate experimental approach therefore requires the continuous recording over time of deformations and forces directly measured on the specific artwork, and of temperature and humidity readings of the surrounding environment. To make a complete analysis, these records need to include the deformations and forces sufficient to characterize the global behaviour of the artwork; and, obviously, all must be carried out non-invasively.

Since 2004, the Mona Lisa's wooden panel (hereinafter "the panel") has been studied by an international research team, including researchers from French and Italian universities and related scientific institutions (Montpellier, Clermont Auvergne, Poitiers, Florence), which carried out several experimental campaigns to understand the panel's mechanical, hygroscopic and shape characteristics and behaviour, to evaluate its present state, and provide related suggestions in order to optimize its conservation. The following main questions were originally posed by the Louvre conservators in 2004, when the team started its activities: **(a)** evaluating climatic specifications for the new display case (on April 6, 2005 the *Mona Lisa* was moved from its previous location in the *Salle Rose*, to its current location in the *Salle des États*), **(b)** assessing the risk of propagation of the ancient crack affecting the panel, **(c)** suggesting possible improvements to the framing conditions of the panel, and **(d)** improving the technological aspects of the monitoring procedure. To provide answers to these questions, the artwork was studied (i) by direct observation and measurements (once a year, during the few hours available on the occasion of the so called "*Journée Joconde*", when it is removed from its climate-controlled display case), (ii) by automatically monitoring continuously the panel's behaviour while in the display case, using a special ad-hoc equipment, and (iii) by developing numerical models simulating the historic artwork's reactions to actual or potential hygro-mechanical stresses. This paper (i) focuses on the experimental approaches, and (ii) discusses the most significant results obtained.

2. Aims

This paper describes an innovative method whose aim is to apply modern scientific techniques to the conservation of historic panel paintings, based on non-invasive testing and continuous monitoring of the artworks in museum display conditions. This method, applied in the last 18 years on the *Mona Lisa*, provides an in-depth knowledge of the artwork, of its construction features, and of its mechanical and hygroscopic behaviour. To obtain such knowledge, thorough monitoring techniques were developed and improved over time, recording simultaneously the forces to which the panel is subjected and its state of deformation. Such data can provide real time information on the panel's condition, measure its response to environmental variations, and thus contribute substantially to optimize its conservation; data from monitoring can be used for advanced analyses, including the development and calibration of digital numerical models, allowing a reliable simulation of the panel's behaviour under many environmental conditions, for optimisation of its framing constraints, for preventive conservation, and for the exploration of risk scenarios. The possibility of adapting such methods to other artworks is also briefly discussed.

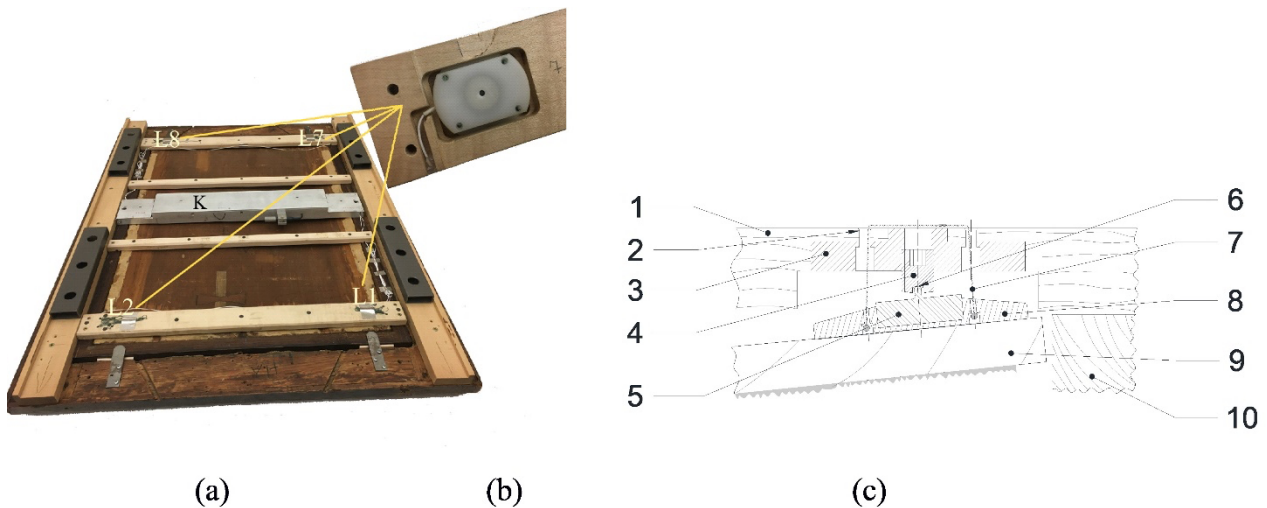


Fig. 2 (a,b,c) – Equipment for measuring and monitoring forces, in use from 2013 to 2021. (a) Overall view of the back of the assembled system. (L1-L2-L7-L8) Locations of the load cells. (K) Aluminium case housing the deflection transducers and the electronic equipment. In the foreground, two of the four metal brackets that secure the auxiliary frame in the gilded frame are clearly visible. (b) View of an end of an overturned crossbeam, and of the swivelling Delrin® presser. (c) Partial longitudinal cross-section of a crossbeam at the level of the load cell. (1) Wooden crossbeam (maple wood). (2) Holes for the passage of the strings. (3) Support embedded in the crossbeam. (4) Steel grub screw. (5) Miniature load cell. (6) Contact pin of the load cell. (7) String. (8) Presser. (9) Panel. (10) Batten of the auxiliary frame.

The *Mona Lisa* is painted on a thin (~13 mm) wooden plank (“the panel”). When left free the panel is presently quite distorted (cupping and bowing) (the reasons for this are briefly outlined in other parts of this paper). To prevent distortions from increasing in time, the panel is maintained flatter than it would be if left free, by compressing it between the auxiliary frame and the crossbeams fixed to this frame with screws (see Fig. 1a and Section 3.2). The auxiliary frame, with the panel inside, is fixed inside the gilded external frame by means of metal brackets (which are not shown in Fig. 1a; two of the four metal brackets are clearly visible in Fig. 2a). A technological analysis of the panel’s structure and assembly is presented in Sections 3.1 to 3.3.

When the surrounding climatic conditions change, the panel’s shape tends to change as well, however the top and bottom crossbeams tend to prevent any deformation at its top and bottom edges; therefore, the reaction forces and the related internal stresses and strains are also constantly changing. Both to monitor the current state of the panel and to formulate and calibrate a numerical model, an accurate continuous monitoring (i.e., automatic measuring and recording) of the forces acting between crossbeams and panel, and of the panel’s deformations, has been implemented (see Sections 3.4-3.7). The data provided by such monitoring proved to be particularly useful for the analysis of the hygro-mechanical behaviour of the panel during its normal display conditions. Additionally, several physical and mechanical measurements on the panel were directly carried out by the authors and by other members of the international team when the conditioned display case was opened (see e.g. [11], [13-15]). This typically takes place on the so-called *Journée Joconde*, when the *Mona Lisa* is subjected to routine checks, observations and measurements by art historians, conservators, and researchers belonging to various disciplines.

3.1 The panel

The panel is a flat-sawn (i.e. subtangential) rectangular board of Poplar wood (*Populus alba* L.), 794 x 534 x 13 mm³, doubly curved (i.e. both transversally and longitudinally) with convexity towards the painted face, which is the “external” one (i.e. the face away from the original log’s pith).

The crack. An ancient crack, about 110 mm long, runs through the panel's thickness from the top edge of the panel down to the *Mona Lisa*'s forehead. The crack length runs along the direction of the wood grain, and its plane is parallel to the local radial direction of wood, so it is inclined by about 34° to the painted surface of the panel; two wooden "butterflies" had been inlaid, possibly during the 19th century, into the panel's thickness to prevent any longitudinal propagation of the crack, one of them now missing and being replaced by a glued canvas strip [16, 17].

Near the tip of the crack the craquelure in the paint layers is organized according to a particular pattern, indicating that the crack formed during the first decades of existence of the artwork, and did not advance further [16].

A reasonable hypothesis regarding the formation of the crack could be the following. The presence of a barb of paint and ground running along some parts of the edge of the painted surface testifies that the ground layer was applied when the panel was already inserted into a grooved frame [17]. Such frame was intended to keep it flat despite the important variations in moisture content (MC) caused by the application of the ground layer, and to the unavoidable subsequent environmental fluctuations [16, 17]. It is well known that when a panel painting is subjected to strong variations in moisture content (e.g. during the application of the preparation layers, or during subsequent drying, or in any case following significant climatic changes) it can develop a strong tendency to cupping. If this cupping tendency is prevented by external constraints such as the grooved frame mentioned above, stress states may develop in the wood such as to produce (in a short or long time) transversal bending breakage, which typically occurs along longitudinal radial surfaces, which are structurally weaker. This mechanism could have caused (perhaps some years after the panel was prepared and painted) the formation of the crack, the opening of which would also have modified the shape of the panel and reduced the magnitude of the internal stresses present in it.

The double curvature, which can be considered typical of a thin panel painted on only one face and blocked along its four sides, resulted in a central deflection of about 11 mm. It was presumably caused by the many MC variations and gradients, producing complex phenomena that can be globally recalled with the term "compression set" [5], [18], combined with the tendency to warp caused by the orientation of the growth rings and of the direction of the wood grain, and with the distortions produced by the formation of the crack. However, a thorough discussion about the localisation and orientation of the wooden panel inside the log from which it was obtained falls outside the scope of this paper and is presented elsewhere [19, 20]

Since its making, the panel underwent only few modifications [17], including: (i) the inlay, possibly during the 19th century, of the two "butterflies", (ii) a light surfacing of the back-face, and (iii) a small width reduction affecting only lateral unpainted parts.

3.2 The restraining system: auxiliary frame and crossbeams

The auxiliary frame is made of oak wood (*Quercus* sp.) battens, whose L-shaped cross section measures 25 x 32 mm² (Fig. 1a). It shows limited stiffness, both flexural and torsional, as compared to those of the panel [21] and of the gilded frame (Section 3.3). It performs important mechanical functions, outlined below. Its rabbet (*feuillure*) is the surface on which the panel rests, and on which the contact forces acting on the front face of the panel are distributed [13]. Together with the crossbeams screwed against its vertical battens it constitutes the system of constraints, which maintains the panel slightly forced in a stable shape and prevents its curvature from gradually increasing over time.

In 2005, the four crossbeams shown in Fig. 1 (25 x 28 mm² in cross-section) were replaced with crossbeams only 15 mm thick, to fit into the extremely narrow space left available in the new location. Due to the double curvature and convexity of the panel the two middle crossbeams do not touch it and merely serve to stiffen the auxiliary frame. On the contrary, the top and bottom crossbeams (both the old and the new ones) force against the panel, and maintain it flatter than it would be otherwise.

In 2005, the new top and bottom crossbeams were made 50 mm wide to provide room for the insertion of load cells measuring the contact forces. They were replaced again in 2013, when new load cells were installed, and in 2021 (70 mm wide), when load-limiting devices were installed [20]. Old and new crossbeams were made of maple wood (*Acer* sp.); all the new ones were carefully manufactured at the University of Florence, from bars obtained by splitting air-seasoned boards, to ensure the direction and regularity of the grain. To manufacture the crossbeams, the above-mentioned bars were then brought to size by planing, and finally shaped by milling. In 2013, the machined bars were sterilised by keeping them for about 6 hours in the oven at 60°C. In 2021, to minimize the risk of deformations of the long and quite thin bars resulting from processing, the sterilisation was carried out by keeping the machined wood bars in a freezer at -18°C for seven days [6]. After sterilisation, the crossbeams were brush treated with a permethrin-based insecticide to prevent future insect attacks – a treatment that loses its effectiveness over time and should be repeated when necessary. Most of the auxiliary frame is invisible to the public when the *Mona Lisa* is exhibited; only the thin lateral faces of its rabbets are barely visible, mostly along the vertical battens, where they are separated from the front surface of the panel by a small gap, whose thickness is variable due to the irregular shape of the panel's surface (see Fig. 1b).

3.3 The gilded frame

The sculpted and gilded external frame, fully visible to the public (see Fig. 1b), is made up of wooden elements with a much larger cross-section than the auxiliary frame and is therefore much stiffer. It houses and supports the auxiliary frame, and the aluminium profiles fixed on its rear face, invisible to the public, that support and keep the *Mona Lisa* in its display position. When the auxiliary frame housing the panel is placed in the gilded frame and pressed against its rabbets by means of tightly screwed metal brackets, the auxiliary frame being significantly less stiff [21] can only yield and adapt to the surface of the rabbets of the stiffer gilded frame. Thus, for several years the accurate force and deformation adjustments obtained by the authors by means of the monitoring system were changed in an unpredictable way when the panel and the auxiliary frame were placed back in the gilded frame, and then in its display case. Finally, during a 2019 opening day, an accurate analysis of the gilded frame's rim surfaces was carried out with pressure sensitive Prescale[®] film, following a procedure like the one implemented by Goli et al. in 2013 [13]. The analysis allowed detecting some significant irregularities on the frame's rabbet, such as some nail's heads slightly protruding from the wooden surface. Their negative effect was promptly eliminated in a totally non-invasive way, by applying on the rabbets (namely in correspondence of the metal brackets) appropriately thin wood spacers, to obtain a regular although discontinuous supporting surface for the auxiliary frame. This precaution avoids unwanted changes in the forces applied to the panel when the auxiliary frame in which the panel is inserted is placed back in the gilded frame.

3.4 The measurement of the forces

The forces exerted by the rabbet of the auxiliary frame on the front face of the panel are balanced by the forces exerted by the crossbeams on the back face, through the four load cells located in L1-L2-L7-L8 (Fig. 2a). In other words, the system formed by the panel, the crossbeams and the auxiliary frame is closed with regards to the contact forces, so that the four load cells are measuring all the significant forces acting on the artwork during the monitoring. Of course, the panel is also subjected to gravity. Therefore, depending on how it is oriented (i.e. vertically in the normal display position, or horizontally as sometimes happens during certain adjustments, measurements or manual tests) gravity can modify the forces measured by the load cells, because of the influence of the panel's weight. Additionally, friction forces can build up on the contact areas between panel and auxiliary frame, both on the panel's face and on its edges. Several tests have been performed to account for these effects, which however do not seem to significantly affect the monitoring results; therefore, they are not discussed here. The equipment described below was designed, repeatedly improved, and

implemented to effectively, safely and non-invasively measure and monitor such forces both under normal display conditions and for manual measurements carried out during the yearly openings of the display case. Until 2013 only the forces exerted on locations L1 and L2 (Fig. 2a) were monitored throughout the year by means of only two load cells inserted in the top crossbeam [11]. Starting from 2013, an improved and still now working force monitoring equipment was installed, based on four miniature load cells (P286.C-S-A/100N, 0-100 N, accuracy 0.5 %; diameter 16 mm, height approximately 6 mm, capacity 100 N; made on purpose by Deltatech, Italy) integrated in the top and bottom crossbeams (Fig. 2b). The load cells are of the strain gage type and are equipped with external miniature supplying-conditioning electronics providing analog outputs, hence their resolution is virtually infinite; however, the Pace-Sci® logger to which they are connected (see Section 3.7) can discriminate a variation of $2.4 \cdot 10^{-2}$ N.

In 2021, when new load-limiting devices were installed, the load cells and their electronic equipment remained the same, but their mechanical assembly was modified [20].

Here the mechanical assembly which was in use from 2013 until 2021 is described in detail (Fig. 2a). Top and bottom crossbeams were equipped with four miniaturized load cells at the four contact locations L1-L2-L7-L8. Each load cell was fitted in a swivelling presser pushing against the back of the panel. A grub screw (hexagonal hollow, cup end, M6x5 mm, inserted in a threaded support embedded in the wooden crossbeam) accommodated the load cell's contact element (a cylindrical pin with a diameter of 1.25 mm) in its cup-shaped end; therefore the load cell was free to oscillate around its contact element (a virtual spherical hinge with its centre at the cup-shaped end of the grub screw), allowing the presser to swivel and adapt to the local inclination of the panel in the contact area. This arrangement also allowed the adjustment of the position of each presser, and hence of the force acting on it, by operating the corresponding grub screw.

Both the support and the presser were made of Delrin®, a plastic material chosen to ensure frictionless and chemically inert contact between the load cell and the back face of the panel.

To facilitate the assembly and disassembly of the crossbeams while the presser was not pushing against the panel, the presser itself was held in position by means of thin sliding strings, which allowed it to assume the inclination of the panel's surface.

The equipment described above was also used during the manual measurements as a loading device for the acquisition of data concerning the mechanical characteristics of the panel. Displacements can be imposed at each load cell independently, by rotating the grub screw controlling its approach towards the panel; to adjust with the greatest possible accuracy such displacement, detachable devices (nicknamed *Jocondometers*) equipped with large goniometers were specifically developed so that the rotation of the screw (and hence its axial displacement) could be controlled accurately and repeatably, with a resolution of ± 0.01 mm. Fig. 3 shows one of such devices. During the measurement each device was firmly fixed against the crossbeam by a couple of tie-rods not shown in the drawing; by turning the knob, connected to the handle of a hexagonal key, one could accurately and repeatably control the rotation (and hence the axial displacement) of the grub screw, thus controlling the advancement or backing of the load cell towards the panel, and hence modifying the force acting on it. The large protractor allowed a resolution of 3.6° (sexagesimal degrees) corresponding to the axial displacement of 0.01 mm of the grub screw. A linear graduation on the lateral ruler indicated the number of entire rotations of the grub screw (1 turn = 1 mm). A soft preloaded coil spring ensured the contact between key and screw whichever way the panel was oriented, without affecting the measured load. In this way it became possible to impose on the panel very accurate displacements in conditions of absolute safety and to measure the force variations by means of the already mentioned load cells. Thus, well linear load-displacement curves, reported in Section 4, were obtained for each measurement location (L1-L2-L7-L8).

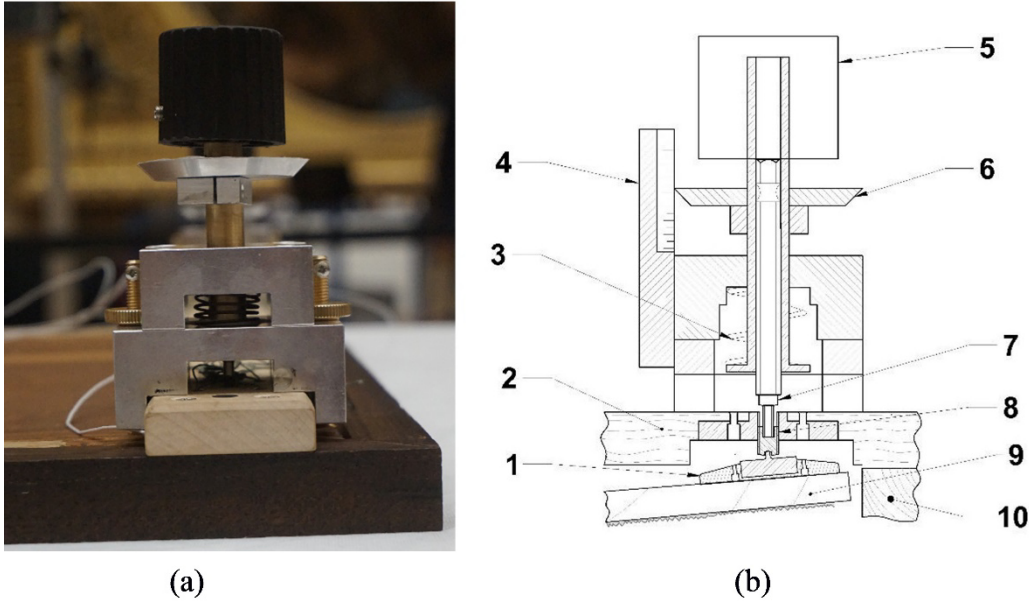


Fig. 3(a,b) – Picture (a), and schematic drawing (b), of one of the four identical removable devices (nicknamed *Jocondometers*), developed to identify the force-displacement relationships. (1) Presser and load cell. (2) Crossbeam, sectioned longitudinally. (3) Coil spring. (4) Lateral ruler. (5) Knob. (6) Protractor. (7) Hexagonal key. (8) Grub screw. (9) Panel. (10) Batten of the auxiliary frame.

3.5 The measurement of the deflections

The auxiliary frame and the crossbeams touch and constrain the panel only near its top and bottom edges; additionally, the panel touches the left vertical batten near its upper end [13]. Otherwise, owing to its longitudinal permanent curvature, the panel's central part does not come in contact with either the crossbeams or the auxiliary frame, and hence is free to move and deform, both transversally (cupping) and longitudinally (bowing). To measure both such deflections three displacement potentiometric transducers (SLS095 by Penny&Giles, stroke 10 mm, independent linearity $\pm 0.5\%$) were installed on the aluminium case fixed on the auxiliary frame (see Fig. 2a). Each transducer measures the deflection through a mechanical system already described in [11], touching the panel's back with a spherical feeler (each contact force amounts to about 1 N, small enough to avoid damaging the wood surface). The contact points of the three feelers are located on the panel's horizontal midline, one at each extreme and one at its centre; the corresponding deflections are thus measured with respect to the rear plane of the auxiliary frame (Fig. 4). Such geometry allows monitoring and computing separately both cupping f_c and bowing f_b as follows:

$$f_c = f_2 - [(f_1 + f_3)/2] \quad (1)$$

$$f_b = (f_1 + f_3)/2 \quad (2)$$

Note. Due to the limited space available behind the *Mona Lisa*, the transducers are positioned parallel to the panel, instead of perpendicular to it. For each of them a twofold pivoting lever system transfers to the cursor the deflection measured by the feeler, which ideally should be perpendicular to the rear plane of the auxiliary frame. Due to this arrangement, the feeler's spherical end moves along a circular rather than a linear path, which causes minor systematic geometric errors. However, given the small entity of the deflection variations (which at most are of the order of 0.5 mm), such non-linearity errors

can be neglected, as well as the error produced by the fact that the slight lateral translation of the feeler causes the contact points to move transversally along the back of the panel, which is locally sloping due to its cupping distortion. The system was considered a good compromise to solve the space issue, despite the presence of the above-mentioned geometric errors which were well known to the authors since the beginning of the work; and which were also partly automatically compensated by the calibration of the system, performed with depth templates in correspondence with its actual working positions.

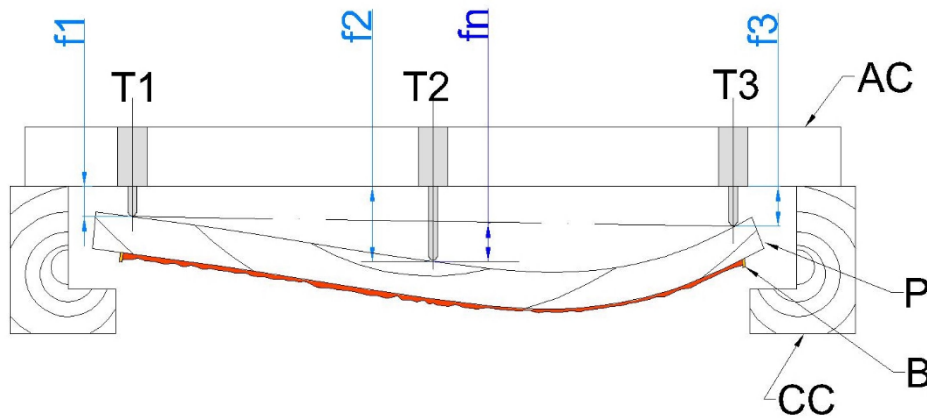


Fig. 4 – Schematic diagram (in cross-section) of the principle and of the equipment for monitoring the panel’s deflections and cupping at mid-height. (CC) Batten of the auxiliary frame. (AC) Aluminium case (slightly shorter than the width of the auxiliary frame). (P) Panel. (B) “Barb” of the ground and paint layers (see Section 3.1 and Fig. 1b). (f_1, f_2, f_3) Deflections of the panel. (f_b) Panel bowing. (f_c) Panel cupping. (T1, T2, T3) Transducers (drawing just outlined: for clarity and simplicity, the actual kinematics of the transducers (see [11] have been omitted).

3.6 The measurement of climate inside the display case

The relative humidity (RH) in the display case is monitored and controlled by a dedicated air conditioning system, while air temperature (T) is determined by that of the room where the artwork is exhibited (the *Salle des États*); both systems are managed by the museum’s technical department. To thoroughly monitor and analyse the panel’s mechanical behaviour and the main factors that determine it, climatic data had to be directly available to the international team, in a format and a timing allowing them to be used in connection with those describing the panel’s forces and deformations. Therefore, data on air T and RH near the panel were also collected by ad hoc sensors and recorded by the same data-logger as the other data, all such equipment being placed in the aluminium case (see Section 3.7). Additionally, a self-powered data logger (HOBO U12- 013 by Onset, accuracy ± 0.35 °C and ± 2.5 %) placed inside the display case measured and recorded independently the T and RH, and was used as a further data source in synchronism with the climate, force and displacement data logged by the main monitoring unit.

3.7 Data collection, storage and wireless transmission

Since 2005, the authors developed an instrumented aluminium case, fixed on the auxiliary frame at mid-height, facing but not touching the back face of the panel, with the function of housing, protecting, and shielding both the deflection transducers and the electronics (including the power supply batteries) of the monitoring equipment. This case was re-designed and replaced several times, according to the evolution of the instrumentation. The latest version (see Fig. 2a) houses (a) the three displacement transducers that monitor the deflection of the panel, (b) the sensors measuring T and RH in close proximity to the panel, (c) the electronic equipment of the load cells, (d) the data logger, and (e) the equipment for wireless data transmission.

Initially, the monitoring of the panel’s hygro-mechanical response to climate fluctuations was limited by the memory size of the data loggers (two HOBO® U12-006 featuring 4 external channels each). In 2006, a new data-logger was adopted, and a new connection apparatus was implemented, as described below. The current data-logger used (XR5-SE by PACE Scientific, 8 external channels + 1 internal monitoring the temperature, 12-bit AD converter, accuracy $\pm 0.35\%$ F.S.) reads the RH sensor, the three displacement transducers, and the four load cells, and stores the readings at the desired time intervals (typically, every 30 minutes throughout the year, when the display case is closed, and at shorter intervals - down to 2 seconds - during manual measurements or other tests). The data can be downloaded – depending on the situation – through a cable connection or wirelessly, by means of the connection apparatus. Such apparatus, named LAB-MoB, of which no equivalent equipment was commercially available at that time, was expressly developed and patented [22]. It is based on a Bluetooth RS232 antenna, interfaced to the data logger using a standard serial communication protocol without proprietary communication modifications. Thanks to such device, not only a logging system with greater capacity was used, but it became also possible to interact with it (including data downloading and modifying at will the sample rate) while staying a few meters away, without opening the display case. To ensure data confidentiality, the Bluetooth access is secured by a password. To keep energy requirements reduced, a super-low consumption ($<90\mu\text{A}$) switch controlled by a remote transmitter, which allows to turn on the connection only when needed. This further possibility also improves the security, preventing any unauthorized connection to the data-logging system, since without the remote transmitter it is impossible to discover the connection ID in the room.

4. Results and discussion

4.1 The climatic conditions

The data obtained from the continuous monitoring provide significant information about the forces and deformations to which the panel is subjected, and about their variations, caused mainly by the inevitable, albeit small, fluctuations of the climatic parameters, namely of the RH. As an example, the fluctuations monitored for one whole year can be observed in Fig. 5, and possibly derive from external (i.e. of the *Salle des États* hall) temperature fluctuations and from the normal functioning of the conditioning plant. The results presented here refer to only one year of monitoring. However, as the climatic conditions within the display case are fairly stable year-to-year, they can be considered representative of the last 18 years. On the other hand, the rare anomalous deviations, commented on below, are probably attributable to occasional openings of the display case.

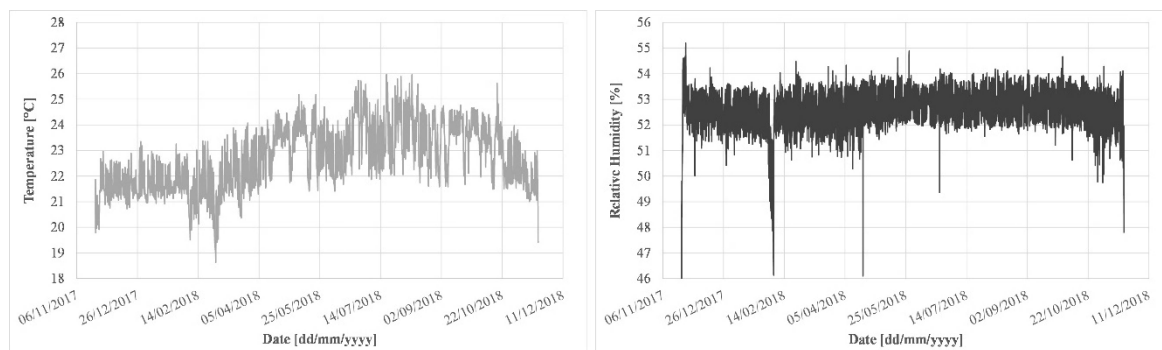


Fig. 5 – Graphs of temperature T (on the left, light grey curve) and relative humidity RH (on the right, dark grey curve) against time, monitored for a period of 12 months (21/11/2017-20/11/2018) in the display case close to the panel’s back face, recorded every 30 minutes.

The analysis of the frequencies for both T and RH (see Fig. 6) confirmed the stability of climate conditions inside the display case.

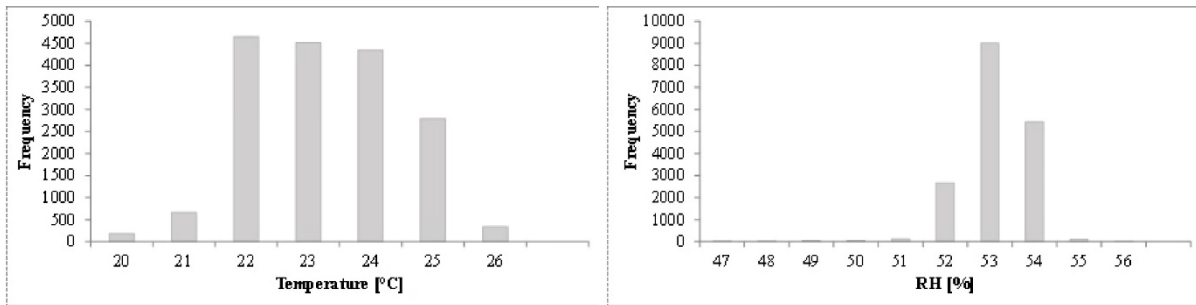


Fig. 6 – Frequency distributions of temperature and relative humidity (RH), with average values of 23 °C (std. dev. ± 1 °C) and 53 % (std. dev. ± 0.7 %) respectively, during the period shown in Fig. 5.

4.2 The mechanical behaviour of the panel

The forces monitored by the four load cells and the deflections measured by the three displacement transducers are shown in Fig. 7 as total force and cupping deflection curves. The yearlong data testify the good quality and reliability of the measurement system, which allows monitoring without interference with the visitor’s experience, or the need to access the artwork. For all the monitored years, the same trend is shown by the total force and cupping deflection curves, which represent the hygro-mechanical response of the *Mona Lisa*’s panel (constantly constrained between the auxiliary frame and the crossbeams) under the action of the T and RH variations in the display case.

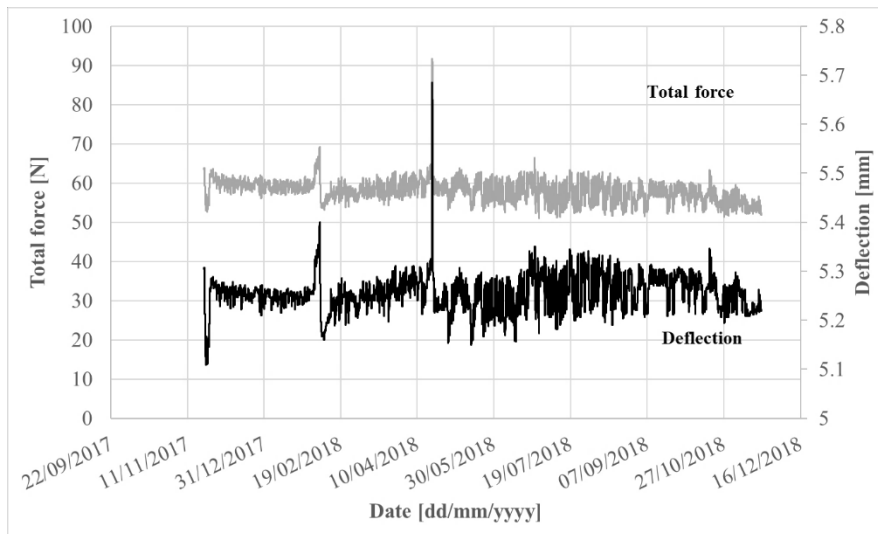


Fig. 7 – Examples of total force (grey line) and cupping deflection (black line) data resulting from the year-long monitoring of the panel’s response to the hygrothermal fluctuations in the display case shown in Fig. 5. Cupping deflection (fc in Fig. 4) and total force (sum of forces measured in locations L1-L2-L7-L8, see Fig. 2a) are plotted against time for the same period. Note. The highest peaks of force (90,7 N) and deflection (5.7 mm) occurring on 19/04/2018 are partially superimposed.

A thorough analysis of the climate conditions inside the display case, and of the resulting panel’s response, is beyond the scope of this paper and will possibly be published in a near future.

The minor climatic fluctuations occurring constantly throughout the year are reflected in similar minor fluctuations in the rather constant force and deflection values. A two-dimensional numerical simulation of the effects of such fluctuations was published in [23].

The three following unusual changes of climatic conditions occurred in the year presented. Two climatic spikes occurred on 19/04/2018 and 21/06/2018, and are reflected in two force and deflection spikes, well noticeable although small in absolute value. A longer lasting climatic perturbation occurred on 02/02 to 05/02/2018; a brief examination of the data collected, and the graphs shown here can provide the following simple indications: (i) both the force and deflection variations are quite small in absolute values, (ii) the panel's response starts approximately 4 hours after the onset of the climatic disturbance, and (iii) the panel takes about 6 days after the end of the disturbance, to reach its 'steady state' conditions again.

The mechanical behaviour of the wooden panel can also be represented by means of the force-deflection graphs plotted in Fig. 8, where for each year the point clouds are well fitted by linear trend lines (R^2 consistently > 0.75); the slight deviations from linearity are probably due to friction, visco-elastic phenomena, hysteresis, and mechano-sorption. In addition, the fact that such fitted lines, which can be interpreted as representing a sort of rigidity of the system, remain parallel to each other over the years, suggests that no irreversible processes have occurred in the panel, and that hence the present climatic conditions can be considered favourable to its conservation. Small changes from year-to-year result from slightly different loading conditions, possibly caused by different adjustments of the load cells after disassembly and reassembly of the system at each opening day.

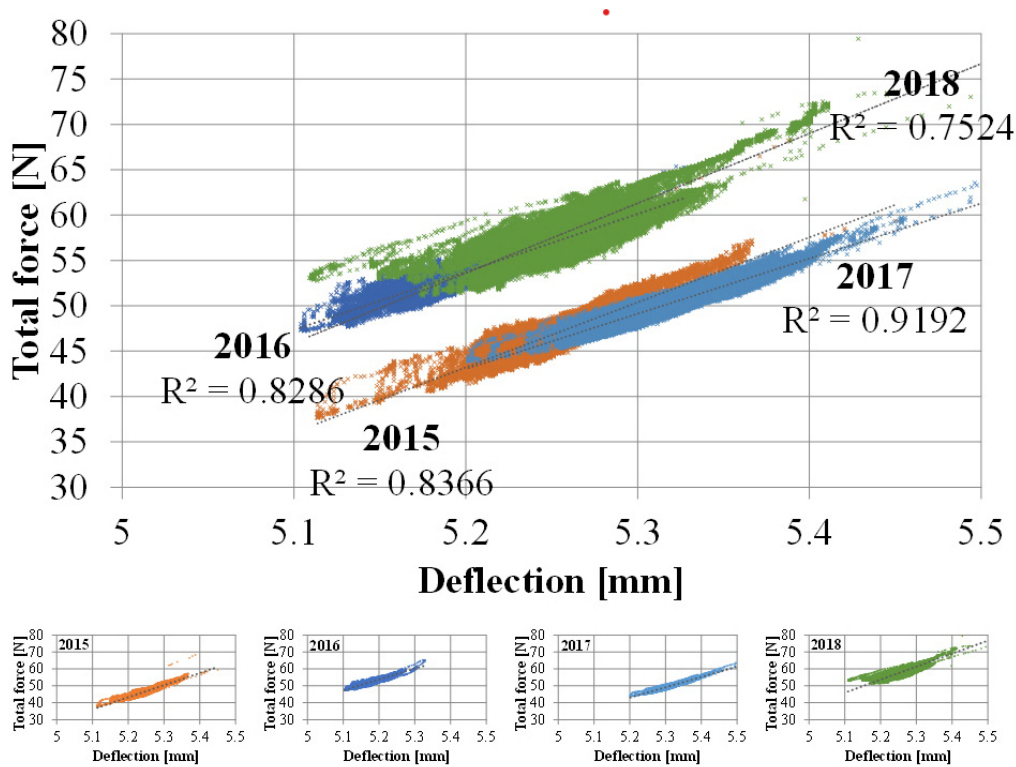


Fig. 8 – Force-deflection graphs plotted for years 2015 to 2018. In the large graph, the data of all years have been presented showing their substantial similarity despite their partial overlapping. The smaller separate graphs enable seeing full data ranges of individual years.

In addition to the yearlong mechanical behaviour shown by the panel while exhibited inside the display case, the results from the punctual test regarding its apparent stiffness (intended as a local

ratio between applied force and measured displacement) are presented below. The experimental data (see Section 3.4) were organised in force-displacement curves (see Fig. 9) showing a linear relationship between the displacement imposed on a load cell and the corresponding increase in the load measured by it. The slope of each curve represents the apparent stiffness of the various parts of the panel, as “seen” from the various loading points L1-L2-L7-L8; in fact, the experimental data show a significantly different slope for each of the four locations (see Table 1). These differences can be attributed to many factors, including wood variability, asymmetry of contacts between panel and auxiliary frame, and the presence of the crack, which certainly influences the mechanical response of the panel.

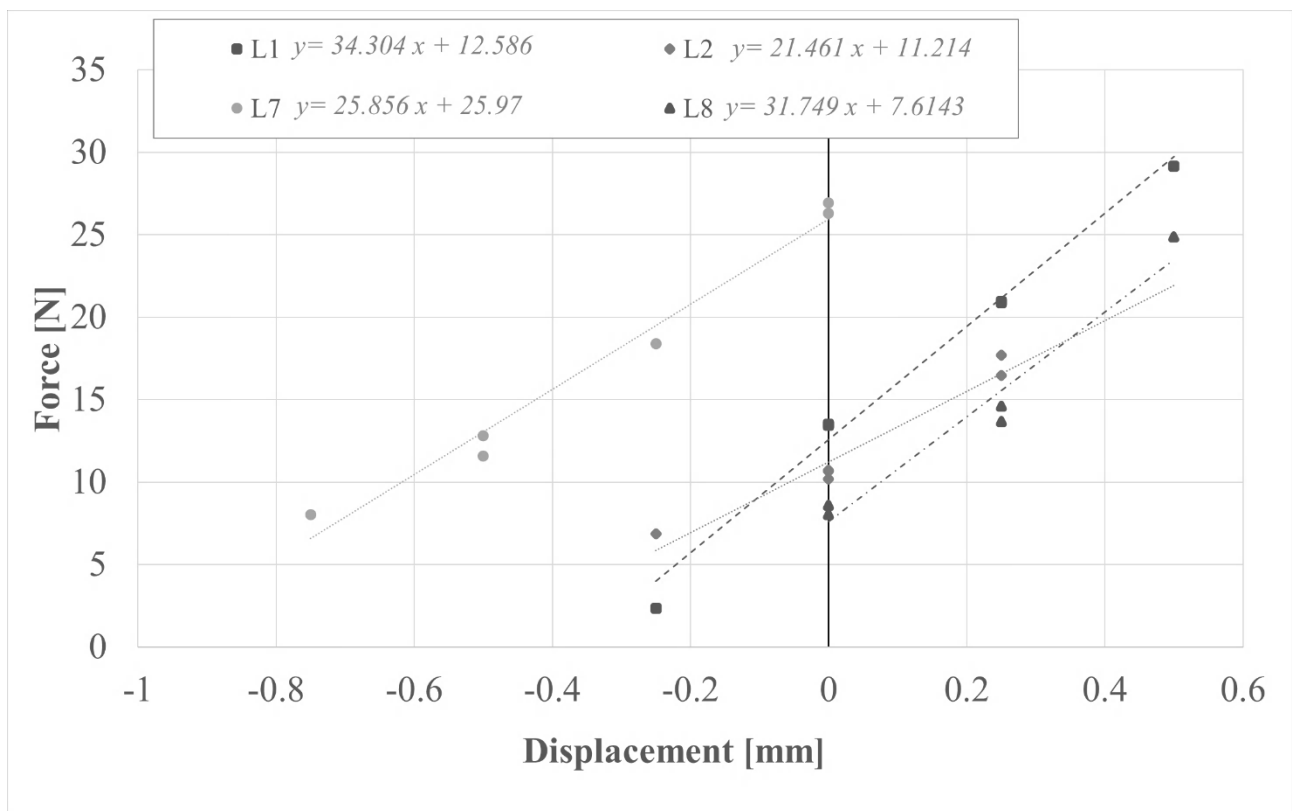


Fig. 9 Force-displacement graphs plotted for each of the four locations (L1-L2-L7-L8); R^2 values larger than 0.95 confirm that the tests were carried out in the elastic range.

Table 1 – Apparent stiffness values of the panel (i.e. force increments produced by 1 mm displacement of the corresponding load cell) in locations L1-L2-L7-L8, derived from the trendline equations shown in Fig. 9.

Location	Force increment per 1 mm displacement [N]
L1	34
L2	21
L7	26
L8	32

It is not the focus of this paper to show comprehensively the results of the monitoring described here; therefore, the above results, derived from elementary graphing and calculations, are reported just by way of example. However, the authors are planning to publish in a near future a further paper, dealing with the mechanical behaviour and the FE-modelling of the *Mona Lisa* panel [24].

5. Conclusions

This paper describes in detail the methods and the equipment developed for continuous monitoring of the mechanical and deformative state of a panel painting under museum display conditions; in our case the panel of the *Mona Lisa* exhibited at the Louvre Museum. This monitoring proved its effectiveness in allowing a more in-depth knowledge of the artwork and of its behaviour, and in providing the data needed for calibrating reliable digital models able to describe accurately the individual panel's response to environmental fluctuations, or to the application of forces and other external actions. Such methods and equipment were developed and improved over time, based on a thorough evaluation of (a) the objectives of the whole project, (b) the constraints constituted by the fact that the research work concerned a famous and delicate historic artwork constantly exhibited to the public, and (c) an accurate technological analysis of the painted panel and of its assembly. After eighteen years of work, it can be concluded that the methods and equipment described in this paper do work correctly and provide reliable results, obtained in a non-invasive way and respecting all the safety and functionality constraints deriving from the artwork's permanent on display status.

A similar approach can be adopted for other panel paintings, to obtain similar results. However, appropriate methods and equipment obviously need to be conceived and adapted to each individual artwork, considering its specific peculiarities and constraints. As for the parameters describing the material properties and the behaviour of wooden artworks, to be used in numerical models and simulations, the author's experience – both on historic panel paintings and on mock-models – indicates that the variability is extremely high, and that using numbers found in the literature provides unreliable, if not completely wrong results.

Some examples of the data collected are also reported in this paper, together with intermediate results deriving from basic processing, such as (a) the force-deformation relationships derived from direct manual tests, (b) the climatic, force and deflection data monitored throughout the whole year, and (c) the force-deflection graphs plotted for years 2015 to 2018, suggesting that the present climatic conditions maintained in the display case can be considered favourable to the panel's conservation. The forces acting on the panel have been monitored in the current constraint conditions and can now be adjusted as required by the conservation needs. The contact conditions between the auxiliary frame and the external gilded frame have been identified and adjusted to prevent the onset of uncontrollable deformations and forces at the time of reassembly.

Acknowledgments

One of the reasons why the work described here can be considered effective, is that it has always been carried out in close, sincere, and fruitful collaboration not only within individual groups, between specialists of different disciplines, and with the expert restorers, but firstly and mostly with the curators in charge of the artwork's management and conservation.

With the hope of not having inadvertently omitted anyone, the authors sincerely thank all those who through cooperation and mutual confidence made in many ways this work possible, including the following (that for practical reasons are divided according to the institutions or professional categories to which they belong, and within them are listed in alphabetical order).

From the Louvre Museum: Sébastien Allard (present head) and Vincent Pomarède (former head) of the Painting Department - Vincent Delieuvin (present chief curator) and Cécile Scaillerez (former chief curator) of Italian painting of the sixteenth century paintings department) – In charge of the climatization equipment: Eric Burgart, Antoine Carnino (†), Olivier Leçon, Philippe Martins

From C2RMF (National Centre for Research and Restoration in French Museums): Michel Menu, Bruno Mottin, Elisabeth Ravaud, Jean-Paul Rioux

From University of Florence (DAGRI, former-GESAAF, University di Florence, Florence, Italy): Linda Cocchi, Marco Fioravanti, Luisa Ghelardini, Lorenzo Vedovato

From University of Lorraine (LerMAB, Univ. Lorraine, Epinal, France): Romain Rémond

From University of Montpellier (LMGC, Univ. Montpellier, CNRS, Montpellier, France): Olivier Arnould, Sandrine Bardet, Delphine Jullien

From University of Paris-Saclay (LGPM, Centrale Supélec, Gif-sur-Yvette, France): Patrick Perré

From University of Poitiers (Institut Pprime, Université de Poitiers, CNRS, Poitiers, France): Fabrice Brémand, Pascal Doumalin, Jean-Christophe Dupré, Franck Hesser, Valery Valle

From INSA Lyon (LaMCos, INSA Lyon, France): Julien Colmars, David Dureisseix

From Art et Métier (LaBoMaP, Arts et Métiers Institut de Technologie, Cluny, France): Bertrand Marcon

Independent restorers and engineers of wooden panels: Jonathan Graindorge-Lamour (Moulins le Carbonnel, 72130 France), Daniel Jaunard (from Paris, one of the historical restorers, retired in 2014), Gilles Tournillon and Cécilia Gauvin (S-MA-C-H, Science and mechanics in conservation of heritage, Le Château, 594 Rte de Suze-la-Rousse, 84290 Sainte Cécile les Vignes)

Florentine Masters of precision machining, having collaborated with competence and passion in practical design and manufacture of the *ad hoc* equipment: Alfredo Canacci (†), Fulvio Smorti

Italian electronic engineers, having collaborated in the design, construction and calibration of the LAB-MoB connection apparatus: Massimo Liggio, Stefano Lucchetti

Manufacturer of the miniature load cells: Gianni Fondriest (†), co-founder of Deltatech (Sogliano al Rubicone, Forli-Cesena, Italy)

References

- [1] L. Uzielli, Historical overview of panel-making techniques in central Italy, The Getty Conservation Institute, Los Angeles, 1998, pp. 110–135.
- [2] J. Wadum, Historical overview of panel-making techniques in northern countries, The Getty Conservation Institute, Los Angeles, 1998, pp. 149–177.
- [3] R. D. Buck, Some applications of mechanics to the treatment of panel paintings, *Studies in Conservation*, 1961, 6 (1): 156–162.
- [4] R. D. Buck, Some applications of rheology to the treatment of panel paintings, *Studies in Conservation*, 1972, 17:1-11
- [5] B. R. Hoadley, Chemical and physical properties of wood, The Getty Conservation Institute, Los Angeles, 1998, pp. 2–20.
- [6] A. Unger, A. Schniewind, and W. Unger, *Conservation of Wood Artifacts, a Handbook*. Springer Berlin Heidelberg, 2001. doi: <https://doi.org/10.1007/978-3-662-06398-9>.
- [7] J. Gril, Ed., Wood science for conservation COST Action IE0601. *Journal of Cultural Heritage*, 2012.
- [8] K. Dardes and A. Rothe, Eds., *The structural conservation of panel paintings: Proceedings of a Symposium at the J. Paul Getty Museum 24-28 April 1995*, The Getty Conservation Institute, Los Angeles, 1998.
- [9] A. Phenix and S. A. Chui, Eds., *Facing the challenges of panel paintings conservation: trends, treatments, and trainings. Proceedings of the symposium 17-18 May 2009*, The Getty Conservation Institute, Los Angeles, 2011.
- [10] M. Ciatti and C. Frosinini, Eds., *Structural conservation of Panel paintings at the Opificio delle Pietre Dure in Florence: method, theory, and practice*. Florence, Edifir, 2016.
- [11] L. Uzielli, P. Dionisi Vici, and J. Gril, “Physical and Mechanical Characterization of the Support,” in *Mona Lisa, inside the painting*, J. P. Mohen, M. Menu, and B. Mottin, Eds. New York, 2006, pp. 48–49.
- [12] D. Hunt, L. Uzielli, and P. Mazzanti, Strains in gesso on painted wood panels during humidity changes and cupping, *Journal of Cultural Heritage*, 2017, 25:163-169.
- [13] G. Goli, P. Dionisi Vici, and L. Uzielli, Locating contact areas and estimating contact forces between the Mona Lisa wooden panel and its frame, *Journal of Cultural Heritage*, 2013, 15 (4): 391-402.
- [14] F. Brémand, P. Doumalin, J. C. Dupré, F. Hesser, and V. Valle, Measuring the Relief of the Panel Support without Contact, in *Mona Lisa, inside the painting*, J. P. Mohen, M. Menu, and B. Mottin, Eds. New York: Abrams, 2006, pp. 43–47.
- [15] F. Brémand, P. Doumalin, J. C. Dupré, A. Germaneau, F. Hesser, and V. Valle, Mechanical structure analysis by Digital Image Correlation and Fringe Pattern Profilometry, Joint focused meeting, COST Actions IE0601 and FP0601, *Non-destructive techniques to study Wooden Cultural Heritage Objects (WCHOs)*, 2011.
- [16] E. Ravaud, The Complex System of Fine Cracks, in *Mona Lisa, inside the painting*, J. P. Mohen, M. Menu, and B. Mottin, Eds. New York, Abrams, 2006, pp. 38–42.
- [17] N. Volle, G. Aitken, D. Jaunard, B. Lauwick, P. Mandron, and J. P. Rioux, Early Restorations to the Painting, in *Mona Lisa, inside the painting*, J. P. Mohen, M. Menu, and B. Mottin, Eds. New York: Abrams, 2006, p. 18-21.

- [18] P. Mazzanti, J. Colmars, J. Gril, D. Hunt, and L. Uzielli, A hygro-mechanical analysis of poplar wood along the tangential direction by restrained swelling test, *Wood Science and Technology*, 2014, 48 (4): 673-687, doi: 10.1007/s00226-014-0633-4.
- [19] E. Ravaud, The Mona Lisa's Wooden Support, in *Mona Lisa, inside the painting*, J. P. Mohen, M. Menu, and B. Mottin, Eds. New York: Abrams, 2006, pp. 32–37.
- [20] L. Uzielli, Personal communication, paper under preparation, 2022.
- [21] D. Dureisseix, J. Gril and O. Arnould, Mechanical Modeling of the Activity of the Flexible Frame, in *Mona Lisa, inside the painting*, J. P. Mohen, M. Menu, and B. Mottin, Eds. New York, Abrams, 2006, pp. 52–53.
- [22] S. Lucchetti and P. Dionisi Vici, Wireless apparatus for remote monitoring of e.g. art objects and, in general, of inaccessible objects of any kind, 2006
- [23] P. Perré, R. Remond, and J. Gril, Simulation of the Effects of Ambient Variations, in *Mona Lisa, inside the painting*, J. P. Mohen, M. Menu, and B. Mottin, Eds. New York, Abrams, 2006, pp. 50–51.
- [24] L. Riparbelli, Personal communication, paper under preparation, 2022.

Hygromechanical behaviour of wooden panel paintings: Classification of their deformation tendencies based on numerical modelling and experimental results

Lorenzo Riparbelli¹, Paola Mazzanti¹, Chiara Manfriani¹, Luca Uzielli¹, Ciro Castelli², Giovanni Guldani^{1,2}, Luciano Ricciardi², Andrea Santacerea², Sandra Rossi², Marco Fioravanti¹

1 DAGRI, University of Florence, Italy

2 Opificio delle Pietre Dure, Florence, Italy

Corresponding author: Paola Mazzanti – paola.mazzanti@unifi.it

Abstract

Wooden panel paintings are among the most important historical and artistic artworks from the Middle Ages and the Renaissance period. Currently, they represent a challenge for conservators and scientists who face complex issues related to their conservation. Panel paintings can be considered multilayer objects, that for brevity can be considered to consist of a wooden support and various paint layers. The wooden support is known to be hygroscopic and is continuously seeking hygroscopic equilibrium with the humidity of the environment, thus it tends to deform. Based on various hygroscopic tests carried out on 6 real panel paintings chosen by expert restorers to represent different periods and construction techniques, this paper describes the deformation tendencies of the selected panel paintings. Among possible variables, three most important variables were identified: a) tree ring orientation of the wooden support, b) stiffness and c) emissivity of the paint layers. The internal equilibrium of the forces, governed by the moisture gradients across the thickness of the wood, changes drastically according to the varying characterisation of these factors. To observe their individual contributions, the 6 panel paintings underwent various humidity cycles, were completely free to deform and were always in complete safety. To characterise the stiffness and emissivity of the paint layers, the 6 panel paintings underwent a few humidity cycles with the front face totally waterproofed; thus, the moisture exchange was forced from the back only, and one of the three variables was eliminated. A complex system emerges where the tree ring orientation of the wooden support, the stiffness and emissivity of the paint layers are strongly coupled and determine the deformation modes of the panel paintings. A numerical analysis was conducted to classify the various general deformation modes of panel paintings and the specific classification of the 6 real panel paintings analysed experimentally. The complexity of the interaction of the variables studied suggests that experimental procedures must be conducted in preparation for numerical analyses of real panel paintings.

Keywords: Wooden panel paintings, conservation, experimental tests, numerical modelling, panel painting deformation tendencies, paint layer emissivity, paint layer stiffness.

1. Introduction

Wooden panel paintings (WPPs) are some of the most valuable cultural heritage artworks. In recent decades, WPP preservation has been the object of several scientific studies [1-5], that have attempted to solve critical questions such as those concerning their interaction with conservation environments.

WPPs have a multilayered structure schematically represented by wooden supports, often made of different boards covered on one side with paint layers (occasionally, the back of the panel was covered by a light coat, historically used to balance the moisture entering from both sides of the panel), and typically equipped on its back with a restraining system. The paint layers are constituted by a ground layer, mainly glue and gesso, sometimes canvas, pigments or dyes included in tempera or oil binders, and often by a varnish layer on top [6,7]. The structural characteristics of WPPs, together with their construction techniques, have changed over time. In Italy, the period between the 12th and the first half of the 15th century was characterised by a wide production of large polyptychs and painted crosses. In this period, the ground layers were solid and strong, including the presence of canvas with a still-valid structural function, when the canvas covered the frame. Later, from the second half of the 15th century, characterised by altarpieces, the ground layers were lighter and thinner [8].

According to Cennini [9], the preparation of the panel began with several coats of animal glue to saturate the porosity of the wood. Several layers of ground, usually made of gesso and animal glue, were subsequently laid down. It is known that the ground layers may have different compositions — glass, kaolin, calcium carbonate, among others, were identified [10] — being in any case the thicker layer, measuring from 250 μm up to 1800 μm [11] without canvas. Canvas could be applied below ground layers to cushion the impact of the moisture-induced movements of the wood on the paint film. The presence of the canvas was discontinuous over time, becoming less common in the late 15th century. On top of the paint layers, the thinner varnish layer strongly contributes to defining the emissivity [12] of the artwork, because it is the most superficial layer and was made of low-hygroscopic materials, such mastic, and other natural resins in the past or resins such as aliphatic, acrylic and urea-aldehyde, among others, in the case of modern restoration resins [13-17]. By contrast, the other layers of the WPP structure are made of hygroscopic materials [1-3], primarily wood and ground layers, which may expand or shrink according to their own properties under climatic variations. Henceforth, for brevity, all these layers will be referred to collectively as the paint layers.

Due to this complex structure, the mechanical and hygroscopic properties of the constitutive materials are quite different; in the case of climatic variations, the shrinking/swelling tendencies contribute to generating inner stresses between the wooden support, the paint layers and at their interface [1,2]. Moreover, when not properly dimensioned, the interaction between the wooden boards and the restraining system can worsen the conservation conditions of the artworks [8] producing damage both on the paint layers [1], [8] and on the wooden support [1,2,3,8], and/or irreversible deformations that determine the typical cupping that can be observed in many panel paintings [8].

Typically, deformations of panel paintings are induced by the variation of the Relative Humidity of the air (RH), and they can be either permanent or transitory [1,18]. In addition, the mechanisms responsible for their origin have not yet been conclusively established, and some of those considered to be the most relevant most likely occur at the same time to determine the deformational behaviour of the paintings, as this paper attempts to demonstrate. For clarity, the most important causes are reported below according to deformation typology.

- a) Permanent deformation:

- tree ring orientation: it is well-known that wood is an anisotropic material for which shrinkage and swelling are twice as high along the tangential direction compared to the radial direction [19]. Such behaviour causes a typical cupping of the tangential boards that also remains at the equilibrium state;

- compression set: namely, the permanent deformation remaining after removal of a force. This is caused by repeated RH cycles that induce internal tension-compression stresses in the wooden support. When the RH varies, a change in the moisture content (MC) occurs, first in the most superficial layers of the exposed back of the boards that consequently produce dimensional changes. However, the inner wood layers that are not yet involved in such a process, do not yet shrink or swell, with the consequent internal stresses within the wood thickness causing permanent cupping of the panel [18,20]. It is possible that a first manifestation of such a mechanism occurs with the preparation of the wooden support when a large amount of water is introduced in the panel by means of animal glue and gesso [21];

- wood ageing: with time, wood loses hemicelluloses from the back surface of the wooden panel towards the inner layers, with a progressive reduction in the hygroscopicity of the surface layer compared to the inner layers [22,23]. This mechanism can produce a 'moisture gradient' across the wood panel that over time can contribute to its permanent deformation;

- panel's mechanical asymmetry: the back of the panel has the mechanical properties typical of the wooden species, whereas the front has mechanical properties heavily influenced by those of the paint layers (ground, paints, and varnish). In fact, wood and paint layers show different hygromechanical properties [14,15], with ground layers stiffer than wood in its transverse directions, and the paint layers due to their complexity and despite their small thickness can significantly affect the deformational behaviour of the whole panel. Their mechanical contribution to the permanent deformation must be taken into account [1,21,24];

b) Transient deformation:

In addition to permanent deformations, transient deformation can also occur as a consequence of RH variations. These variations arise from the hygroscopic asymmetry between the two faces of the panel painting, the bare wood on the back and the painted face on the front. This transient state is characterised by the onset of asymmetric moisture gradients across the panel thickness, that may produce a typical deformation known as flying wood [25,26]. A note: [25] uses the term flying wood to describe the deformations of wooden boards with an asymmetric hygroscopicity with large mechanosorption effects; in the panel paintings conservation, the same term flying wood describe deformations where the mechanosorption effects can be considered negligible, and this is the meaning of the term used in this paper;

Within this theoretical framework, this paper presents the results from an experimental campaign carried out on six historic panel paintings. The WPPs, dated from the 15th to 16th century, were subjected to several cycles of controlled RH variations that were compatible with RH fluctuations already sustained by paintings (determined according to EN15757:2010 [27]) in the restoration environment, without any damage visible when analysed by restorers, and their actual time history of deflection was monitored. The experimental tests allowed us to establish the main mechanisms causing the deformations in the panel paintings, together with their specific contribution. In addition, a numerical model was developed and was able to interpret such behaviour and highlight the complexity of the phenomenon acting through the interaction of these mechanisms.

The aim of the research is to understand the deformation dynamics in a population of WPPs chosen by experienced restorers as representative of both different techniques and construction typologies relevant to the Italian school in the periods between the 15th and 16th centuries and to establish the existence of various deformation modes within the examined structural typologies.





The hygroscopic behaviour of wood is well described in the literature; however, the deformation tendencies of panel paintings are more complex because they are also influenced by the interaction of the hygromechanical behaviour of the wooden support with the hygromechanical behaviour of the paint layers that may have a moisture barrier and mechanical stiffening behaviour. For the experimental validation, the present study assumes that the main variables influencing the actual deformation dynamics of WPPs are a) the stiffness of the wood and the paint layers, b) the moisture diffusion of wood and emissivity of wood and paint layers, and c) the tree ring orientation of the wooden panel. Thus, a numerical model was developed (a) to classify the hygromechanical behaviour of the panel paintings and (b) to explore how the complex interaction among these three variables affects such behaviour.



2. Materials and methods

2.1 Panel paintings and monitoring equipment

Six panel paintings were chosen for testing. Table 1 shows images (front and back) of the investigated paintings, along with the name, dimensions, age and painting technique specifications. They are labelled by 'WPP' followed by a progressive number, as follows: WPP1 corresponds to '*Madonna with Child*', WPP2 to '*Saint Lodovico and Saint Giuliano*', WPP3 to '*Dominican Saint*', WPP4 to '*Madonna with Child, Saint John and monk*', WPP5 corresponds to '*Crucifixion with Madonna and Saint John*', and WPP6 to '*Madonna with Child*'. These WPPs, whose wooden support is made of poplar wood (*Populus alba* L.), were chosen according to OPD (Opificio delle Pietre Dure, restoration laboratory in Florence, Italy) art conservators' observations; they are considered representative of historical changes (see Section 1) during a time span between the 15th and 16th century for construction features, ground layer and painting/artistic technique, or conservation conditions.

Table 1 Description of the six paintings and their dimensions, period, and materials.

	Painting	Dimensions	Age	Materials and artistic technique
1	<p>Madonna con Bambino <i>Madonna with Child</i></p> 	530x900x14 mm	15th century	<ul style="list-style-type: none"> • Wood species: Poplar • Number of boards and orientation: two vertical tangential (around 4 cm from the pith), respectively 275 mm e 255 mm wide • Preparation and painting technique: thick gesso and animal glue preparation with the use of canvas; egg tempera paints.
2	<p>S. Lodovico e S. Giuliano <i>Saint Lodovico and Saint Giuliano</i></p> 	67x1310x33 mm	15th century	<ul style="list-style-type: none"> • Wood species: Poplar • Number of boards and orientation: three vertical radial boards (around 2 cm from the pith), respectively 170 mm, 380 mm, and 145 mm. • Preparation and painting technique: thick gesso and animal glue preparation with the use of canvas; egg tempera paints.
3	<p>Santa Domenicana <i>Dominican Saint</i></p> 	700x1370x25 mm	15th century	<ul style="list-style-type: none"> • Wood species: Poplar • Number of boards and orientation: four vertical boards; the first looking from the back is tangential (5 cm from the pith) and 18,5cm wide; the other three are radial (around 2 cm from the pith) and respectively 165 mm, 13,0 cm e 220 mm wide • Preparation and painting technique: thick gesso and animal glue preparation with canvas; tempera paints and gold leaf. • Previous conservation treatment: application of a waterproof coating (60% bee wax, 30% paraffine, 10% colophon) on the back face
4	<p>Madonna con Bambino, S. Giovannino e Monaco <i>Madonna with Child, Saint John and monk</i></p> 	645x775x23 mm	16th century	<ul style="list-style-type: none"> • Wood species: Poplar • Number of boards and orientation: two vertical tangential boards, 210 mm and 435 mm wide • Preparation and painting technique: thick gesso and animal glue preparation; thick oil paints.
5	<p>Crocifissione con Madonna e S. Giovanni apostolo <i>Crucifixion with Madonna and Saint John</i></p>	655x855x30 mm	16th century	<ul style="list-style-type: none"> • Wood species: Poplar • Number of boards and orientation: two vertical tangential (around 5 cm from the pith) poplar wood boards, 295 mm and 360 mm wide • Preparation and painting technique: thin gesso and animal glue preparation; rose primer; thin oil paints.

				
6	<p>Madonna con Bambino <i>Madonna with Child</i></p> 	650x890x28 mm	16th century	<ul style="list-style-type: none"> • Wood species: Poplar • Number of boards and orientation: three vertical boards; the first looking from the back is radial and 225 mm wide; the other two are tangential (around 6 cm from the pith) and 320 and 105 cm wide respectively • Preparation and painting technique: thin gesso and animal glue preparation; thin oil paints.

Each panel painting was equipped with a Deformometric Kit (DK) to measure the deformation behaviour, the panel shrinking and swelling and, by means of data processing and trigonometrical calculations, the variations in cupping angle (φ , °) and maximum deflection (δ_{\max} , mm) induced by climatic fluctuations [28]. The DKs geometrical parameters are presented in Table 2. All sensors were connected to a Pace Scientific XR5-SE data logger (accuracy $\pm 0.25\%$) that powered the instruments and logged the data every 15 min. The collected data were elaborated through a customised data code.

Table 2: Schematic diagram of the most relevant geometrical parameters of the DK. The convention concerning positive (front face convex) and negative (front face concave) values of the cupping angle is also shown. Key to symbols; e: distance between the axes of the two columns, where they intersect the back face of panel (variable in time); m: distance between the centres of the ball joints of the two transducers on the same column (constant, determined by construction); r: radius of curvature of the base lines (variable in time); z: distance between the centre of the ball joint of the lower transducer, and the back face of the panel, along the axis of the column (constant, determined by construction) [28].

Geometry of the DKs			
Painting	e [mm]	m [mm]	z [mm]
WPP1	174.35	113.35	11.55
WPP2	170.61	114.27	12.175
WPP3	173.19	92.8	14.67
WPP4	167.6	92.8	14.6
WPP5	173.28	113.25	11.85
WPP6	166.83	92.7	14.6

To obtain a controlled and stable environment, an RH-controlled box (120 x 180 x 200 cm, 4.32 m³ volume total) was constructed using a wooden frame and thermoinsulated panels. The temperature (T) was not controlled and depended on the controlled ambient conditions of the OPD Lab, and the small variations were mitigated by the insulated panels. RH was controlled using a Preservatech miniOne humidity generator. Ventilation was guaranteed by 6 fans together with the typical functioning of the humidity machine. The temperature and the relative humidity inside the box were measured by an Onset Hobo U12-013 (accuracy ± 0.35 °C and $\pm 2.5\%$) and logged every 15 min. A remote-control system was also implemented; two CEAM LoRa-C Smart digital sensors were installed in the experimentation area, one inside the box and one outside, and connected to T/RH probes (accuracy $\pm 2\%$ and ± 0.5 °C), with a sampling interval of 15 minutes. The data were continuously collected through the CEAM CWS software, an integrated platform for supervision, monitoring and shared management based on the web-cloud-IoT technology.

2.2 Preparatory conditions of panel paintings and RH cycles

Since the aim of the research is to observe the deformational behaviour of the WPPs, the artworks were tested free from their restraining systems. The restraining system was removed to measure the complete deformation of each panel painting, otherwise such deformation is contained by the restraint system. This allowed (a) comparison of the experimental results and (b) exclusion of nonlinear behaviour, such as monolateral contacts and friction, among others, that would not have allowed a clear comprehension of the measurements. Thus, the complete free deformation was observed and measured. WPP2 had a painted frame glued on the front face that could not be removed. However, it did not affect the tests, because the frame is considered to be a structural feature of the artwork, typical of a precise historical period and useful for characterisation of such objects. Inside the box, a rack was prepared to house the WPPs in a vertical position, the contact areas at the bottom were covered by stripes of PTFE to minimise the friction, and on the top, a fork covered by foam was fastened on the rack to keep the panel vertical. Prior to the tests, the panel paintings were kept inside the box at 52% RH for 20 days to reach the equilibrium state to avoid moisture gradients.

Together with the restorers and conservators, the climatic range was set between 50 and 65% RH for the objects' safety and to be representative of their typical conservation conditions. The RH% variations were determined by applying the standard EN 15757:2010 [27] and the concept of historical climate that it introduces. Thus, the conservation climatic conditions were analysed, and the maximum variation of 10% RH% in the range between 50-65% was considered safe, in agreement with conservators.

Seven tests were carried out, three in the adsorption mode and four in the desorption mode. The climatic conditions of the tests are described in Figure 1 and in Table 3.

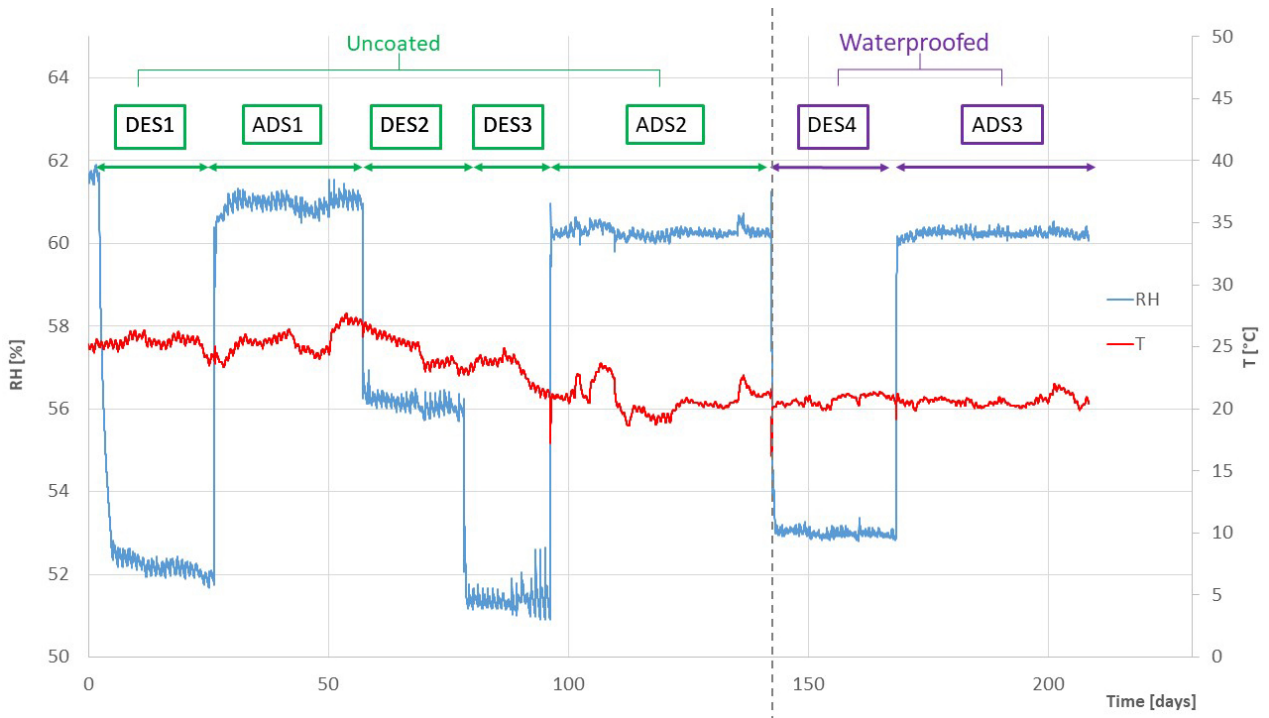


Figure 1 Relative humidity (RH) cycles for all of the tests performed. The labels indicate the tests, and waterproofing/no waterproofing is reported. In addition, the temperature (T) was reported.

Table 3 Average values of RH and T for each cycle, calculated starting within 3 hours from the RH change applied till the next change and their standard deviations.

Test name	Average Δ RH [%]	Sd RH [%]	Average T [°C]	Sd T [°C]
ADS 1 Not waterproofed	52-61	± 0.2	25.5	± 1.0
ADS 2 Not waterproofed	51-60	± 0.1	20.7	± 1.1
ADS 3 waterproofed	53-60	± 0.1	20.6	± 0.4
DES 1 Not waterproofed	62-52	± 0.4	25.4	± 0.5
DES 2 Not waterproofed	61-56	± 0.2	24.8	± 1.1
DES 3 Not waterproofed	56-51	± 0.3	23.5	± 1.0
DES 4 waterproofed	60-53	± 0.3	20.7	± 0.5

The procedure of the tests (hereafter called ADS#/DES#) consisted of equilibrating the panel paintings to a specific RH value and then changing the settings on the humidity generator to produce the desired Δ RH (the complete cycles of RH variations imposed are reported in Figure 1). The new equilibrium condition was considered to be reached when the deformation became flat and stable. During each test, the derivative of the deflection curves was determined repeatedly. Once the derivative is calculated to be zero for at least 6 h, the WPP was considered to be equilibrated to the new RH conditions.

Two of the RH cycles imposed on the paintings, namely, DES4 and ADS3, were performed with waterproof protection applied on the painted face. This is done to evaluate the hygroscopic behaviour of the WPPs when the influence of the emissivity of the front face is nullified and one of the three variables assumed by the study is excluded. Prior to applying the aluminium foil, the four edges of the panel paintings were prepared with Japanese paper glued on the four edges with animal glue, on which the foil was fastened. The choice to protect the edges of the wooden panel by placing Japanese paper made the operation safe and reversible. Then, the painted face was covered by aluminium foil and sealed by silicone tape on Japanese paper. The aluminium foil is impervious to water vapour [29] and much less stiff than wood, with a much lower thickness than that of the wooden supports. In addition, the aluminium foil was chosen to be larger than the artworks to avoid tensions on the painted face.

Since the analysed RH cycles vary in different quantities, the data are normalised to the 5% RH variation; that is, the deflection was scaled to a 5% variation in RH. The normalisation is based on the assumptions that the isotherm was explored within its linear part from 51 to 62% RH, where the behaviour is completely reversible, and the plastic phenomena excluded. The viscoelasticity was considered to be a linear phenomenon as well. In addition, to enable comparison of the results for the six WPPs, the data are normalised for the span of the DKs. For both cases, the data were divided by a constant (the initial span of the specific DK or the RH variation) and multiplied by a) 5 to normalise for the RH, which is the minimum hygroscopic variation (Figure 1) imposed on the WPPs, and b) 300 to normalise for the span, which is the width arbitrarily chosen for the modelling to avoid edge effects because an average width of 400 mm was arbitrarily chosen (see Section 2.3).

2.3 Numerical Modelling

The numerical modelling is applied to assess, through a sensitivity study, the influence and the mutual interactions of the identified dimensioning variables (layers stiffness, moisture diffusion and emissivity, anatomical cut) in determining the deformation of the painted board. It is important to emphasise that the aim of this numerical model is to create an interpretative method to improve the understanding of the experimental results and in particular of the relationships between certain variables in the theoretical physical model.

For the simulation of moisture diffusion in wood, a simplified approach consisting of an isotropic version of Fick's theory that merges the multiple diffusion mechanisms in wood into a single mechanism [30] was used.

Following [31], the moisture flow is described by

$$\mathbf{q}_m = -\rho_0 \cdot \underline{\mathbf{D}} \cdot \nabla m_c \quad (1)$$

where ρ_0 is the wood density in dry conditions, m_c is the moisture content, and $\underline{\mathbf{D}}$ is the tensor of the diffusion coefficients that in our case has the following form:

$$\underline{\mathbf{D}} = \begin{bmatrix} D_0 \\ D_0 \\ D_0 \end{bmatrix} \quad (2)$$

where D_0 is a value of isotropic moisture diffusion. This approach was already applied by [32,33] and particularly by [34]. Furthermore, it is theoretically supported by [35,36], because at room

temperature, vapour movement makes only a small contribution to the total transfer movements. This is because bound water movement through the cross walls between cells is two or three times slower than movement across the cell cavity and therefore controls the overall transport rate. Furthermore, [37-39] evidence in the tests carried out using a vacuum sorption balance shows that there are no appreciable differences in the rate of absorption for the specimens in the tangential direction or in the longitudinal direction. Finally, the time-dependent form of Fick's law is

$$\frac{\partial m_c}{\partial t} = \nabla \cdot (\underline{D} \cdot \nabla m_c) \quad (3)$$

Assuming it exists, the isotherm of the paint layers is unknown and presumably it varies strongly among the artworks. Similar to [40], we applied the following boundary condition to model its emissivity:

$$\frac{q_t}{\rho_0} = K \cdot (m_{c,air} - m_{c,sur}) \quad (4)$$

where $m_{c,air}$ is the wood equilibrium moisture content corresponding to the air humidity, $m_{c,sur}$ is the moisture content of the wood surface immediately below the ground calculated by the solver, and \mathbf{K} is the global effective emissivity of the paint layers. This corresponds to the assumption of perfect adherence between the ground preparation and wood.

First-order hexahedral finite elements were used for the hygroscopic analysis, while second-order hexahedral finite elements were used for the mechanical model.

The applied mechanical model is homogeneous orthotropic linear elastic [41] in cylindrical coordinates with the centre in the pith and considers shrinkage/swelling in cylindrical coordinates. The ground layers were modelled using two-dimensional elements, in accordance with the Kirchhoff-Love theory, that share their nodes with the corresponding nodes of the wood surface. The geometry and discretisation were carried out with the open-source software Salome-Meca developed by EDF (Électricité de France), the simulations with the open-source solver code_aster [42], and the handling of cylindrical coordinates in the solution of the computational model with the open-source software Mfront [43].

The geometric model is made of 9 boards typologies of 400x30 mm, where each board has the same side (front, the right in Figure 2) covered by paint layers and the opposite one (back, the left in Figure 2) free to exchange moisture with the environment. Boards 1-4 represent the common cut for the construction of the WPPs [8], board 5 is a radial cut, and boards 6-9 represent the WPPs 'painted backwards' (a panel painting with paint layers on the 'opposite' face than the most common cases found in conservation literature). The selected WPPs (Table 1) are associated with the model boards as follows: WPPs 2 and 3 are associated with virtual boards 4 and 5, and WPPs 1, 4, 5 and 6 are associated with virtual board 4. The thickness of the paint layers was chosen as 0.5 mm as an approximate average value among those found in [11]. The boards have a uniform thickness along the longitudinal direction of the wood, with no diffusion phenomenon allowed in this direction; they are also isostatically free to deform. However, the influence of D or thickness is not decisive for the

classification of deformation tendencies because their different values manifest the same typological characteristics.

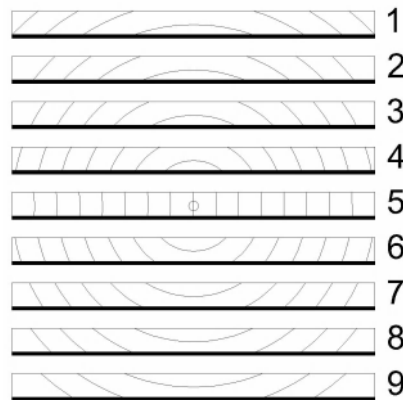


Figure 2 The geometric model consists of 9 boards typologies virtually obtained by a flat sawn tree trunk. Their dimensions are specified in the drawing. The black area on each board represents the front with the paint layers

The material properties used for poplar wood reported in Table 4 are based on [40, 44].

Table 4 Mechanical and physical properties of Poplar wood used.

Young moduli	$E_L=10060 \text{ MPa}$	$E_R=641 \text{ MPa}$	$E_T=306 \text{ MPa}$
Shear Moduli	$G_{RT}=200 \text{ MPa}$	$G_{TL}=640 \text{ MPa}$	$E_{LR}=860 \text{ MPa}$
Shrinkage	$\alpha_L=0.39\%$	$\alpha_R=1.92\%$	$\alpha_T=3.45\%$
Diffusion	$D_0=1.52 \cdot 10^{-4} \text{ mm}^2 \text{ s}^{-1}$		

Through the numerical model, the deflection of the central span, measuring 300 mm (see Section 2.2) of each of the 9 boards, is extracted and plotted over time, drawing a point every 24 hours for 60 days.

For these simulations, the following simplifications have been applied:

- 1) all materials are homogeneous, and their characteristics are not moisture-dependent;
- 2) all materials behave purely elastically, and phenomena such as viscoelasticity, mechanosorption and plasticity are not taken into account;
- 3) the diffusion along the radial and tangential directions is considered to be the same to reduce the number of significant variables, because for now it is not possible to quantify them experimentally;
- 4) the water vapour resistance of bare wood on the back of painted boards is neglected as it is not known a priori, considering that various products were often applied on the back of the artworks to stabilise its deformational behaviour, in addition to the natural ageing phenomenon of the exposed back;
- 5) at the initial equilibrium conditions, the whole body does not present stresses and strains, and it is planar in the initial conditions;
- 6) Since, due to their physical structure, paint layers have much lower shrinkage and swelling coefficients [14] than wood in transverse directions, the effect of mechanical hygroexpansion is neglected in the mechanical modelling of paint layers.

A -1% step variation in the equilibrium moisture content (EMC) is used in the modelling.

To understand the mechanical interaction of the paint layers stiffness with their emissivity, a sensitivity study was carried out by varying their stiffness values, with constant hygromechanical parameters of the wood (Table 4). The sensitivity study is presented in Table 5, where the 50 simulated cases are reported. The table is divided into 5 blocks, each representing a specific rigidity of the pictorial layers, starting from pictorial layers hypothetically with zero rigidity arriving to the maximum, which for this work is considered 10^4 MPa, representing the maximum stiffness value identified in [45]. For each block, the pictorial layer emissivity imposed is also reported.

Table 5 The sensitivity study, with indication of paint layers rigidity and, emissivity for the 50 cases analysed.

Model id	Paint Layers Rigidity [MPa]	Paint Layers Emissivity [mm·s⁻¹]	Model id	Paint Layers Rigidity [MPa]	Paint Layers Emissivity [mm·s⁻¹]
1	no rigidity	bare wood	26	5000	1.00E-05
2	no rigidity	1.00E-04	27	5000	7.50E-06
3	no rigidity	7.50E-05	28	5000	5.00E-06
4	no rigidity	5.00E-05	29	5000	2.50E-06
5	no rigidity	2.50E-05	30	5000	insulated
6	no rigidity	1.00E-05	31	7500	bare wood
7	no rigidity	7.50E-06	32	7500	1.00E-04
8	no rigidity	5.00E-06	33	7500	7.50E-05
9	no rigidity	2.50E-06	34	7500	5.00E-05
10	no rigidity	insulated	35	7500	2.50E-05
11	2500	bare wood	36	7500	1.00E-05
12	2500	1.00E-04	37	7500	7.50E-06
13	2500	7.50E-05	38	7500	5.00E-06
14	2500	5.00E-05	39	7500	2.50E-06
15	2500	2.50E-05	40	7500	insulated
16	2500	1.00E-05	41	10000	bare wood
17	2500	7.50E-06	42	10000	1.00E-04
18	2500	5.00E-06	43	10000	7.50E-05
19	2500	2.50E-06	44	10000	5.00E-05
20	2500	insulated	45	10000	2.50E-05
21	5000	bare wood	46	10000	1.00E-05

22	5000	1.00E-04	47	10000	7.50E-06
23	5000	7.50E-05	48	10000	5.00E-06
24	5000	5.00E-05	49	10000	2.50E-06
25	5000	2.50E-05	50	10000	insulated

3. Results

The experimental results relevant to the RH cycles applied to the six WPPs are presented in graphs and tables in this section. Here, the deformation behaviour and the quantitative results of the experimental tests are presented separately from the sensitivity study carried out by numerical modelling.

3.1 Deformational behaviour and quantitative results

The graphs reported in Figure 3 show the evolution of the deflection δ [mm] between the two columns of the DKs over time in the group of monitored WPPs. The deflection is calculated as the distance between the midpoint of the (imaginary) line constructed between the bases of the DK columns and its projection normal to the back surface of the painting; therefore, the deflection is calculated in the central 300 mm of the 400 mm virtual table.

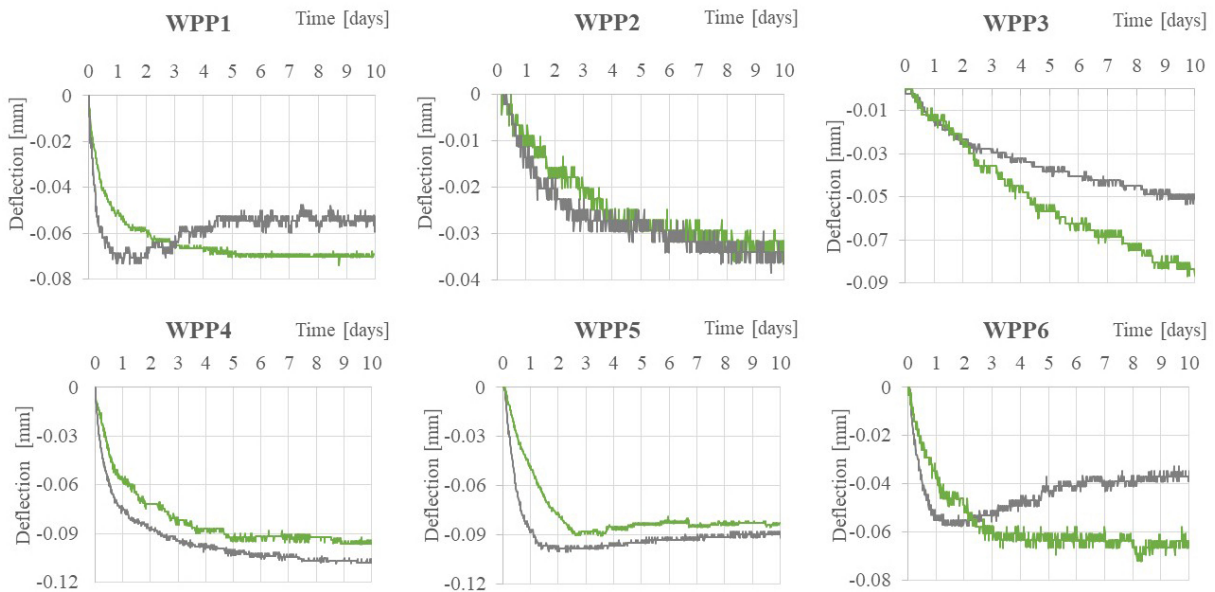


Figure 3 The hygroscopic deformation behaviour of the 6 panel paintings monitored. The green curves represent the deflection of the WPPs under free exchange of humidity, and the grey curves represent the deflections when the front of the panel is waterproofed by the aluminium foil.

The deflection curve of each of the WPPs tested shows two distinct phases (Figure 3): the initial phase with a very steep change and the second phase where the curve flattens out. This behaviour is typical of any wooden board during a moisture cycle, where the initial faster moisture adsorption or desorption is followed by a weakening of adsorption or desorption rate when the new equilibrium is approaching. The curves in Figure 4 refer to the rate of reaction of WPP3 during the different cycles carried out in both adsorption and desorption modes. The rate of reaction was calculated by dividing the deflection data by the average deflection at the equilibrium of test DES1 that produced the greatest deflection for WPP3. Figure 4 shows the clear presence of hysteresis in the deformation panels that is caused by the different equilibrium moisture content that the wood exhibits depending on whether it is in the adsorption or desorption phase. However, these differences appear to make a negligible contribution to the qualitative and quantitative amount of deformation.

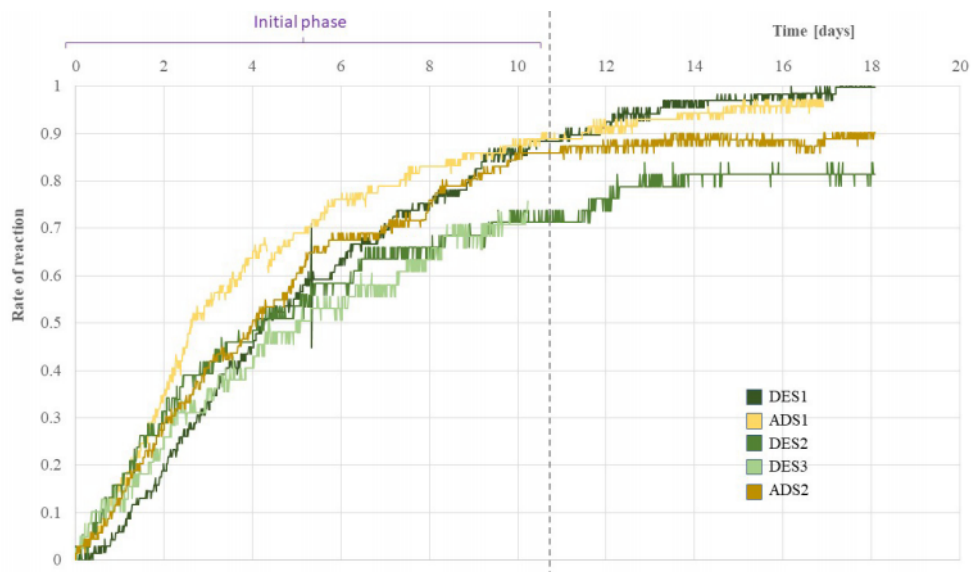


Figure 4 Representation of the deformational behaviour of WPP3 subjected to different moisture cycles. Each curve represents a different moisture cycle carried out in adsorption (green) or desorption (yellow). All curves show the normalised data and a positive deflection both for adsorption and desorption tests to make the data easier to compare.

In all examined paintings (Figure 3), the first phase is typically concluded within the first 9 days, a time during which the moisture gradients triggered by the different emissivities of the two surfaces of the WPP play a significant role in driving the panel deformation. The deformation at the new equilibrium is the result of the interaction between the anatomy (i.e., growth ring arrangement) of the wooden board and the stiffening caused by the presence of the paint layers. Among the WPPs (Figure 3, green curves), only WPP5 shows the so-called 'flying wood' (FW): the typical deformational behaviour induced in the presence of a significant hygroscopic and/or mechanical asymmetry of the two opposite faces in a wooden panel. Although hygroscopic and mechanical asymmetry is certainly present to the same extent in all the other paintings, their deformation curve does not show FW behaviour. This experimental evidence appears to suggest that in addition to hygroscopic asymmetry, flying wood deformation can also be generated by the effect of other variables and of their combinations that influence the deformational behaviour of the WPPs.

To assess the existence and the possible influence of a moisture emissivity of the paint layers, the same RH cycles were repeated modifying the hygroscopic behaviour of the painted surface, with the introduction of the waterproofed barrier that increased the hygroscopic asymmetry between the two surfaces of each WPP (this facilitates the build-up of steep moisture gradients and, as a consequence, the possible occurrence of transient deformations of flying wood [46]). The results obtained show in general a different deformation behaviour of the WPPs, with a new set of deflection curves over time.

These curves (grey lines in Figure 3) differ in both shape and rate of deflection from those shown by the same panel in the nonwatertight mode, with a certain variability among the panels with the same constraint conditions and between the same artwork with different constraint conditions.

For almost all WPPs, the very initial segment of the two curves is characterised by an overlapping of the two phases (this is particularly clear in WPP3, where the treatment applied on the back prolongs this stage). In this initial stage, the paint layers, even in free conditions, exert an effective barrier to moisture diffusion; the point at which the two curves separate can be interpreted as an indication of the specific emissivity to moisture diffusion of each singular WPP.

WPP2 did not show any significant variation between the two cycles. This behaviour can be explained considering the stiffening effect caused by the presence of the wooden cusp frame at the front of the painting.

In all other WPPs, the waterproofed deformation curves are steeper than those with no-waterproofing barriers (typical condition of the panel paintings), highlighting the potential importance of gradients (that are certainly higher in the first case) on the transient behaviour of panel deformation.

However, the most interesting aspects are represented by the difference in the amounts of deformation between the two cycles at the new equilibrium, as shown by WPPs 1, 3, and 6 (WPPs 1 and 3 are both characterised by a thin support and thick ground layers). If the deformation depends only on the anatomical cutting of the wooden board, in the steady state, the curves in the two test conditions should converge to almost the same values as those in WPPs 4 and 5, where the differences are less evident. This different behaviour suggests a nonlinear moisture-dependent behaviour of the paint layers, whereas a cause related to the hysteretic behaviour of the wood appears to be ruled out, considering that this differentiation does not occur in the other paintings and that both cycles were carried out in desorption mode. Thus, it appears that the stiffness of the paint layers may influence the anatomical behaviour of the wooden panel, allowing the hypothesis that the interaction of paint layers with moisture may change both its mechanical properties and behaviours (in uncovered conditions, the painted layers appear to be less stiff).

With the front face waterproofed, WPP5 confirmed the same FW behaviour that was also observed in WPP1 and WPP6 in this hygroscopic cycle. This observation is a clear demonstration that in some cases, the paint layers exhibit an emissivity that does not allow the formation of a significant gradient between the two faces of the panel. By contrast, when the emissivity is artificially increased, the formation of a strong hygroscopic asymmetry leads to FW behaviour, as theoretically expected. On the other hand, WPP3 and WPP4 maintained the same nonflying wood behaviour observed in the non-waterproofed tests, even when hygroscopic asymmetry was induced. In WPP 4, the thick gesso layer and the thick oil pigments almost completely insulated moisture diffusion, and the paint layer behaved in almost the same manner in both free and waterproofed conditions.

The quantitative aspects of the abovementioned observations are reported in Table , where for each WPP, the maximum deflection (δ_{\max}), the time that occurred to reach it and the time to reach equilibrium are presented.

Table 6 Quantitative deformational behaviours of the no-waterproofed WPPs studied. It should be noted that the time to reach the deflection and the time to reach the equilibrium are the same for all the WPPs, except for WPP5 which is the only one to show the FW behaviour.

	δ_{\max} [mm]	Time to reach δ_{\max} [days]	Time to reach equilibrium [days]
WPP1	-0.074 ± 0.003	8	8
WPP2	-0.030 ± 0.003	9	9
WPP3	-0.087 ± 0.003	9.5	9.5
WPP4	-0.209 ± 0.003	6	6
WPP5	-0.094 ± 0.003	3.5	6.5
WPP6	-0.067 ± 0.003	5.5	5.5

3.2 Sensitivity Study on the six studied panel paintings

The influence and the mutual interactions of the variables assumed to be the most important on the deformation behaviour of WPPs can be better understood through the sensitivity analysis carried out by numerical modelling (see Section 2.3). The main results of this study are presented in Figure 5.

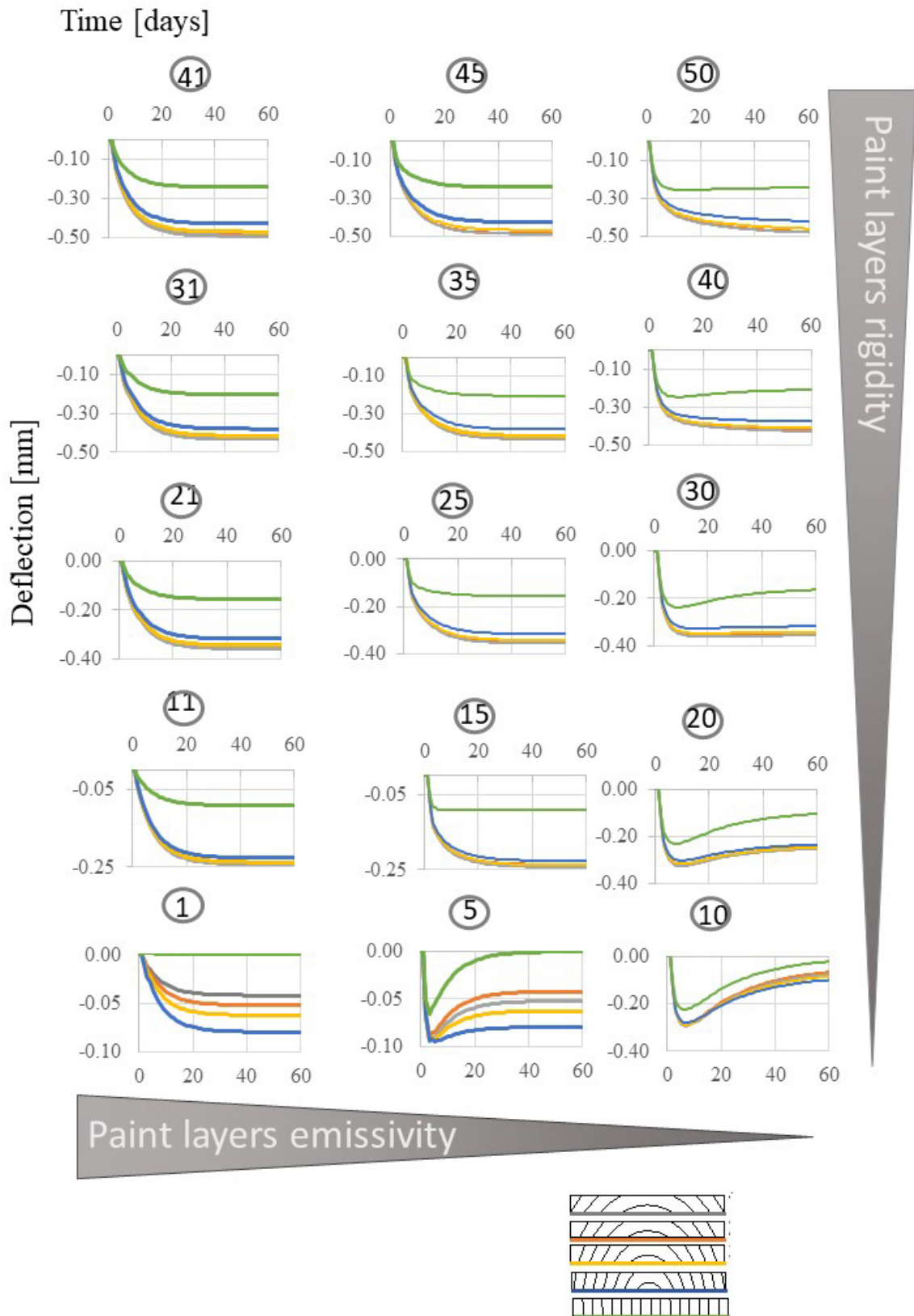


Figure 5 Results from the sensitivity study. The numbers represent the model ID of the analyses of Table 5; for simplicity, 15 cases among 50 were chosen, and the deflection [mm] versus time [days] is shown in the graphs, when a hypothetical decrease in RH corresponding to a 1% moisture content occurs. The graphs are sorted according to both paint layer rigidity (mainly of the ground layers) and emissivity. The latter increases from right to left, while the rigidity increases from bottom to top according to the values in Table 5. Case 10 represents the lowest rigidity and the lowest emissivity, while

case 41 represents the highest rigidity and the highest emissivity. Moreover, case 1 represents the greatest paint layer emissivity and lowest paint layer rigidity; by contrast, case 50 represents the lowest emissivity and the greatest rigidity. The lower part of the figure shows the geometric reference model for each type of board that was associated with a different colour for each anatomical orientation. The values of the ordinates are proportional to the estimated deformation values to allow a better understanding of the deformation behaviour.

Here, each diagram represents a hygro-mechanical transient simulation in terms of maximum deflection (δ_{\max}) for boards 1-5 (Figure 2). Boards 6-9 were omitted from this study because they are a very rare occurrence in WWPs. Each single row of Figure 5 can be interpreted as the effect produced on the deformational behaviour by the progressive reduction in the emissivity of the paint layers (i.e., cases 1 and 5 will degenerate into 10, cases 11 and 15 into 20 and so on). The column relative to the lowest emissivity can be considered to be a direct estimate of the stiffness of the paint layers; notably, the waterproofed panel paintings with stiff layers will not show flying wood, unlike panel paintings with less stiff layers.

Note that some of the situations represented in Figure 5 are well described in wood science:

1. Graph 1 is simply the case of boards desorbing equally from both sides with unstiffened surfaces (hygroscopic and mechanical symmetry);
2. Graph 10 shows the case of a board free to exchange moisture on one side only, and the opposite face is completely waterproofed (maximum hygroscopic asymmetry);
3. Graph 41 shows the case of boards free to exchange moisture on both sides and strongly stiffened on one face only (maximum mechanical asymmetry).

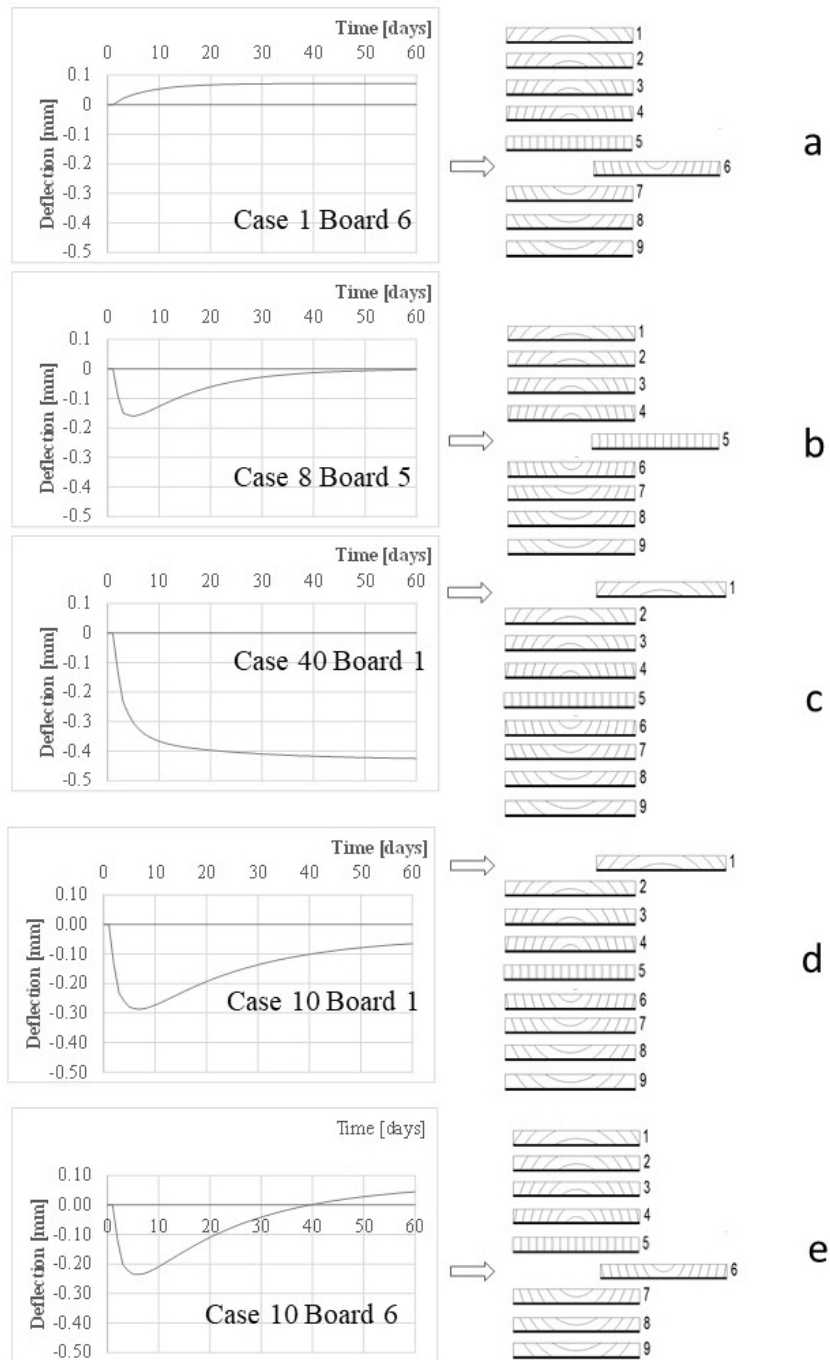


Figure 6 The macrocategories of the deformation behaviour of the WPPs.

The models provide evidence for the presence of five macrocategories, as shown in Figure 6, characterised by

- a. Non-Flying wood behaviour with an asymptotic concave deformation relative to the painted face, typical of WPPs 'painted backwards' and with paint layers with low stiffness;
- b. Flying wood behaviour without residual concavity relative to WPPs painted on a radial board with low-to-high stiffness of the paint layers;

- c. Non-Flying wood behaviour with convex asymptotic deformation relative to the painted face, typical of WPPs painted on a tangential board with high stiffness and low emissivity;
- d. Flying-wood-type behaviour with a concave asymptotic deformation relative to the painting face, typical of WPPs 'painted backwards' on a tangential board with low emissivity and stiffness of the paint layers;
- e. Flying wood-type behaviour with convex asymptotic deformation relative to the painting face, typical of WPPs painted on a tangential board with low emissivity and stiffness.

Cases c and d represent the actual effect of the stiffness of the paint layer in a radial board that are cases where the anatomical component of the deformation tendency is absent.

It is observed that the FW and non-FW behaviours can be associated to the extreme (low and high) values of both stiffness and emissivity but also that they can coexist with the same stiffness and emissivity of the paint layers but with hypothetical different anatomical cutting of the boards (e.g., cases 30, 40, and 50 in Figure 5 and Figure 7). This suggests that the three parameters, namely emissivity, stiffness, and anatomy of the wooden board, either acting by themselves or coupled with each other, identify a conceptual domain of panel deformation, within which the actual deformation behaviour of a specific panel painting may occur.

Despite the simplifications introduced in the model, the deformation modes derived from the model application demonstrate a variability and a high degree of complexity of the phenomenon studied to strongly question whether it is truly possible to determine a priori the deformation tendencies of an individual WPP in the absence of a specific characterisation.

Aggregating all of the patterns of Figure 7, it is possible to determine the existence domain of deformation of a WPP when wood species and panel thickness are given (Figure 8).

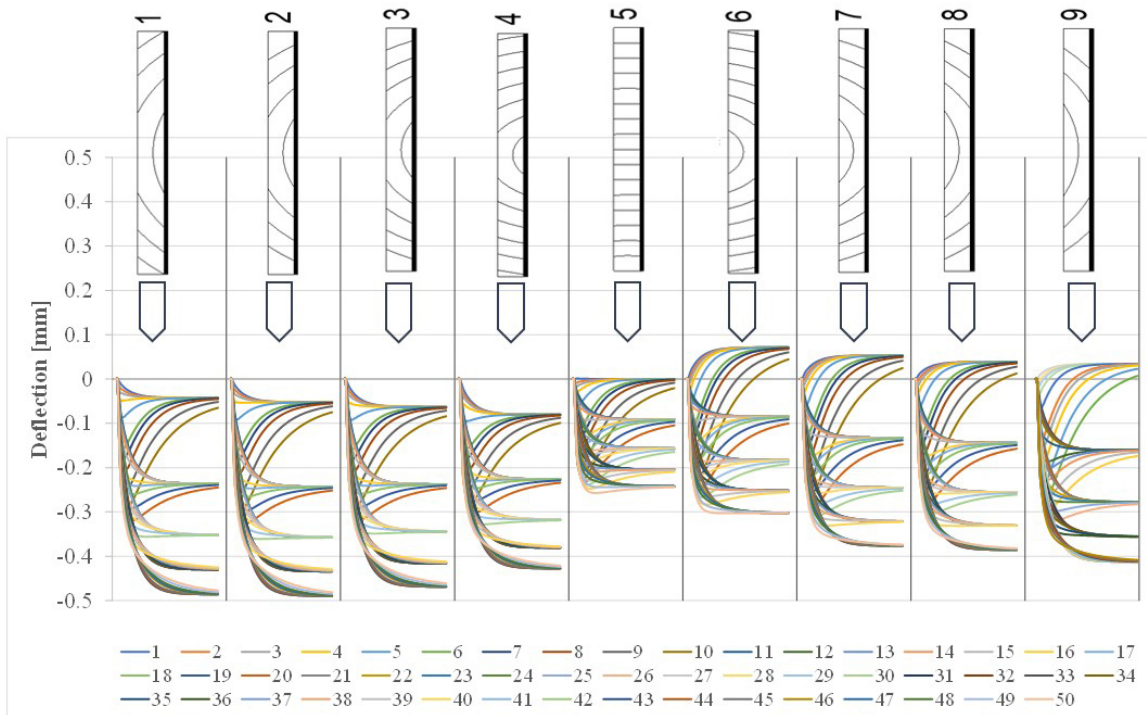


Figure 7 Deformation tendency of wooden panel paintings examined by anatomical cut, depending on paint layer emissivity and ground layer rigidity. Each family of curves represents the 50 calculated models (Table 5) for each different cut of the table: this shows the enormous variability of values that can occur both within the same table and between different tables. It is emphasised that within the same table, variations in the stiffness of the paint layers and their emissivity alone can reduce the deformation tendency by up to an order of magnitude.

Although the simulation reported in Figure 8 represents a simplified condition with a constant board thickness of 30 mm, it suggests that the effect of the three variables considered and their reciprocal interactions can produce a hypothetical field of variation, here labelled the 'existence domain', that is highly articulated and has been confirmed by the experimental observations. This consideration introduces the possibility of considering the WPPs as a complex system that shows evolutionary — materials modification with time — and nonlinear behaviours.

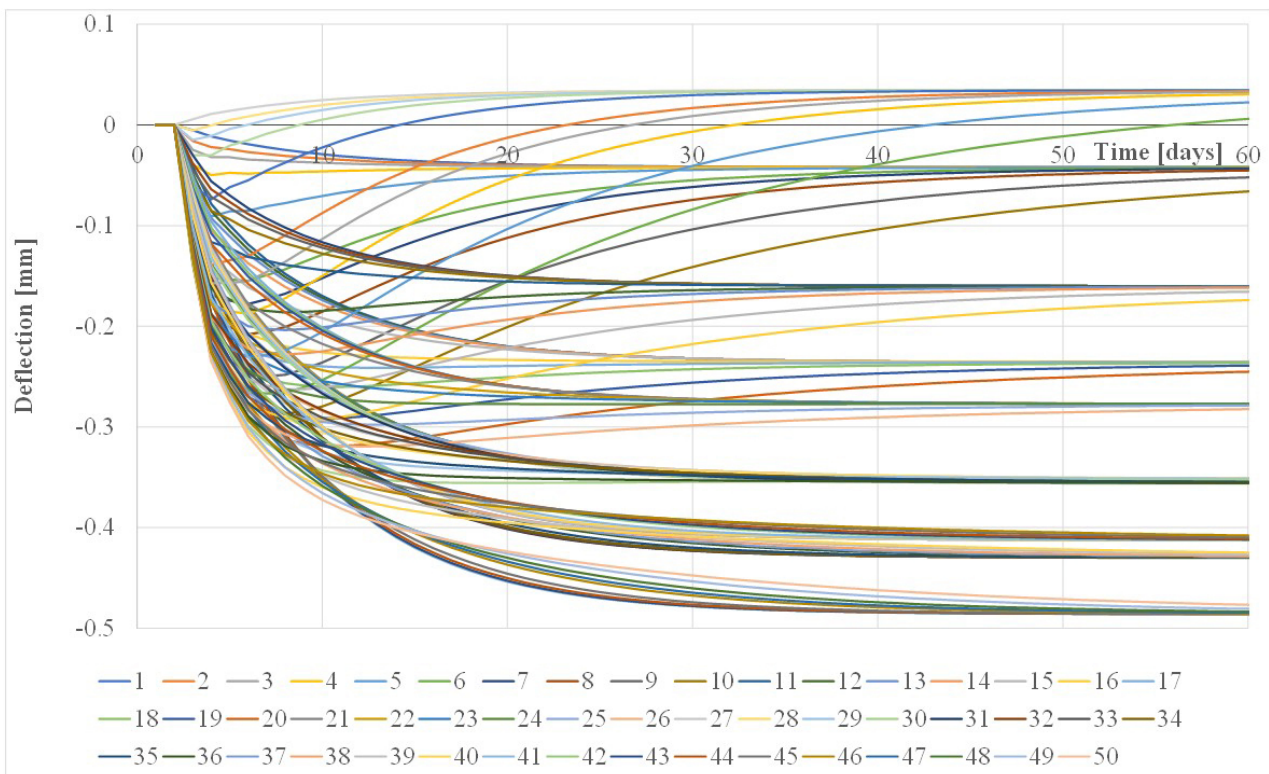


Figure 8 The existence domain of the deformation of a WPP with a thickness of 30 mm and properties reported in Table 4, according to variations in the anatomical cutting of the board, the paint layer emissivity and the ground layer rigidity.

4. Discussion

The analysis performed directly on the experimental data (Figure 4), leads to the following observations:

- Most of the WPPs studied under normal conditions, without waterproofing foils, show nonflying wood behaviour, and only WPP5 shows FW behaviour in every test condition. This suggests that the combination of the main considered variables (i.e., emissivity and stiffness of paint layers) does not produce the same deformation behaviours even among panel paintings with similar constructive typologies (see WPP5, WPP6) and anatomical cuts (all paintings studied are assimilable to the cutting typology number 4 of Figure 2).

- Each painting behaves differently if tested with the painted surface free to exchange humidity with the environment or in waterproofed condition. This indicates a nonnegligible moisture transfer through the ground and the paint layers that plays a significant role as a driver of deformation for the wooden support.

- The face waterproofing led some paintings to assume FW behaviour, which does not occur under normal conditions. In the performed tests, all of the variables remained the same except for the induced hygroscopic asymmetry (only the back was allowed to exchange humidity), and it can be deduced that the internal moisture gradient has a critical influence on panel behaviour. As stated in [24], the rigidity of the ground layers can cause a lack of FW behaviour. However, the presented numerical modelling and experimental results clearly demonstrate the necessity to couple the rigidity and the emissivity of the paint layers. Based on the experimental results produced in the present work, the generalised stiffness of the preparation (intended as the stiffness of the material and its thickness) and its water vapour emissivity appear to be two strongly coupled and interdependent variables in determining the actual deformation tendencies in a specific WPP.

- A third ancillary observation is that all paintings, chosen a priori by conservators as representative of different historical typologies, behave differently in terms of deformation tendencies, either with a free-to-exchange front or with its total insulation.

The experimental observation allowed us to establish three main families of behaviour:

1. Panel paintings that do not present flying wood in both configurations (WPP3, WPP4);
2. Panel paintings that do not have FW behaviour under normal conditions but do show FW behaviour with the waterproofing of the painted face (WPP1 and WPP6);
3. Panel paintings with flying wood in both configurations (WPP5).

Overlapping the results of the sensitivity study with those obtained from experimental observations for real cases allows us to collocate the studied paintings within the existence domain identified by the modelling.

In Figure 9, a correlation between the WPP behaviours and the diagrams Figure 4 is shown. The approximate location of each painting and its deformation state transition due to the waterproofing of the paint surface are shown on a paint layer rigidity/emissivity diagram.

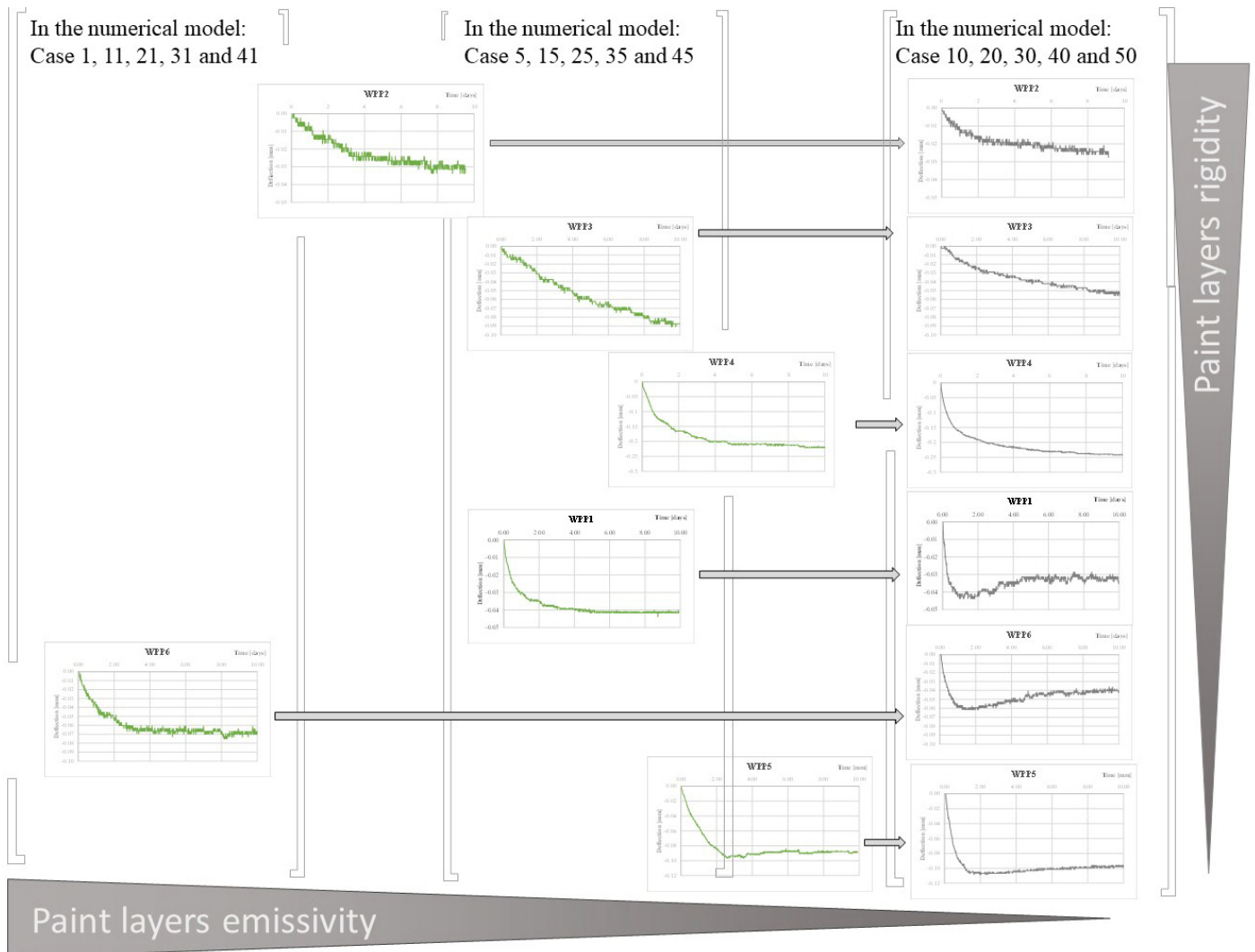


Figure 9 Experimental results are qualitatively placed in a graph similar to Fig. 5. The waterproofing of the paint layers allows us to reduce the problem of their emissivity variable and leads us to identify its level of stiffness and its deformation consequences. This is realised in the row of diagrams in the last column on the right. The location of the WPPs is approximate.

As a result, the three previously identified families can be related to decreasing values of the stiffness of the paint layers relative to the stiffness of the wooden support.

In Figure 9, it is clearly observed that the application of the aluminium foil makes the paintings comparable in terms of their general deformation mode, bringing them into the vertical zero-emissivity zone on the right part of the diagram. Thus, overall, 3 panel paintings express a low stiffness of the paint layers, and the other 3 show a pronounced stiffness to prevent flying wood due to the strongest possible asymmetry of the internal moisture gradient. The deformation mode of WPP 4 is dominated by the stiffness of the ground layer, while in WPPs 1 and 6, the low stiffness of the paint layers makes the emissivity of the ground layer the dominant driver of the deformation tendency. Finally, experiments show that the case of WPP 5 represents the limiting case of low emissivity and low stiffness of the paint layers.

5. Conclusions

The present experimentally examined WPPs matched with comparative results obtained by numerical modelling and applied to understand and characterise their deformation behaviour.

Experimental analysis of a significant sample of WPPs subjected to environmental hygrometric variations revealed the complexity of these objects and a high level of variability in terms of materials and deformation behaviours.

Once the species and thickness of the wood panel were established, three variables were identified as determining factors: the emissivity and stiffness of the paint layers and the cut of the panel in relation to the pith of the tree (anatomy). Each of these factors independently can determine not only the extent of maximum deformation of the paintings but also the deformation behaviour. Therefore, the obtained results suggest that in the presence of hygroscopic variations, these factors are strongly coupled in determining the WPP deformation.

Moreover, the waterproofing of the paint layers demonstrated that (i) the front layers show a nonnegligible flow of humidity; (ii) it is possible to evaluate the deformative effect of the stiffness of the paint layers (iii) as well as the actual effect of the emissivity of paint layers on the global deformation behaviour of the panel; and (iv) it is possible to identify deformation families. For conservation, the deformation tendency of the panel determines the choice and sizing of any restraining system, such as crossbeams and frames, and, together with reactivity, the design of any climatic control system. Its nature as a complex system, as appears from this study, underlines the necessity to consider every panel as unique object, the state of which needs to be characterised prior to the implementation of any conservation treatment or preventive conservation and climate control plan. Each WPP is also a complex and unique system affected by nonlinear state-dependent behaviour. Each of the parameters characterising these artworks (layers hygroscopicity, mechanical stiffness, anatomical cutting, and conservation environments) constitute a set of interconnected and interacting physical subsystems, whose temporal evolution (the rules by which they evolve over time), which is not random, is highly dependent on knowledge of the initial conditions, boundary conditions and inner structural mechanics characterisation. Since a small difference in these conditions can lead to very different characteristics and behaviour of the system, as any other state-dependent nonlinear system, WPP may not be predictable even if the variables and equations governing them are known. Therefore, for this artefacts, deterministic models based on the use of generic material characteristics and/or on the results of accelerated ageing cycles could yield very modest, if not misleading, results in the interpretation of the behaviour of systems and particularly in the prediction of the evolutionary behaviour of individual works. Similar to other complex systems, in the case of WPP, behaviour cannot be predicted but only measured. By contrast, if all material properties and boundary conditions are specifically determined through direct experimentation on real works of art — as in the methodology introduced in this work — then results of the numerical simulations can be accurate and correspond to the actual behaviour of the works. In any case, numerical simulations are useful for classifying real objects and explaining observed phenomena; this means that numerical methods should be used to extend the knowledge provided by experimental results.

Declarations

List of abbreviations: not applicable

Availability of data and materials: the datasets generated and analysed during the current study are available from the corresponding author on reasonable request.

Competing interests: absence of any conflict of interest.

Funding: PREMUDE Project - Tuscany Region – POR-FSE 2014 – 2020
Modelli innovativi per la conservazione PREventiva in ambienti MUseali e DEpositi temporanei post-emergenza

Authors' Contributions:

L.Riparbelli designed the tests, discussed the results, developed and discussed the numerical model, analysed and discussed the physics of the panel paintings, wrote and revised the paper.

P.M. designed the tests, processed and discussed the experimental data, participated in discussing the model results, wrote and revised the paper.

C.M. processed the data, prepared table 1-3 and 6 and figure 1, revised the paper.

L. U. designed the tests and revised the paper.

G.G. observed and described the six panel paintings.

L. Ricciardi, S.R., A. S. and C. C. chose and provide the six historical panel paintings, participated in designing the tests and revised the paper.

M.F. participated in designing the tests, discussed the experimental data and the numerical model results, wrote and revised the paper, coordinator of the project.

Acknowledgements: not applicable

References

- [1] Buck RD. Some applications of mechanics to the treatment of panel paintings, in *Recent Advances in Conservation*, International Institute for the Conservation of Historic and Artistic Works (IIC), London: G. Thomson, 1963, pp. 156–162.
- [2] Buck RD. Some applications of rheology to the treatment of panel paintings, *Studies in Conservation*, 17 (1), pp. 1–11, 1972.
- [3] The structural conservation of panel paintings: Proceedings of a Symposium at the J. Paul Getty Museum 24-28 April 1995. Dardes K. and Rothe A. (Eds.). The Getty Conservation Institute, US 1998. ISBN 0-89236-384-3.
- [4] Facing the challenges of panel paintings conservation: trends, treatments, ad trainings. Proceedings of the symposium 17-18 May 2009. Phenix A. and Chui SA. (Eds). The Getty Conservation Institute, US 2011. ISBN 978-0-9834922-2.1.
- [5] Wood science for conservation COST Action IE0601. Gril J. (Ed). Supplement of *Journal of Cultural Heritage*. 13 (3S), 2012, doi: <https://doi.org/10.1016/j.culher.2012.06.001>.
- [6] Uzielli L. Historical overview of panel-making techniques in central Italy, in *Proceedings of a Symposium at the J. Paul Getty Museum 24-28 April 1995*, The Getty Conservation Institute, US1998, pp. 110–135.
- [7] Wadum J. Historical overview of panel-making techniques in northern countries, in *Proceedings of a Symposium at the J. Paul Getty Museum 24-28 April 1995*, The Getty Conservation Institute, US 1998, pp. 149–177.
- [8] Structural conservation of Panel paintings at the Opificio delle Pietre Dure in Florence: method, theory, and practice. Ciatti M. and Frosinini C. (Eds). Edifir, 2016. ISBN 978-88-7970-792-3.
- [9] C. Cennini, *Il libro dell'arte*, Neri Pozza. Frezzato F., 2009. "*The art book*" in *Italian*.
- [10] Federspiel B. Questions about Medieval Gesso Grounds, in *Historical painting techniques, materials, and studio practice: Preprints of a Symposium*, University of Leiden, the Netherlands, 26-29 June 1995, The Getty Conservation Institute, US 1995, pp. 58–64.
- [11] Martin E., Sonoda N., Duval A. Contribution a l'etude des preparations blanches des tableaux italiens sur bois, *Studies in Conservation*, 37(2), pp. 82–92, 1992, doi: <https://doi.org/10.2307/1506400>.
- [12] Siau J.F., Avramidis S. The surface emission coefficient of wood, *Wood and Fiber Science*, 28 (2), pp. 178–185, 1996.
- [13] Cremonesi P. Le vernici finali per i dipinti, *Progetto Restauro*, 29, pp. 16–28, 2005. "*The varnishes for panel paintings*" in *Italian*.
- [14] Mecklenburg M., Tumosa C., Erhardt D. Structural response of painted wood surfaces to changes in ambient relative humidity, in *Painted Wood: History and Conservation*, The Getty Conservation Institute, US 1998, pp. 464–483.
- [15] Allegretti O., Raffaelli F. Barrier effect to water vapour of early European painting materials on wood panels, *Studies in Conservation*, 53 (3), pp. 187-197, 2008, doi: [10.1179/sic.2008.53.3.187](https://doi.org/10.1179/sic.2008.53.3.187).
- [16] De Backer L., Laverge J., Janssens A., de Paepe M. Evaluation of the diffusion coefficient and sorption isotherm of the different layers of early Netherlandish wooden panel paintings, *Wood Science and Technology*, 52 (1), pp. 149–166, 2018.
- [17] Hendrickx R., Desmarais G., Weder M., Ferreira E.S.B., Derome D. Moisture uptake and permeability of canvas paintings and their components, *Journal of Cultural Heritage*, 19, pp. 445–453, 2016, doi: [10.1016/j.culher.2015.12.008](https://doi.org/10.1016/j.culher.2015.12.008).
- [18] Hoadley B. Chemical and physical properties of wood, in *The structural conservation of panel paintings: Proceedings of a Symposium at the J. Paul Getty Museum 24-28 April 1995*, US, 1998, pp. 2–20.

- [19] Wood handbook—Wood as an engineering material. FPL-USDA, 2010. [Online]. https://www.fpl.fs.fed.us/documnts/fplgtr/fpl_gtr190.pdf
- [20] Mazzanti P., Colmars J., Hunt D., Uzielli L. A hygro-mechanical analysis of poplar wood along the tangential direction by restrained swelling test, *Wood Science and Technology*, 48, pp. 673–687, 2014, doi: 10.1007/s00226-014-0633-4.
- [21] Hunt D., Uzielli L., Mazzanti P., Strains in gesso on painted wood panels during humidity changes and cupping, *Journal of Cultural Heritage*, 25, pp. 163–169, 2017, doi: <https://doi.org/10.1016/j.culher.2016.11.002>
- [22] Sassoli M., Characterization of Wood Aging by means of Volatile Organic Compounds (VOCs) Analysis, PhD Thesis, University of Florence, Italy, 2018.
- [23] Esteban L., Gril J., De Palacios P., Casasus A. Reduction of wood hygroscopicity and associated dimensional response by repeated humidity cycles, *Annals of Forest Science*, 62 (3), pp.275-284 2005, doi: 10.1051/forest:2005020.
- [24] Allegretti O., Bontadi J., Dionisi-Vici P. Climate induced deformation of Panel Paintings: experimental observations on interaction between paint layers and thin wooden supports, *International Conference Florence Heri-tech: the Future of Heritage Science and Technologies*, vol. 949, 2020, doi: 10.1088/1757-899X/949/1/012018.
- [25] Brandao A., Perré P. “The Flying Wood” – A quick test to characterise the drying behaviour of tropical woods, 5th iufro W.D.C., Quebec 1996, pp. 315-324.
- [26] Arends T., Pel L., Huinink H.P., Schellen H. L. Dynamic Bending of an Oak Board Due to a Moisture Content Gradient, *Poromechanics 2017 - Proceedings of the 6th Biot Conference on Poromechanics*, 9-13 July 2017, Paris, France, pp. 386-394.
- [27] EN 15757:2010 - Conservation of Cultural Property - Specifications for temperature and relative. <https://standards.iteh.ai/catalog/standards/cen/ad03d50b-22dc-4c57-b198-2321863f3870/en-15757-2010>.
- [28] Uzielli L., Cocchi L., Mazzanti P., Togni M., Julien D, Dionisi-Vici P. The Deformometric Kit: A method and an apparatus for monitoring the deformation of wooden panels, *Journal of Cultural Heritage*, S13: (3) S94–S101, 2012.
- [29] Siau J., Wood: influence of moisture on physical properties, Virginia Polytechnic Institute and State University. 1995.
- [30] Saft S., Kaliske M. Numerical simulation of the ductile failure of mechanically and moisture loaded wooden structures, *Computers&Structures*, 89 (23–24): 2460–2470, 2011, doi: <https://doi.org/10.1016/j.compstruc.2011.06.004>.
- [31] Fortino S., Mirianon F., Toratti T. A 3D moisture-stress FEM analysis for time dependent problems in timber structures, *Mechanics of Time-Dependent Materials*, 13 (4): 333-356, 2009, doi: <https://doi.org/10.1007/s11043-009-9103-z>.
- [32] Marcon B., Mazzanti P., Uzielli L., Cocchi L., Dureisseix D., Gril J. Mechanical study of a support system for cupping control of panel paintings combining crossbars and springs, *Journal of Cultural Heritage*, S13 (3): S109–S117, 2012, doi: 10.1016/j.culher.2012.04.003.
- [33] Marcon B., Goli G., Fioravanti M. Modelling wooden cultural heritage. The need to consider each artefact as unique as illustrated by the Cannone violin, *Heritage Science*, 8 (1): 24, 2020, doi: 10.1186/s40494-020-00368-1.
- [34] Rachwał B., Bratasz Ł., Łukomski M., Kozłowski R. Response of Wood Supports in Panel Paintings Subjected to Changing Climate Conditions, *Strain*, 48 (5): 366–374, 2012, doi: 10.1111/j.1475-1305.2011.00832.x.
- [35] Choong E. Diffusion coefficients of softwoods by steady-state and theoretical methods, *Forest Products Journal*, 15 (1): 21–27, 1965.
- [36] Skaar C. Wood-water relations. Springer-Verlag, 1988.
- [37] Christensen G., Kelsey K. The rate of sorption of water vapor by wood, *Holz Roh Werkst*, 17: 178–188, 1959.

- [38] Christensen G. The rate of sorption of water vapour by wood and pulp, *Appita J.*, 13: 112–123, 1959.
- [39] Engelund-Thybring E., Zelinka S., Glass S. Kinetics of Water Vapor Sorption in Wood Cell Walls: State of the Art and Research Needs, *Forests*, 10 (8): 704, 2019, doi: ; doi:10.3390/f10080704.
- [40] Dureisseix D., Marcon B. A partitioning strategy for the coupled hygromechanical analysis with application to wood structures of cultural heritage, *International journal for numerical methods in engineering*, 88 (3): 228–256, 2011.
- [41] Bodig J., Jayne B.A. *Mechanics of Wood and Wood Composites*. Van Nostrand Reinhold, 1982.
- [42] EDF - Électricité De France, Finite element Code_Aster: Analyse des Structures et Thermo-mécanique pour des Etudes et des Recherches, 2022. *Finite element Code_Aster: Analysis of the Structure and Thermo-mechanics to the Study and Researc, in French*.
- [43] Helfer T., Michel B., Proix J-M., Salvo M., Sercombe J., Casella M. Introducing the open-source mfront code generator: Application to mechanical behaviours and material knowledge management within the PLEIADES fuel element modelling platform, *Computers & Mathematics with Applications*, 70 (5): 994–1023, 2015, doi: <https://doi.org/10.1016/j.camwa.2015.06.027>.
- [44] Mazzanti P., Togni M., Uzielli L. Drying shrinkage and mechanical properties of Poplar wood (*Populus alba L.*) across the grain, *Journal of Cultural Heritage*, S13 (3): S85–S89, 2012.
- [45] Gauvin C. Etude expérimentale et numérique du comportement hygromécanique d'un panneau de bois : application à la conservation des tableaux peints sur bois du patrimoine, PhD Thesis, LMGC - Laboratoire de Mécanique et Génie Civil, Université de Montpellier 2, France, 2015. *Experimental study and numerical modeling of the hygromechanical behaviour of wood applied to the conservation of panel paintings, in French*.
- [46] Dionisi-Vici P., Mazzanti P., Uzielli L. Mechanical response of wooden boards subjected to humidity step variations: climatic chamber measurements and fitted mathematical models, *Journal of Cultural Heritage*, 7 (1): 37–48, 2006.

Modelling of hygro-mechanical deformations of wooden panel paintings: model calibration and artworks characterisation.

Riparbelli Lorenzo¹, Mazzanti Paola¹, Helfer Thomas², Manfriani Chiara¹, Uzielli Luca¹, Castelli Ciro³, Santacesaria Andrea³, Ricciardi Luciano³, Rossi Sandra³, Gril Joseph^{4,5}, Fioravanti Marco¹

1 DAGRI, Università di Firenze, Florence, Italy

2 CEA, DES, IRESNE, DEC, Cadarache F-13108 Saint-Paul-Lez-Durance, France

3 Opificio delle Pietre Dure, Florence, Italy

4 Université Clermont Auvergne, INRAE, PIAF, Clermont-Ferrand, France

5 Université Clermont Auvergne, CNRS, Institut Pascal, Clermont-Ferrand, France

Corresponding author: Paola Mazzanti, paola.mazzanti@unifi.it

Abstract

Wooden Panel Paintings (WPP) are among the most significant historical and artistic artifacts from the Middle Ages and Renaissance and pose a challenge to conservators and scientists in both their comprehension and conservation. From a structural point of view, they can be considered as multi-layered objects, consisting of a wooden support and several pictorial layers. The wooden support, hygroscopic in nature, constantly seeks equilibrium with the humidity of the environment, and consequently deforms. Based on a series of hygroscopic tests carried out on six original WPP, the present work aims to model their deformation tendencies induced by moisture changes and to characterise them by means of an inverse identification process. The sensitivity analysis of this study provided valuable insights into the complexity of the phenomenon of WPP deformation: even small variations in input variables (board anatomy, stiffness and emissivity of pictorial layers) led to significant changes in the deformation trend over time, highlighting the high variability of the physical problem under investigation. Sobol's analysis variance confirmed this complexity, demonstrating the different levels of influence of input variables and the existence of interactions between them. Overall, the results of this analysis highlighted the need to carefully evaluate the interactions and uncertainties in input variables to fully understand the complexity of the system. The iterative optimization process led to numerical results tending to agree with experimental data, with most results showing a very high correlation. This suggests that the chosen variables and modelling assumptions sufficiently described the physical system and that numerical models can be accurately calibrated. The proposed concept of 'learning from objects', by conducting experimental investigations specifically dedicated to understanding the deformation tendencies of the artwork, is essential. In this approach, numerical analysis is used in conjunction with experiments to gain a deeper understanding of the artwork, characterise it and extract valuable information.

Keywords: Wooden Panel Paintings, conservation, experimental tests, numerical modelling, panel painting deformation tendencies, paint layer emissivity, paint layer stiffness.

1. Introduction

Wooden Panel Paintings (WPPs) represent one of the most important categories of cultural artefacts, whose conservation is challenging due to their interaction with environments. Although the early treatises [1] attempt to codify both structure and construction techniques, WPPs, while maintaining common denominators over time, may differ from case to case according to different schools and workshops [2,3], resulting in a wide panorama of morphological, constructional and manufacturing diversities, which is combined with the intrinsic variability of wood. This structure, together with its interaction with the environment, can lead to the appearance of mechanical stresses that can be critical for the conservation of a WPP, being at the origin of permanent deformations, cracks, or damages to paint layers. Each artwork shows its own deformation behaviour that may be explained through generative causes such as:

1. Wood hygroscopicity: wood being a hygroscopic and anisotropic material, environmental hygrothermal fluctuations can produce permanent deformations, induced by the combined effect of wood anisotropy with respect to the board cut, transient deformation induced internal humidity gradients, and the compression set phenomenon (i.e. the permanent deformation deriving from the succession of environmental fluctuations over time[4]).
2. Mechanical asymmetry: stiffness asymmetry within the thickness may be due to differences between the wood and paint layers, to the wood itself as it presents a non-homogeneous stiffness following growth rings and main anatomical directions, and to the interaction with any restraining system such as frames and crossbeams. Moreover, the shrinking-swelling behaviour of wood is orders of magnitude bigger than that of the paint layers [5].
3. Ageing: over time biological, physical, and chemical agents may cause permanent modification (ageing phenomena) that can affect the behaviour of wood, of paint layers, of glues and of their mutual interactions.
4. Anthropic: past human interventions such as restoration, size adjustments, accidents and tampering, exposure to sudden winter heating, etc.

Each of these aspects has been the object of several specific research works. Studies and monitoring of original works have been carried out in the past [6-8] including using optical measurement methods to correlate deformation fields with the mechanical characteristics of the paint layers [9]. Materials used to make the WPPs were object of characterisation by [5,10, 11] for the wooden support, as well as [12] for the stiffness and [13-15] for the emissivity characteristics of the painted layers. Most parts of this latter studies were carried out on new materials, because sampling on original components of WPPs is impossible, producing a limited representativity of the behaviour of real materials subjected to centuries of ageing and interacting each other inside the structure, as a recent research shows [16]. Such paper shows that the main parameters responsible of the hygro-mechanical behaviour of the WPPS are the tree ring orientation of the wooden panels, the stiffness of the ground layers and the emissivity of the varnishes (and their interactions). Within the same research, a classificatory model was developed which shows that the hygro-mechanical behaviour of the WPPs is complex and hardly predictable if the characteristics of the material making the WPP are considered independent. It is their interaction, indeed, which strongly affects the hygro-mechanical behaviour of the WPP.

Models of the dynamics of panel paintings have been also developed [17,18], sometime considering a painting with a complex structure subject to environmental variations [19]. To these studies shall also be added those on wood-moisture interaction [20], on cracking phenomena of paint layers [21], on the response of painted panels to humidity variation [22], and finally one on the analysis of the effect of relative humidity cycles [23]. Some studies were also carried out on replicas and simulacra [21, 24-26].

Numerical studies mainly use literature values to define hygro-mechanical characteristics, opening up the risk of reaching unrealistic solutions [27]. In fact, key variables such as anatomical directions, stiffness and emissivity of the paint layers can generate a wide field of deformation patterns both qualitatively and quantitatively, as it has been demonstrated by numerical modelling and monitoring of original artworks [16]. This approach is certainly the most applied in literature, and operates with a logic where the behaviour of a WPP results from the linear additive contribution of each singular component of the system.

The present work takes a different methodological perspective, considering the WPP as a complex system, where initial conditions, time history and evolution are unknown. This implies that small variations of individual variables, and even more so the variations of these variables in relation to the values of others [16], cannot be predicted through studies conducted on artificial samples, copies, materials that have not been aged or subjected to artificial ageing cycles. The resulting top-down approach starts from the awareness that the behaviour of complex systems can often only be measured and needs to be addressed through a direct experimentation logic, without aprioristic considerations on aspect that cannot be directly measured and observed. It is based on known hygro-mechanical models and aims to calibrate their characteristics through non-destructive experimental tests conducted on individual artworks. This approach consists in not worrying aprioristically about the structural composition, but representing all the physical entities with characteristics that, in their interaction, provide us with a model that behaves similarly to an original when subjected to experimental characterisation tests. In this interpretation, after an established theoretical approach and sound physical-mathematical methods have been set up, the numerical analyses become a way of extracting advanced information from experimental evidence that does not provides it directly.

The aim of the present study is to broaden the current spectrum of knowledge of the main deformation drivers of real WPPs from an experiment on six original paintings subjected to micro changes in humidity, and to draw analytical conclusions.

The research builds on a previous work [16] that was carried out by means of experimental tests on 6 original WPPs subjected to slight variations in humidity inside a climatic chamber and the measurement of the resulting deflection. The cycles were repeated after applying an aluminium foil to waterproof the painted face of the panel paintings, in a way that does not affect the rigidity of the painted layers. This allowed the stiffness and emissivity characteristics of the original paintings to be qualitatively determined by non-invasive experimental tests.

In continuation of this work, the present research proposes to determine, in a non-invasive manner, the hygro-mechanical characteristics of the six original WPPs studied and to calibrate their respective numerical models. The work presents a reproducible method, based on a finite element calculation, for the direct characterisation of a WPP by means of an experimental test in which the work is subjected to a slight change in humidity [16].

2. Materials and methods

2.1 The panel paintings and experimental set up

The study was carried out on six original WPPs of the Italian painting school. Each one is made of poplar wood (*Populus* sp) and was selected based on its representativeness in terms of construction period, structural typology, thickness of the preparatory layers, presence or absence of canvas. Their main technical specifications are given in Table 1 and in [16].

Table 1 Description of the six paintings: dimensions, materials and characteristics. R board: quartersawn board, cut along a radius of the stem; T board: flatsawn board, cut orthogonally to a radius of the stem, at a certain distance from the pith estimated on a face [16].

	WPP1	WPP2	WPP3	WPP4	WPP5	WPP6
Dimensions	530x900x14 mm	67x1310x33 mm	700x1370x25 mm	645x775x23 mm	655x855x30 mm	650x890x28 mm
Wood Species	<i>Populus alba</i> L.	<i>Populus alba</i> L.	<i>Populus alba</i> L.	<i>Populus alba</i> L.	<i>Populus alba</i> L.	<i>Populus alba</i> L.
Boards	2 T boards (~40 mm from pith), 275 and 255mm wide	3 R boards 170, 380 and 145 mm wide.	4 boards; 1 T (~50 mm from pith) 185 mm wide; 3 R 165, 130 and 220mm wide	2 T boards (~20 mm from pith), 210 and 435 mm wide	2 T boards (~50 mm from pith), 210 and 435 mm wide	3 boards; 1R 225 mm wide; 2 T (~60 mm from pith), 320 and 105 mm wide
Ground layer	thick	thick	thick	thick	thin	thin

Each panel was equipped with a Deformometric Kit (DK), as described in section 2.2, and subjected to controlled variations of relative humidity (RH) to measure its hygroscopic deformation. The restraint system was removed to allow only hygroscopic deformation without influence of the crossbeams. A special climatic box was built in the Opificio delle Pietre Dure restoration laboratories; the RH was controlled by means of a humidifier (Preservatech miniOne) and ventilation was provided by means of 6 fans and the usual operation of the humidifier itself. RH and temperature (T) were monitored in real time using URT Smart CEAM LoRa-C ($\pm 2\%$ e ± 0.5 °C), 1 point every 15 minutes. The data were continuously collected by means of CEAM CWS software, an integrated platform for monitoring, control and shared management based on web-cloud-IoT technology. The panel paintings were arranged in the climatic box in a vertical position, and the contact area was covered with PTFE to eliminate friction. Inside the box, the RH values varied between 50% and 65%, such interval was determined according to the historical climate approach as determined by EN 15757 [28]. Seven humidity cycles were performed: 3 desorption and 4 adsorption tests. The hygroscopic tests were carried out under two different boundary conditions: a) the front face free to exchange moisture with the environment (2 in desorption and 3 in adsorption) and b) the front face sealed by an aluminium foil (1 in desorption and 1 in adsorption). This method makes it possible to measure the actual emissivity of the front surface, i.e. the paint layers and varnish, and its effect on the deformation behaviour of the artworks. Details are given in [16].

2.2 The measure of the cupping angle

The Deformometric Kit (DK, [29]) is a measuring device conceived for monitoring the deformation dynamics of wooden objects, mainly in relation to fluctuations of the surrounding environmental conditions; it has been used in many study campaigns, mainly on WPPs [7, 30-33].

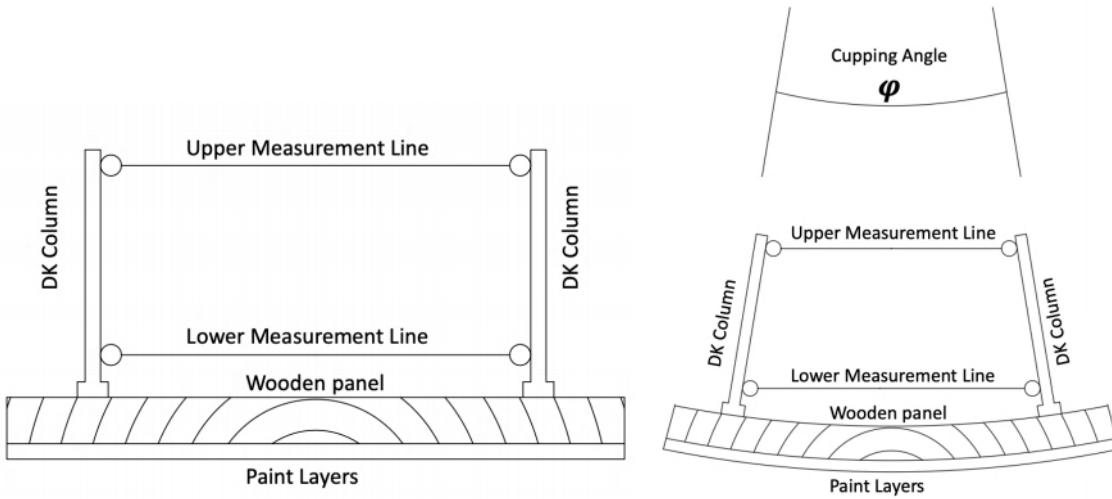


Figure 1 - On the right the general set up of DK on a wood board of a WPP, on the right the physical meaning of the cupping angle and its measurement with the DK

Since the objective of this study is the calibration of a model, we considered parameters that were not subject to any assumptions, but only to direct measurement: the deformation, or equivalently the change in length, of the measurement lines, and the derived cupping angle. These measurements are agnostic to both the physical phenomenon that generated the variation in relative inclination between the two sections and the characteristics of the material that lies between the two columns. Therefore, the deformations of both measurement lines were chosen as parameters for calibrating the numerical models.

Furthermore, this parameter has a clear, well-known and understandable physical meaning in the field of WPP conservation.

Optimisation procedures (described below in section 2.4) require that the correct experimental value can be determined at any given time, so the raw data were treated according to [34]. An interpolation procedure was applied to all data, locally fitted to a second order polynomial curve using a Gaussian kernel to weight the data. The standard deviation used for the kernel (50000 s) represents the window in which the polynomial interpolation is performed.

2.3 Numerical Modelling

For the objectives of this study, the role of the numerical model is to serve as a means of interpreting and enhancing comprehension of the experimental findings, and to reveal the interdependent relationships among the variables that influence the behaviour of the underlying physical model. In this respect, numerical modelling has been used to evaluate, through an optimization algorithm, the influence and the mutual interactions of the identified dimensioning variables (layers stiffness, moisture diffusion and emissivity, anatomical cut) in determining the deformation tendency of the painted board.

For general modelling principles we refer to [16], listing below only those elements in which this modelling differs.

We applied the following boundary condition to model the global emissivity of the rear, bare wood, face:

$$\frac{q_t}{\rho_0} = E_{c1} \cdot (m_{r,air} - m_{r,sur}) \quad (5)$$

where $m_{r,air}$ is the wood equilibrium moisture content corresponding to the air humidity, $m_{r,sur}$ is the moisture content of the rear wood surface calculated by the solver, and E_{e1} is the global effective emissivity of the back of the painting, taking into account also possible aging effects and protective treatments that may affect the emissivity of this surface.

The geometry and discretisation were carried out with the open-source software Salome-Meca developed by EDF (Électricité de France), the simulations with the open-source solver code_aster [40], and the handling of cylindrical coordinates in the solution of the computational model, both for elasticity and swelling, with the open-source software Mfront [41], see Annex 1.

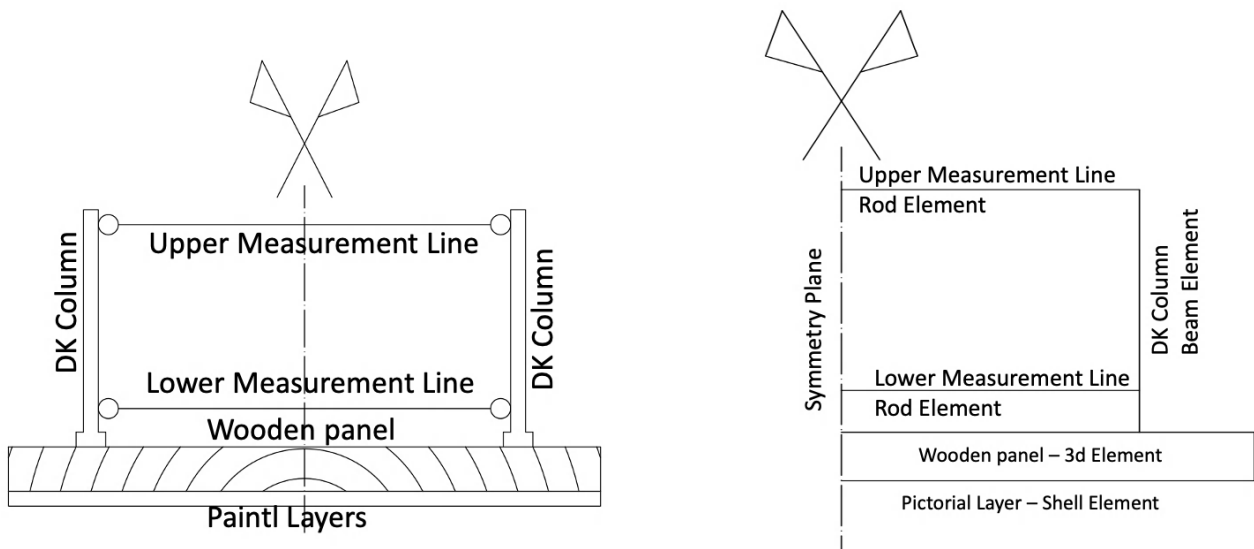


Figure 2 - Scheme of the modelling: on the left the real case, on the right the optimization simplified case with the optimization choices in terms of finite elements

As both the optimization process and the sensitivity study are computationally intensive, it was essential to reduce the degrees of freedom of the system as much as possible. The following assumptions were made in the modelling:

- The length parallel to the grain of the wood panels was reduced to 400mm (a preliminary feasibility study showed that mechanical edge effects lose their influence at a distance of about 150mm from the longitudinal ends in a WPP without crossbeam).
- In the transversal direction, considering that the DKs were mounted in the exact centre of symmetrical panels, only half a panel was modelled with symmetry constraints and isostatic condition.
- The edge effect between adjacent boards is considered negligible considering that they are glued at the edge, the preservation of plane sections, the absence of stiffeners or cross beams and the freedom to deform given the external isostatic constraints (verified in the preliminary feasibility study).
- The thickness of the panel was sliced into 30 layers to capture small local variations due to the internal moisture gradient.
- The panel equipped with the DK is not subjected to external forces; it deforms only as a result of internal hygroscopic interactions.

The output parameters are the deformations of the two measurement lines and, derived from them, the cupping angle, defined as the angular rotation of the section below the DK column. This ensures the biunivocality of the boundary conditions between the numerical model and the experimental data. A similar method for comparing experimental results and numerical models is described in [16].

2.4 Computation of the equilibrium moisture content

The calculation of the equilibrium moisture content (EMC) is required to attribute the correct hygro-mechanical boundary conditions for the moisture. It was made following [42] that permits to calculate and describe the sorption isotherms in wood, with changing temperature and partial cycles. The model is based on [41], that relates relative humidity (RH) to EMC value, noted w , as follows:

$$w = w_{ad}(RH, T) = w_s(T) \cdot [\varphi_{ad} \cdot \ln(RH) \cdot \exp(\alpha_{ad} \cdot RH)] \quad \text{for adsorption} \quad (6)$$

$$w = w_{de}(RH, T) = w_s(T) \cdot [\varphi_{de} \cdot \ln(RH) \cdot \exp(\alpha_{de} \cdot RH)] \quad \text{for desorption} \quad (7)$$

with w_s the EMC value at 100%RH; $w_{ad}(RH, T)$ and $w_{de}(RH, T)$ the adsorption and desorption curve, respectively, for a given temperature T ; α_{ad} , α_{de} , φ_{ad} , φ_{de} constant values. The effect of the temperature, following [43] and based on the work of [44], is concentrated on FSP leading to a general form of $w_s(T)$:

$$w_s(T) = \left(w_s^0 + \frac{C_{anh}}{C_w} \right) \cdot \exp \left(-\frac{C_w}{L} \cdot T \right) - \frac{C_{anh}}{C_w} \quad (8)$$

with w_s^0 the FSP at 0°C , C_{anh} the heat capacity of the oven dry material, C_w the heat capacity for the bound water, L the latent heat of state change.

For the calculation of the EMC evolution from a given condition given by w_0 and RH_0 , the situations of adsorption and desorption are distinguished:

$$\left(\frac{dw}{dRH} \right)_{ads} = \frac{A \cdot (w_0 - w_{ad})^C \cdot w'_{de}(w_0) + (w_{de} - w_0)^C \cdot w'_{ad}(w_0)}{(w_{de} - w_{ad})^C} \quad \text{with} \quad \left(\frac{dw}{dRH} \right)_{ads} > 0 \quad (\text{adsorption}) \quad (9)$$

$$\left(\frac{dw}{dRH} \right)_{des} = \frac{(w_0 - w_{ad})^C \cdot w'_{de}(w_0) + B \cdot (w_{de} - w_0)^C \cdot w'_{ad}(w_0)}{(w_{de} - w_{ad})^C} \quad \text{with} \quad \left(\frac{dw}{dRH} \right)_{des} < 0 \quad (\text{desorption}) \quad (10)$$

where the constants A and B define the slope ratio for a path toward the absorption or the desorption isotherm, respectively, and C is a calibration coefficient.

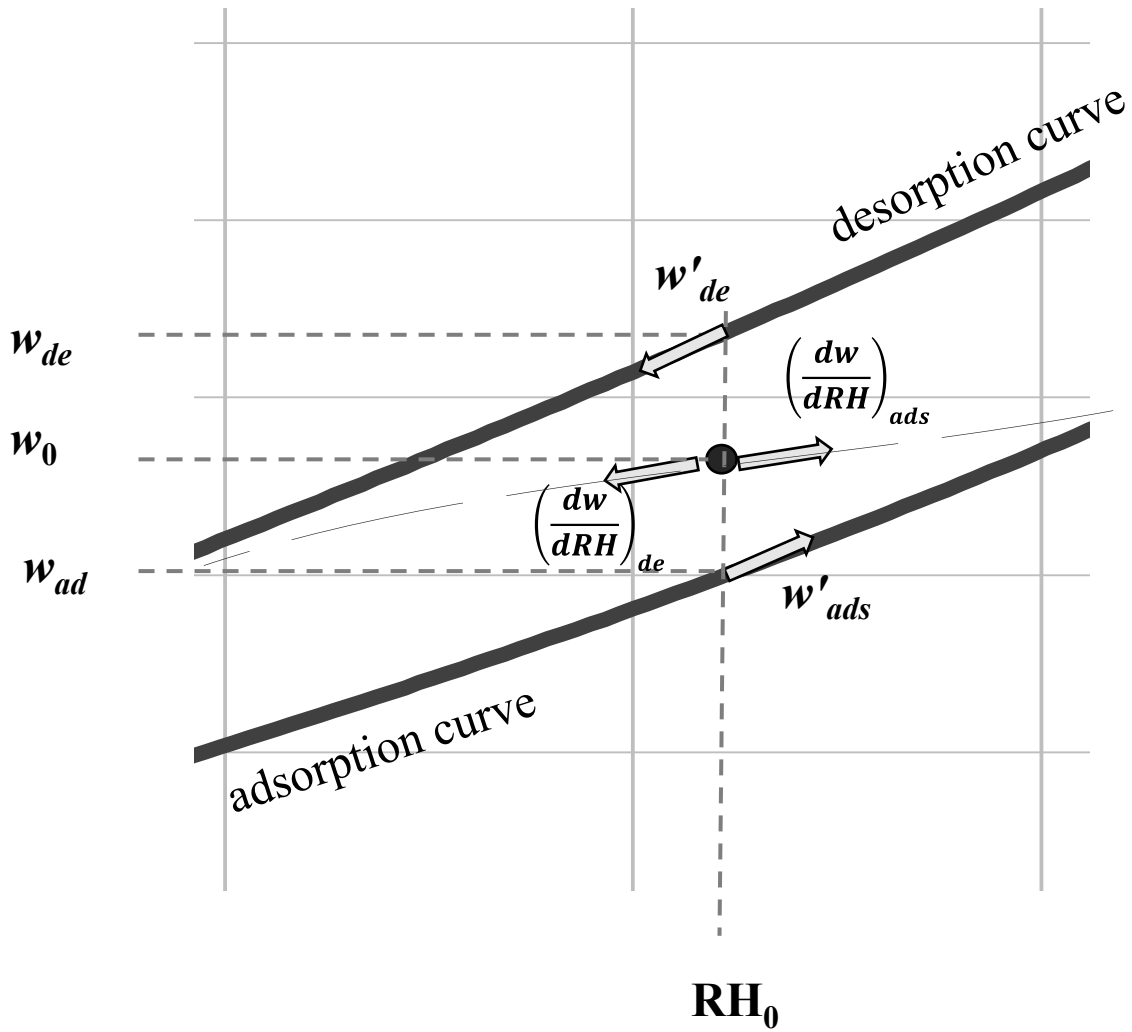


Figure 3 Partial isotherm behaviour. The parameters are from equations (9) and (10).

The material coefficient chosen for the current study, given in Table 2, are those proposed by [42].

Table 2 – Values for the moisture content evaluation

A	B	C	w_0	φ_{ad}	α_{ad}	φ_{de}	α_{de}
0.4	0.06	1.5	0.3236	0.8490	1.647	0.8520	1.088

The time-history of RH and T variation described in [16] was modelled on the basis of the above theory, using a simplified step-wise approximation of RH history and constant T, as shown in Figure 4. The results in terms of MC for each experimental step is given in Table 3. The values then chosen as boundary conditions for the steps used in the optimization process are listed in Table 4.

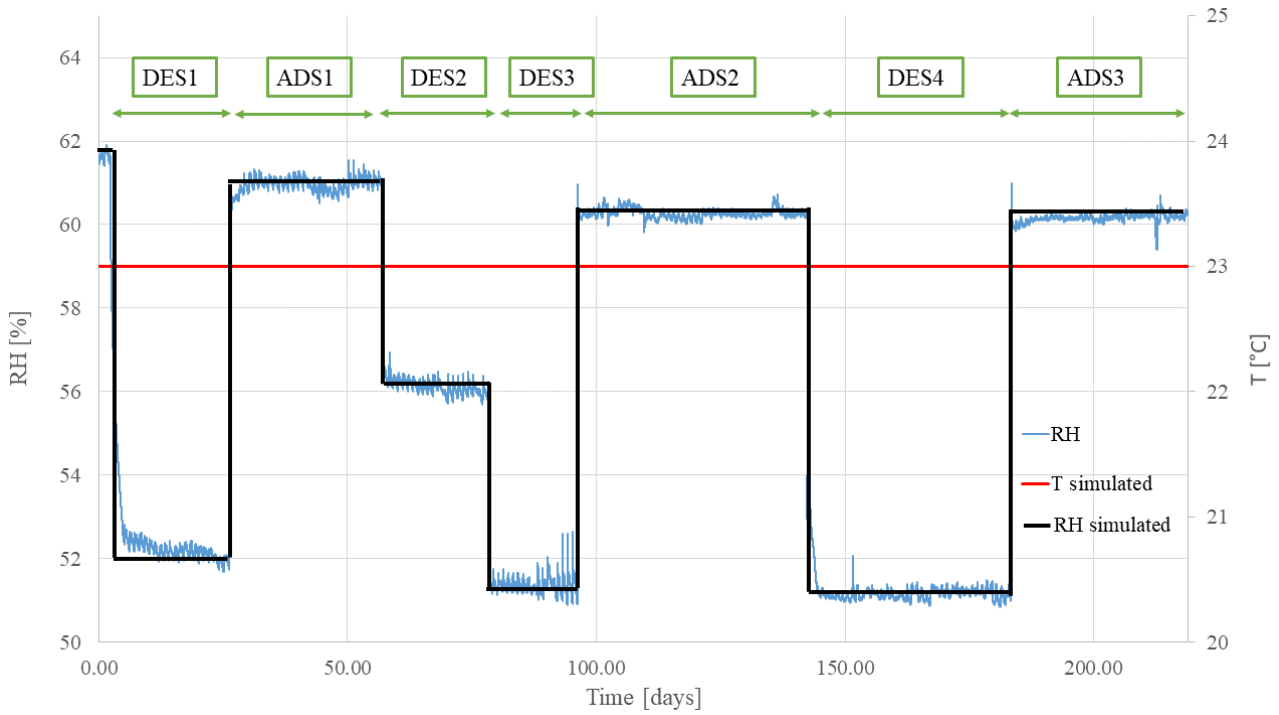


Figure 4 - Time History of Temperature (T) and relative humidity (RH) over the whole experimental campaign: in blue the measured RH, in black the simplified RH used for the EMC calculation

Table 3 – Relative humidity steps, Temperature, and, based on that, calculated EMC variation for all tests

Test name	Δ RH Step [%]	T [°C]	Δ EMC Calculated [%]	Step
DES 1 Not waterproofed	62-52	23	-0.98	
ADS 1 Not waterproofed	52-61	23	0.74	
DES 2 Not waterproofed	61-56	23	-0.43	
DES 3 Not waterproofed	56-51	23	-0.44	
ADS 2 Not waterproofed	51-60	23	0.62	
DES 4 waterproofed	60-53	23	-0.63	
ADS 3 waterproofed	53-60	23	0.59	

Table 4 - Values of the EMC steps used for modelling.

WPP	Delta EMC waterproofed [%]	Delta EMC not waterproofed [%]
1	0.59	0.74
2	-0.63	-0.44
3	-0.63	-0.44
4	-0.63	-0.44
5	-0.63	-0.98
6	-0.63	-0.44

The previous RH history being unknown, in the initial state the value of w was assumed to be mid-way between absorption and desorption isotherms.

2.5 Optimization

An iterative optimization algorithm was chosen to calibrate the numerical model to fit the experimental data, allowing to calculate the hygro-mechanical parameters for each of the six planks. The cost functional J , object of the minimization, is given as a function c , vector of the n parameters to be identified:

$$J(c) = \|\varepsilon - \varepsilon_{exp}\| \quad (11)$$

where ε are the values of time-history of deformation of the DK measurements lines calculated via numerical methods, ε_{exp} are the corresponding experimentally determined values and $\|\cdot\|$ is a norm on L , space of the observable values. Minimisation was performed by means of a technical solution [45] based on the succession of a genetic algorithm followed by a Nelder Mead-type minimisation scheme. This proves to be a very effective method [46, 47] for finding solutions when, in general, a small variation in the coefficients objects of the minimization generates considerable variations in the results.

The parameters subjected to the identification process are as follows:

1. The coefficient of diffusion D_0
2. The emissivity of the back E_{cl}
3. The Young modulus of the paint layer E_p
4. A coefficient X that multiplies the tensor of hygromechanical deformation $\underline{\underline{\varepsilon_{hyg}}}$:

$$\underline{\underline{\varepsilon_{hyg}}} = X \cdot \underline{\underline{\alpha}} \cdot \Delta w \quad (12)$$

Where $\underline{\underline{\alpha}}$ is the tensor of hygroexpansion rate and Δw is the variation of moisture content. The significance, therefore, of this coefficient is to globally calibrate the hygroscopic strain variation associated with a change in moisture content; for this reason, it is simultaneously a multiplier of both the shrinkage/swelling coefficient and the Delta w value obtained from the Varnier-Merekeb-Pedersen theory used here. In fact, on the one hand the aforementioned theory uses a variety of coefficients that cannot be calibrated to the individual painting, mainly due to the fact that they require dangerous humidity variations or destructive investigations, on the other hand it is not possible to precisely establish the climatic history of the paintings prior to the start of the tests and therefore the starting point within the hygroscopic hysteresis is arbitrary and chosen by us as equidistant between the limit isotherms of absorption and desorption. It should also be pointed out here that it is not possible to dissociate the two components in a heuristic characterisation process because the two components have the same effect on the overall deformation behaviour, making their dissociation impossible. For all these reasons we decided to calculate, via optimization, two different X value (X_{wp} , Waterproofed – $X_{no\ wp}$, not Waterproofed) for the two kind of tests done.

5. A Y coefficient that multiplies/divides the fourth-order compliance tensor in the following way:

$$\underline{\underline{Y^{-1} \cdot S_{ij}^0}} = \begin{pmatrix} Y^{-1}S_{11}^0 & Y^{-1}S_{12}^0 & Y^{-1}S_{13}^0 & 0 & 0 & 0 \\ Y^{-1}S_{12}^0 & Y^{-1}S_{22}^0 & Y^{-1}S_{23}^0 & 0 & 0 & 0 \\ Y^{-1}S_{13}^0 & Y^{-1}S_{23}^0 & Y^{-1}S_{33}^0 & 0 & 0 & 0 \\ 0 & 0 & 0 & Y^{-1}S_{44}^0 & 0 & 0 \\ 0 & 0 & 0 & 0 & Y^{-1}S_{55}^0 & 0 \\ 0 & 0 & 0 & 0 & 0 & Y^{-1}S_{66}^0 \end{pmatrix} \quad (13)$$

6. The emissivity of the paint layers E_c

The rigidity components, the initial shrinking/swelling coefficients and the initial diffusion used for poplar wood reported in Table 5 are based on [10] and [18].

Table 5 Mechanical and physical initial properties.

Wood Young moduli	$E_L=10060$ MPa	$E_R=641$ MPa	$E_T=306$ MPa
Wood Shear Moduli	$G_{RT}=200$ MPa	$G_{TL}=640$ MPa	$G_{LR} =860$ MPa
Wood Poisson's Ratios	$\nu_{RT}=0.7$	$\nu_{LT}=0.47$	$\nu_{LR} =0.46$
Wood Shrinkage	$\alpha_L=0.39\%/%$	$\alpha_R=1.92\%/%$	$\alpha_T=3.45\%/%$
Coefficient of moisture diffusion in wood	$D_0=1.52 \cdot 10^{-4}$ mm ² s ⁻¹		
Front Emissivity	$E_c=1.0 \cdot 10^{-5}$ mm·s ⁻¹		
Back Emissivity	$E_{c1}=1.0 \cdot 10^{-5}$ mm·s ⁻¹		
Paint Layers Young Modulus	$E_p=1000$ MPa		
Paint Layers Poisson's Ratio	$\nu_p =0.2$ – not subjected to optimization		
X	1		
Y	1		

A first optimisation process is carried out on parameters 1-6 on the cupping angle time history of the painting with the waterproofed front; in fact, in this case, the flow of moisture transiting the painting surface is identically null and the calculation of the emissivity of the painting front is meaningless.

A second process is subsequently performed on parameters 4 and 6, on the painting with the non-waterproofed front, leaving parameters 1,2,3,5 identified in the previous optimisation process unchanged.

This process also provides us with a cross-validation in the second analysis of the results obtained in the first one; in fact, the fitting of the second one takes place for internal moisture distributions that are completely different from the first one, varying only two variables, emissivity of the front and coefficient of hygroexpansion. Therefore, its conformity with the experimental data confirms the goodness of the first analysis carried out, whose results in terms of (wood diffusion, back emissivity, wood stiffness, paint layer stiffness) remained identical in the second.

2.6 Sensitivity analysis

In order to be able to use an inverse identification system, it is necessary to carry out a sensitivity study on the parameters under study.

Sensitivity analyses allow us to understand which inputs to a model contribute most to the variability of the output, and more specifically to understand input-output relationships, determine the magnitude of the contribution of input uncertainties on the model's output, identify the significance and magnitude of the inputs on the output, and guide modelling and experimental choices.

The opensource software Persalys [48], which is based on the highly industry-validated openTurns methods [49] was used to handle uncertainties and variability. This software can be easily coupled with code_aster, allowing investigations, in our case of sensitivity, to be performed on a finite element model in a fast and rigorous manner.

A Sobol sensitivity analysis is a type of statistical analysis that helps to identify which variables in a model have the most significant impact on its output. In the context of a finite element model, this means that Sobol's method is used to determine which input variables (such as material properties or boundary conditions) are most responsible for affecting the behaviour of the model.

One of the main advantages of using Sobol's method is that it is able to handle non-additive, non-monotonic, and non-linear systems. In other words, it can accurately assess the influence of input variables even when the relationships between those variables and the model output are complex and nonlinear.

However, Sobol's method is computationally intensive, meaning that it can be time-consuming and resource-intensive to implement. Despite this, it is still a valuable tool for exploring all areas of the input space, as it allows for the consideration of interactions and nonlinear responses. This means that it can help to identify unexpected relationships between variables and their impact on the model output, which might not be apparent through other methods of sensitivity analysis. Overall, the use of Sobol's method in a sensitivity analysis on a finite element model can provide important insights into the behaviour of the model and the variables that most strongly influence its output. Following the work of [50] and [51], in our sensitivity analysis we want to represent the studied model as:

$$Y = \mathcal{H}(X_1, \dots, X_n) \quad (14)$$

where the scalar Y denotes the variable of interest, here the cupping angle; \mathcal{H} is the model, deterministic or stochastic, that governs the problem, here the finite elements model; and X_1, \dots, X_n are the input variables.

The variance of Y can be decomposed as:

$$V(Y) = \sum_i V_i + \sum_i \sum_{j>i} V_{ij} + \dots + V_{123\dots n} \quad (15)$$

with $V_i = V(E(Y|X_i))$ the first-order partial variance, $V_{ij} = V(E(Y|X_i, X_j)) - V_i - V_j$ the second-order partial variance, and so on. V_i quantifies the influence of X_i on the dispersion of Y , while V_{ij} measures the second-order interaction contribution between X_i and X_j to $V(Y)$.

Normalizing the partial variances $V_i, V_{ij}, \dots, V_{123\dots n}$ with the total variance we obtain the Sobol sensitivity indices, here for first and second orders:

$$S_i = \frac{V_i}{V(Y)}, S_{ij} = \frac{V_{ij}}{V(Y)} \quad (16)$$

We may derive also a Sobol total index [52] for the input i variable, as:

$$ST_i = 1 - \frac{V(E(Y|X_{-i}))}{V(Y)} \quad (17)$$

where X_{-i} is the vector of all parameters except i .

For a general X_i the difference between the total index and the first-order index is the amount of interaction that X_i contributes to.

In a Sobol sensitivity analysis, the first-order index and total index are two commonly used measures of the sensitivity of a model output to its input parameters.

The first-order index measures the fractional contribution of an individual input parameter to the overall variance of the model output. It quantifies the extent to which changes in the value of that input parameter alone affect the variability of the output, without considering any interaction effects with other input parameters. Specifically, it is defined as the ratio of the variance of the model output due to the variation of the individual input parameter, to the total variance of the model output. The first-order index is a measure of the individual importance of a single input parameter, and can be used to rank the input parameters in terms of their relative importance.

The total index, on the other hand, takes into account the effects of interactions between input parameters of different orders. It evaluates the full range of parameter space by considering all possible combinations of input parameters and their interactions. Specifically, it measures the total contribution of each input parameter, including its first-order effects and all higher-order interactions, to the overall variance of the model output. The total index provides a more comprehensive measure of the impact of an input parameter on the model output, by considering not only its individual effect but also its combined effect with other input parameters.

In summary, the first-order index measures the sensitivity of the model output to a single input parameter, while the total index measures the sensitivity of the model output to all input parameters, including their interactions. Both indices are important measures in a Sobol sensitivity analysis as they help identify the most important input parameters in the model and provide insights into the overall behavior of the model [53].

In a finite element analysis sensitivity study, Sobol's method can be used to identify the impact of input variables (such as material properties, boundary conditions, or geometric parameters) on the output parameters of the model (such as stress, displacement, or strain). Overall, Sobol's method can be a useful tool for improving the accuracy and reliability of finite element analyses by providing insights into the behavior of the model and its sensitivity to input parameters.

3. Results

3.1 General sensitivity study

Figure 5 reports the result of a sensitivity study of the 'local' type, as in [16,17], where each variable is varied while the others remain unchanged. This analysis shows the qualitative appropriateness of the choice of parameters, objectified in two main characteristics:

1. Each variation of an individual variable must have a significant impact on the output, in our case the cupping angle.
2. It must give rise to a different curve compared to that generated by the other variables: two variables yielding the same global variation over time would not be distinguishable in an identification process, making it indeterminate.

In order to improve the readability of the graph in Figure 5 only the results relevant to WPP5 are shown (the others did not show significant differences). They were obtained by applying the variations listed in Table 6 with respect to the values determined in Section 3.3. Here, the emissivity of the painted front is excluded from the sensitivity studies, since it was carried out primarily physically, by waterproofing and excluding this variable.

Table 6 - Values of the hygro-mechanical properties used for the sensitivity study. In bold the values varied from the reference situation

Model	D ₀	E _p	E _c	E _{c1}	X	Y
	[m ² ·s ⁻¹]	[MPa]	[m·s ⁻¹]	[m·s ⁻¹]	waterproofed	
Reference	1.10 10 ⁻⁰⁹	1952	1.0 10 ⁻¹⁰	2.6 10 ⁻⁰⁷	1.27	1.29
Emissivity	1.10 10 ⁻⁰⁹	1952	1.0 10 ⁻¹⁰	3.1 10⁻⁰⁷	1.27	1.29
Diffusion	2.10 10⁻⁰⁹	1952	1.0 10 ⁻¹⁰	2.6 10 ⁻⁰⁷	1.27	1.29
X	1.10 10 ⁻⁰⁹	1952	1.010 ⁻¹⁰	2.6 10 ⁻⁰⁷	1.52	1.29
Y	1.10 10 ⁻⁰⁹	1952	1.0 10 ⁻¹⁰	2.6 10 ⁻⁰⁷	1.27	1.39
Paint Stiffness	1.10 10 ⁻⁰⁹	2452	1.0 10 ⁻¹⁰	2.6 10 ⁻⁰⁷	1.27	1.29

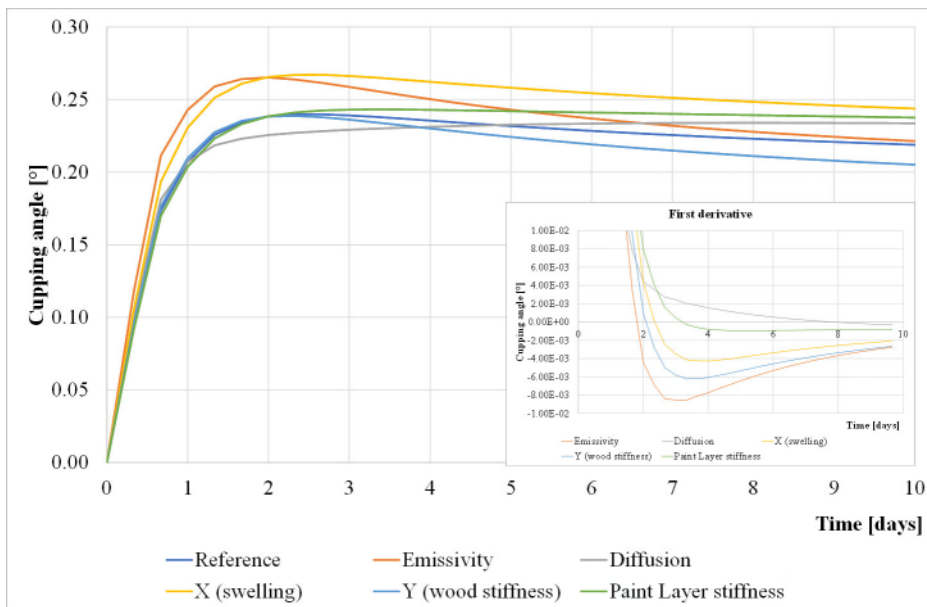


Figure 5 – Results for the sensitivity study according to Table 6. In the window, the first derivative of the curves of the sensitivity study.

The graph in Figure 5 clearly shows that all the variables considered have a significant effect on the variation of the cupping angle over time and that each of them can determine curves whose time evolution is significantly different from each other, as clearly shown by the first derivative calculation of these curves (window in Figure 5). However, the limitation of local sensitivity analysis is that it evaluates one parameter at a time and does

not capture the consequences of simultaneous changes in all model parameters, as well as the interactions between parameters.

3.2 Sobol Sensitivity study

Despite performing a global sensitivity analysis using the Sobol method on five panel paintings, the results were found to be similar in nature. Therefore, only the results related to one specific painting (WPP5) are presented here. The output variable for the analysis was the cupping angle, which was calculated at three different time points (3, 6, and 9 days) after a step change in moisture content ($\Delta w = -1\%$) was applied as a boundary condition for both the front and back faces. To obtain the Sobol analysis results, 10,000 different numerical analyses were performed. The variability range explored for the variables of interest, intended as uniform distribution, is given in Table 7.

Table 7 - Intervals of evaluation of the hygro-mechanical properties for the Sobol analysis

	D_o [$m^2 \cdot s^{-1}$]	E_{c1} [$m \cdot s^{-1}$]	E_p [MPa]	X	Y
Lower bound	$5.0 \cdot 10^{-10}$	$5.0 \cdot 10^{-09}$	1000	0.5	0.5
Upper bound	$5.0 \cdot 10^{-09}$	$5.0 \cdot 10^{-07}$	5000	1.5	1.5

In general, the Sobol sensitivity study comes to the same conclusions as the generic sensitivity study, confirming the significance of the choice of variables; when different values at different moments of a time history are obtained for different input parameters in the Sobol analysis, it means that these parameters have a different effect on the model output. It appears that the level of interaction of each variable (the difference between the total index and the first order index) does not stay constant during the physical evolution of the phenomenon.

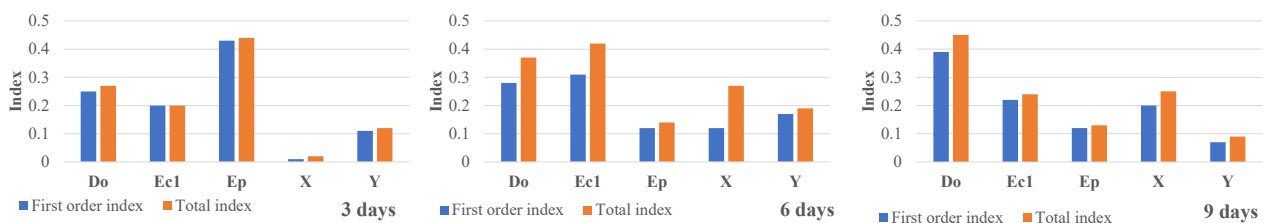


Figure 6 Sobol's sensitivity analysis for the cupping angle value obtained after 3, 6 and 9 days after the humidity step change (D_o - Diffusion coeff., E_{c1} Back side emissivity, E_p Rigidity of paint layers, X and Y corrective coeff.s.).

Table 8 Sobol's sensitivity analysis for the cupping angle value obtained after 3, 6 and 9 days after the humidity step change (D_o - Diffusion coeff., E_{c1} Back side emissivity, E_p Rigidity of paint layers, X and Y corrective coeff.s.).

Index	3 days		6 days		9 days	
	First order index	Total index	First order index	Total index	First order index	Total index
D_o	0.25	0.27	0.28	0.37	0.39	0.45
E_{c1}	0.2	0.2	0.31	0.42	0.22	0.24
E_p	0.43	0.44	0.12	0.14	0.12	0.13
X	0.01	0.02	0.12	0.27	0.2	0.25
Y	0.11	0.12	0.17	0.19	0.07	0.09

3.2 Hygro-mechanical identification

Figure 7 shows, in the case of waterproofed WPP 5, the results of the optimisation process carried out on the two individual measurements lines of the DK (upper and lower), the quantity actually measured by the system.

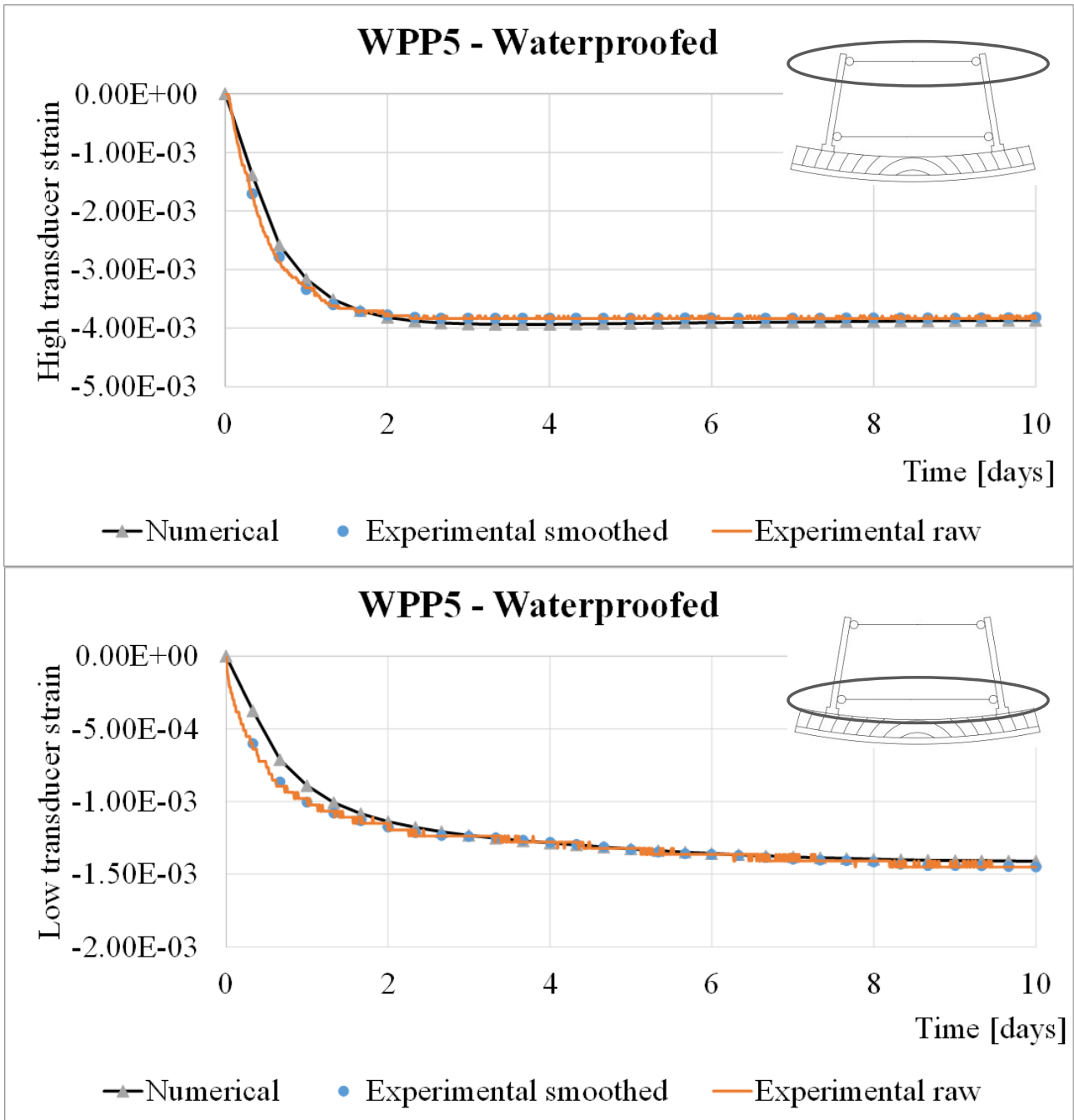
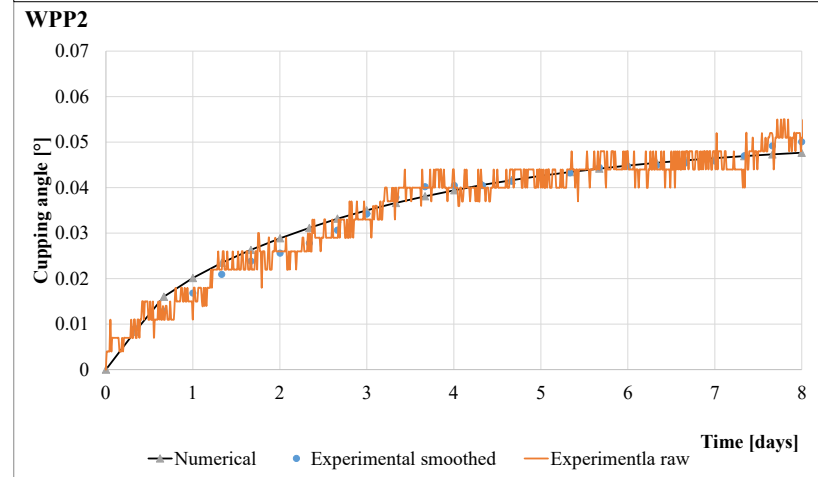
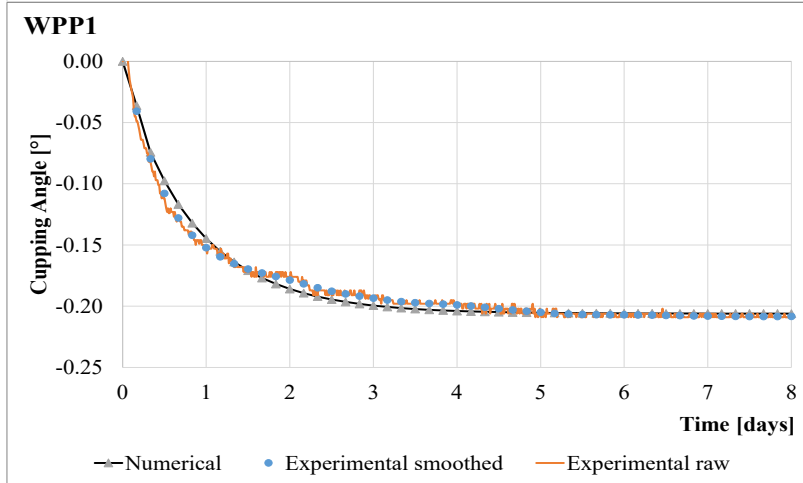
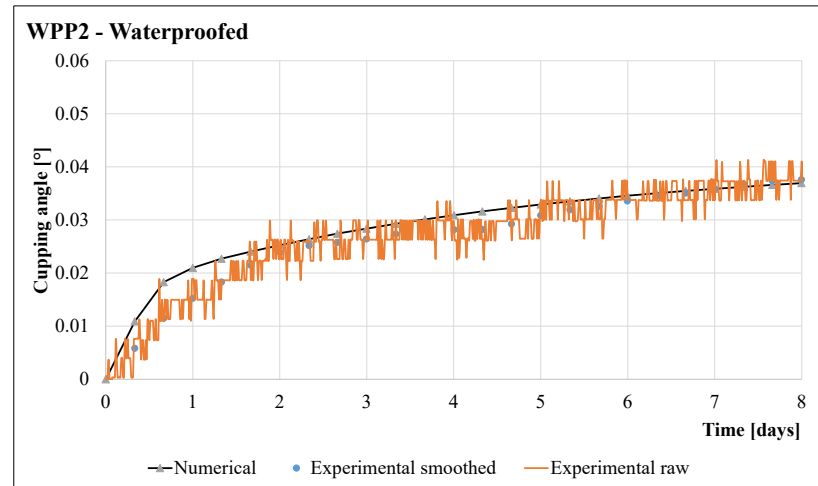
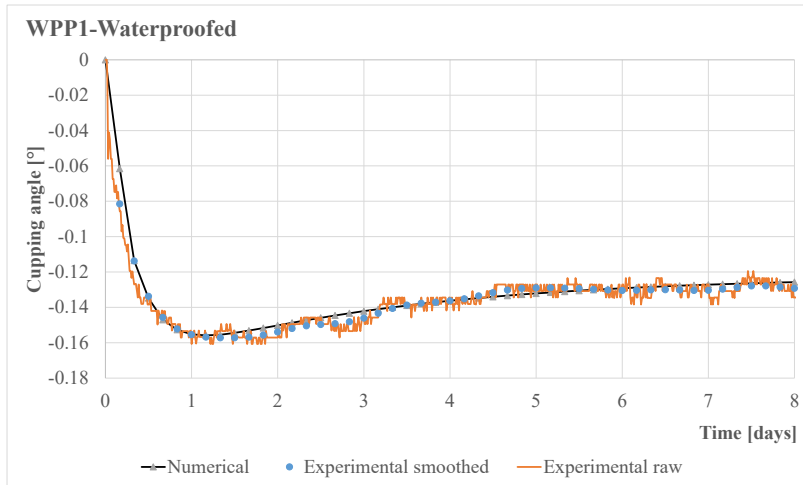


Figure 7 The results of the optimisation of each DK measurement line (strain [m/m]) from which the cupping angle is derived. High line at the top and low line at the bottom.

Table 9 Summary of the calculated hygro-mechanical values for the studied WPPs (D_0 -Diffusion coeff., E_{c1} Back side emissivity, E_p Rigidity of paint layers, X and Y corrective coeff.s.; wp means waterproofed and no wp means no-waterproofed

	$D_0 [m^2 \cdot s^{-1}]$	$E_p [MPa]$	$E_c [m \cdot s^{-1}]$	$E_{c1} [m \cdot s^{-1}]$	X_{wp}	$X_{no wp}$	Y
WPP1	$4.0 \cdot 10^{-10}$	1506	$7.5 \cdot 10^{-8}$	$9.0 \cdot 10^{-8}$	0.47	0.62	0.82
WPP2	$4.5 \cdot 10^{-9}$	2613	$4.0 \cdot 10^{-8}$	$1.1 \cdot 10^{-7}$	0.3	0.3	0.57
WPP3	$1.6 \cdot 10^{-8}$	11467	$4.3 \cdot 10^{-8}$	$5.0 \cdot 10^{-8}$	0.51	0.8	0.93
WPP4	$6.0 \cdot 10^{-10}$	10500	$3.0 \cdot 10^{-8}$	$1.8 \cdot 10^{-7}$	2.2	2.05	1.5
WPP5	$1.1 \cdot 10^{-9}$	1952	$1.0 \cdot 10^{-10}$	$2.6 \cdot 10^{-7}$	1.27	1.29	0.55
WPP6	$9.0 \cdot 10^{-10}$	563	$3.0 \cdot 10^{-7}$	$5.0 \cdot 10^{-7}$	0.67	1.2	0.45

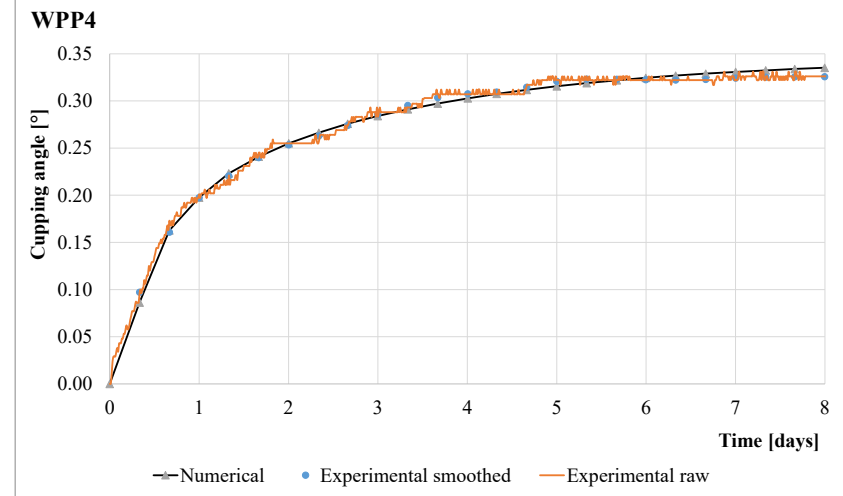
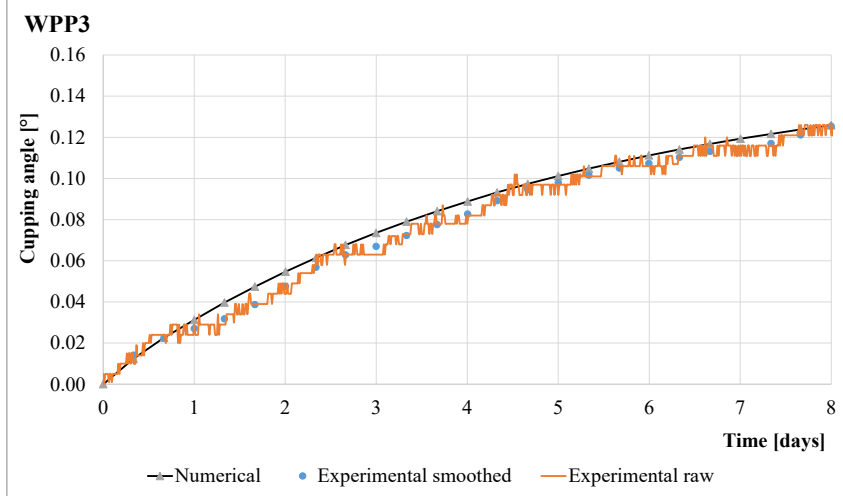
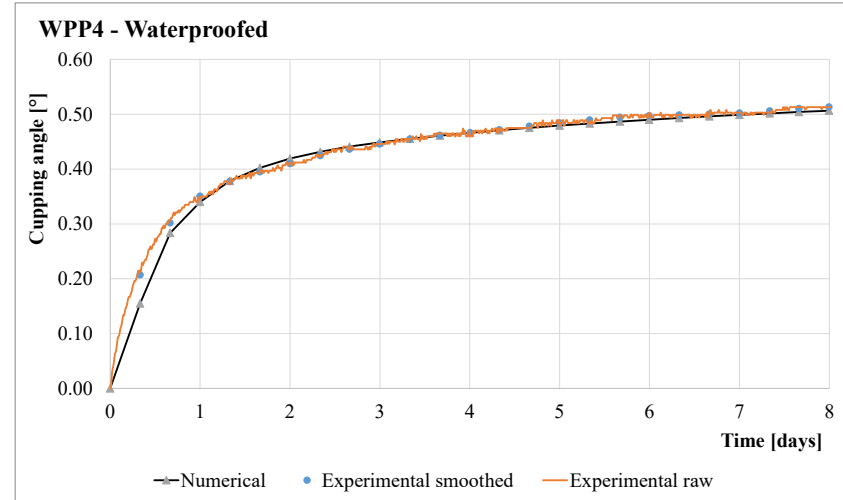
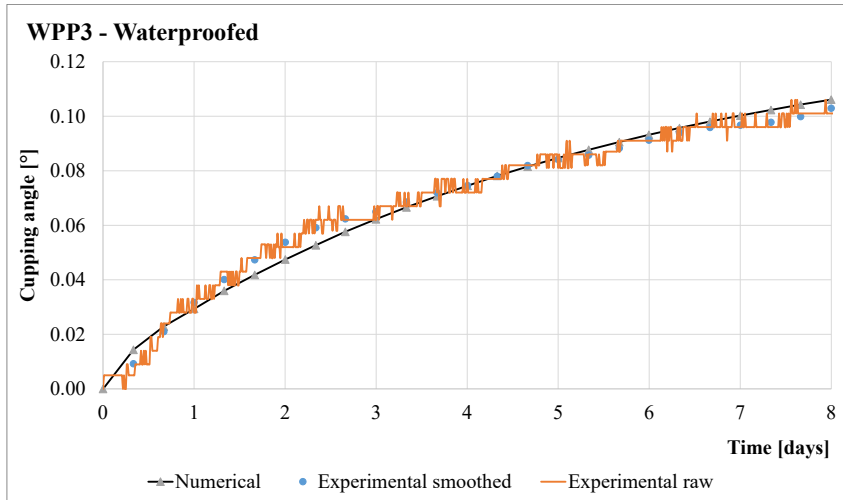
In Figure 8, Figure 9 and Figure 10 the results of the case-by-case optimisation are shown in terms of the angle of curvature; for the sign convention of the angle of curvature, we use the convention described in [29]. Each graph gives the raw data of cupping angle (experimental raw), the data obtained from the smoothing and interpolation process (experimental smoothed) and the numerical results (numerical) at the end of the optimisation, accompanied by the R^2 value calculated between the experimental smoothed and numerical.



D_0	E_p	E_c	E_{c1}	X	X	Y	R^2	R^2
$[\text{m}^2 \cdot \text{s}^{-1}]$	$[\text{MPa}]$	$[\text{m} \cdot \text{s}^{-1}]$	$[\text{m} \cdot \text{s}^{-1}]$	wp			wp	
$4 \cdot 10^{-10}$	1506	$7.5 \cdot 10^{-8}$	$9 \cdot 10^{-8}$	0.47	0.62	0.82	0.95	0.99

D_0	E_p	E_c	E_{c1}	X	X	Y	R^2	R^2
$[\text{m}^2 \cdot \text{s}^{-1}]$	$[\text{MPa}]$	$[\text{m} \cdot \text{s}^{-1}]$	$[\text{m} \cdot \text{s}^{-1}]$	wp			wp	
$4.5 \cdot 10^{-9}$	2613	$4 \cdot 10^{-8}$	$1.1 \cdot 10^{-7}$	0.3	0.3	0.57	0.99	0.99

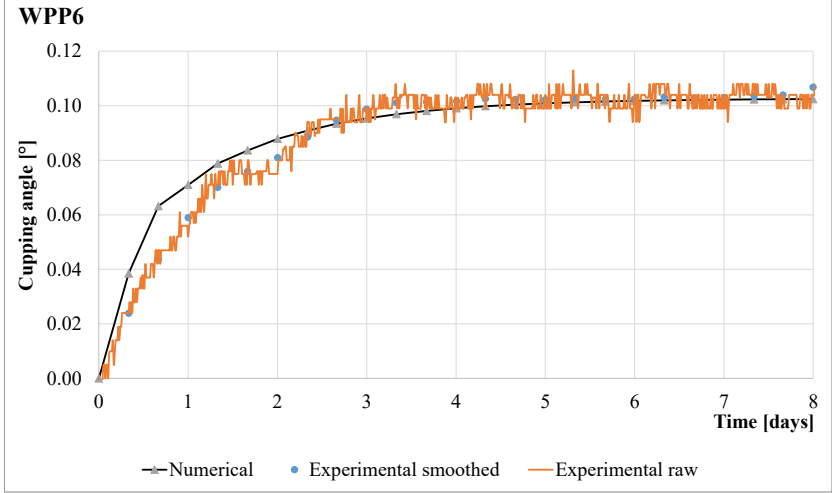
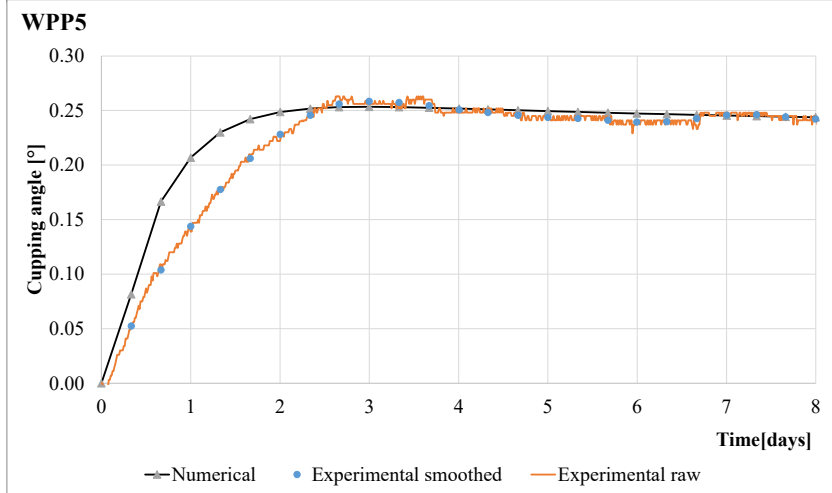
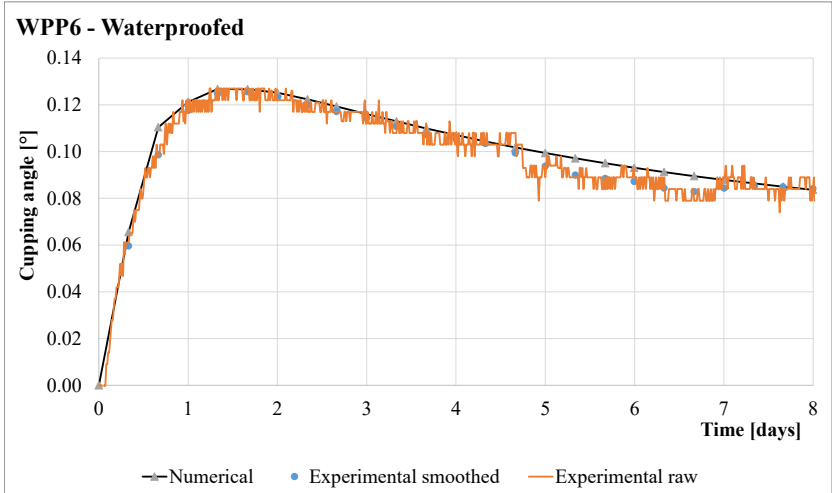
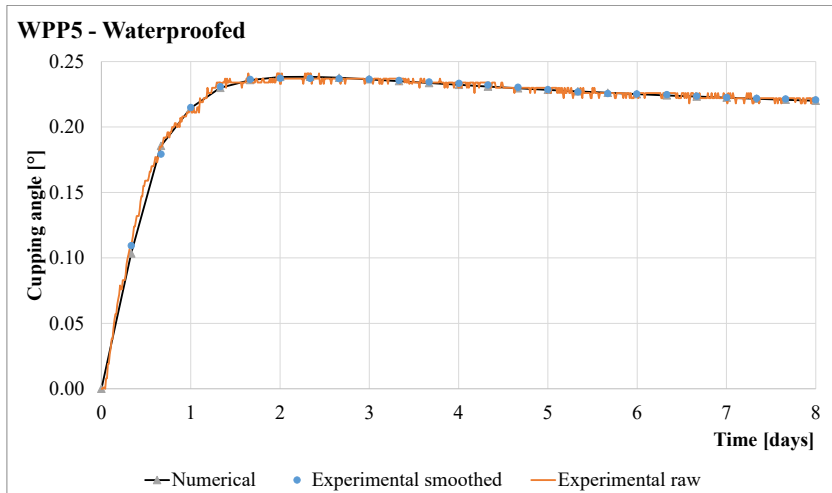
Figure 8 Results of the optimisation for WPP1 (on the left) and WPP2 (on the right). For each WPP, on top the optimisation when waterproofed and below when no-waterproofed. The table resuming the hygro-mechanical characteristics and correlation coefficients (D_0 -Diffusion coeff., E_{c1} Back side emissivity, E_p Rigidity of paint layers, X and Y corrective coeff.s.; wp means waterproofed, if wp is not present the results are for no-waterproofed WPPs)



D_0	E_p	E_c	E_{c1}	X	X	Y	R^2	R^2
$[\text{m}^2 \cdot \text{s}^{-1}]$	$[\text{MPa}]$	$[\text{m} \cdot \text{s}^{-1}]$	$[\text{m} \cdot \text{s}^{-1}]$	wp			wp	
$1.6 \cdot 10^{-8}$	11467	$4.3 \cdot 10^{-8}$	$5 \cdot 10^{-8}$	0.51	0.80	0.93	0.99	0.99

D_0	E_p	E_c	E_{c1}	X	X	Y	R^2	R^2
$[\text{m}^2 \cdot \text{s}^{-1}]$	$[\text{MPa}]$	$[\text{m} \cdot \text{s}^{-1}]$	$[\text{m} \cdot \text{s}^{-1}]$	wp			wp	
$6 \cdot 10^{-10}$	10500	$3 \cdot 10^{-8}$	$1.8 \cdot 10^{-7}$	2.2	2.05	1.5	0.99	0.99

Figure 9 Results of the optimisation for WPP3 (on the left) and WPP4 (on the right). For each WPP, on top the optimisation when waterproofed and below when no-waterproofed. The table resuming the hygro-mechanical characteristics and correlation coefficients (D_0 - Diffusion coeff., E_{c1} Back side emissivity, E_p Rigidity of paint layers, X and Y corrective coeff.s.; wp means waterproofed, if wp is not present the results are for no-waterproofed WPPs)



D_0	E_p	E_c	E_{c1}	X	X	Y	R^2	R^2
$[m^2 \cdot s^{-1}]$	[MPa]	$[m \cdot s^{-1}]$	$[mm \cdot s^{-1}]$	wp			wp	
$1.1 \cdot 10^{-9}$	1952	$1 \cdot 10^{-10}$	$2.6 \cdot 10^{-7}$	1.27	1.29	0.55	0.99	0.89

D_0	E_p	E_c	E_{c1}	X	X	Y	R^2	R^2
$[m^2 \cdot s^{-1}]$	[MPa]	$[m \cdot s^{-1}]$	$[m \cdot s^{-1}]$	wp			wp	
$.9 \cdot 10^{-10}$	563	$3 \cdot 10^{-7}$	$5 \cdot 10^{-7}$	0.67	1.2	0.45	0.97	0.98

Figure 10 Results of the optimisation for WPP1 (on the left) and WPP2 (on the right). For each WPP, on top the optimisation when waterproofed and below when no-waterproofed. The table resuming the hygro-mechanical characteristics and correlation coefficients (D_0 -Diffusion coeff., E_{c1} Back side emissivity, E_p Rigidity of paint layers, X and Y corrective coeff.s.; wp means waterproofed, if wp is not present the results are for no-waterproofed WPPs)

4. Discussion

The sensitivity analysis provides interesting insights, firstly, in term of the level of complexity of the phenomenon. Any variation in the input variables leads to a consistent variation in the trend of the curves, imposing completely different slopes on the time history. This, confirming [16], shows the great variability of the physical problem under consideration; even a single incorrectly calibrated variable can lead to results far from reality. Sobol's analysis is a powerful tool for investigating the sensitivity of a model's output to its input parameters. In this context, the analysis reveals a high level of complexity in the deformation tendency of the board, as measured by the cupping angle, and how it varies over time. The analysis also provides a hierarchy of the influence of the input variables on the deformation tendency of the board, highlighting the most significant factors at different time points. The analysis shows that the indices for individual input variables vary greatly over time, while remaining significant, indicating the complex and dynamic nature of the problem. This suggests that the deformation tendency of the board is affected by a combination of factors, with their relative importance changing over time. Additionally, the analysis reveals that there is generally a significant deviation between the first-order index and the total index in the 6-day and 9-day analyses, while they coincide to a first approximation in the 3-day analysis. The first-order index measures the sensitivity of the model output to individual input parameters, while the total index takes into account the interactions between input parameters of different orders. The deviation between the two indices in the 6-day and 9-day analyses indicates the presence of higher-order interactions between input parameters, which have a significant impact on the deformation tendency of the board. This further highlights the complex and dynamic nature of the problem, and the importance of considering higher-order interactions in the sensitivity analysis. Overall, Sobol's analysis provides valuable insights into the sensitivity of the model's output to its input parameters, revealing the complex and dynamic nature of the deformation tendency of the board and the changing importance of input parameters over time. The analysis highlights the importance of considering higher-order interactions in the sensitivity analysis, which can help improve the accuracy and reliability of the model. This difference has the significance of denoting an interaction of the input variables, i.e. the extent to which the distribution of one variable can be influenced by the variation in the distribution of another variable. In simplified terms, we can say that two inputs have an interaction if their combined effect on the output is greater than the sum of their effects considered separately. This is equivalent to saying that variations in the ambient RH cause a variation in the MC of the hygroscopic materials of which the work is composed, and as a result it manifests a deformation behaviour that is the result of the interaction between the anatomy of the boards and the stiffness and diffusivity of the preparation layers and the colour. The fact that the interaction of variables with each other makes them more significant is therefore a fact that should not be underestimated and shows us that it is necessary to evaluate them precisely in their interaction, i.e. in the actual physical situation. It also shows us a strong system effect, which, coupled with the consideration that in this context small variations in the input variables lead to large variations in the kinetic configuration of the system, is typical of systems with a high level of complexity.

Sensitivity analysis also can be evaluated in how uncertainties in the input variables are carried into the model's response; in this view we can easily observe how the use of material properties not calibrated to the work, but, for example, extracted from literature values or simulacra, lead to enormously valuable variations on the solution, confirming the results of [16].

Regarding the results of the optimization process, it can be observed that the iterative process leads us to numerical results that tend to agree with the experimental data, with the majority of the results presenting a determination coefficient (R^2) of 0.99. The most important indications from this are that the chosen variables and modelling assumptions are essentially a sufficient description of the physical system, and that numerical models can be successfully calibrated.

The logical consequence is that the input parameters of the model can be considered as representative of those that can be associated with the real phenomenon. In any case these are averaged parameters, subject to constitutive and modelling assumptions, underlying a stringent assumption of material homogeneity, etc., and

are therefore themselves subject to margins of uncertainty, but nevertheless they allow a model built on them to behave like the real object.

The numerical values obtained from the optimization process (tables in Figure 8, Figure 9 and Figure 10), show a large dispersion in the numerical values of each parameter between the different WPPs studied. In particular the values obtained for the stiffness of the paint layers are very variable, in the range identified by [9], and allow us to identify in WPP1, WPP5, WPP6 as panels with paint layers of low stiffness, which doesn't prevent their flying-wood behaviour in the sealed state, confirming the qualitative analyses of [16].

WPP3 requires a special attention as the support wood is found to have a high transverse diffusivity. Observing the artwork, the restorers pointed out the presence of a protective layer of impregnating waterproofing beeswax on the back. One hypothesis to explain this early restoration choice, made in the distant past and undocumented, is that the work was probably extremely reactive and the restorers wanted to balance the emissivity of the back against the front by using of a waterproofing product. The result is in fact a board with a very high diffusivity in general, with both sides having the same emissivity, which then moves with almost symmetrical internal gradients, due to the cylindrical anisotropy characteristics of the shrinkage/swelling and the stiffness relationship between the wood and the preparation.

The optimisation process failed to find consistent parameters to fit the first part of uncoated WPP5 test. It is difficult to understand the cause of this localised deviation, given the excellent agreement of the waterproofed test. In fact, it should be noted that only the emissivity of the painted surface and the hygroscopic strain multiplier vary between the first and the second test; if the multiplier essentially leads to a vertical shift of the curve, there is no emissivity value that leads to the match. In our opinion, the cause of this could be a material inhomogeneity just below the interface between the preparation layers and the wood, or an experimental problem whose cause we could not understand.

In general, the numerical results are qualitatively slightly different from the experimental evidence in the very early stages of the transient. As shown by the local sensitivity study, at this early stage the differences that the different variables have on the initial part of the ramp are not discernible. Apart from the fact that this phase was also the most critical for the humidity generator, which needs time to stabilise the humidity in the chamber after the change, it seems to us that the main cause of this discordance is due to a local inhomogeneity in the first layers of the wood back. In these first transient moments, the internal moisture gradient of the wood only affects the first few millimetres, which act as a deformation motor for the rest of the section, which tends to maintain its size, still at the previous moisture content. The most likely causes are: ageing, damage, general inhomogeneity such as insect infestation. In any case, this is an interesting topic for future research.

4. Conclusions

Based on experiments on original paintings subjected to controlled thermo-hygrometric variations, a simplified physical model was developed. After methods of uncertainty analysis were applied to analyse the complexity and sensitivity of the problem, the model was calibrated on experimental tests, leading to hygro-mechanical characterisation of each studied panel.

Based on the results presented, the study demonstrated the possibility of non-invasively characterising a WPP in its complexity through direct observation of its behaviour. The parameterisation of the variables obtained by this approach then makes it possible to model its behaviour and virtually explore hypothetical conservation scenarios. While taking into account the classical limitations associated with inverse identification methods, such as the strong dependence on the physical model chosen and the enormous computational burden, the characteristics identified - an approximation to the real ones, assuming that they can be unambiguously identified in the real object - allow the construction of numerical models whose behaviour is highly congruent with the real one.

The research has also shown that, in order to understand and model the hygromechanical phenomena that govern the deformation tendencies of paintings on panels, it is necessary to consider a strategy of direct analysis on the object, which, at the current state of knowledge, seems to be the only way to avoid obtaining results that have nothing to do with reality. The strategy that this study proposes, beyond the characterisation tools and techniques that can be applied or implemented, is that of "learning from objects". We therefore start by asking the object what its deformation tendencies are, through experimental investigations. In this context, numerical analysis becomes a method to be developed in parallel with experiments and which helps to increase the level of knowledge and extract as much information as possible.

Annex 1

Description of the implementation of the elastic orthotropic behaviour of the wooden panel in MFront

This appendix describes how the of the elastic orthotropic behaviour of the wooden panel has been implemented using the open source-code generator MFront co-developed under strict assurance quality constraints by CEA, EDF and Framatome in the context of a numerical platform dedicated to the simulation of the nuclear fuel elements named PLEIADES. MFront is distributed as part of the Salomé-Méca platform and is tightly integrated with code_aster.

Notations used

Symbol	Description
$\underline{\varepsilon}$	Total strain in the reference system
$\underline{\varepsilon}^*$	Total strain in the material frame
$\underline{\varepsilon}_{hyg}$	Hygromechanical strain in the reference system
$\underline{\varepsilon}_{hyg}^*$	Hygromechanical strain in the material frame
$\underline{\mathbf{C}}$	Stiffness tensor in the reference system
$\underline{\mathbf{C}}^*$	Stiffness tensor in the material frame

In the material frame, the orthotropic elastic behaviour amounts to the following relationship between the total strain $\underline{\varepsilon}^*$ and the stress $\underline{\sigma}^*$:

$$\underline{\sigma}^* = \underline{\mathbf{C}}^* : \left(\underline{\varepsilon}^* - \underline{\varepsilon}_{hyg}^* \right) \quad (18)$$

where $\underline{\mathbf{C}}^*$ denotes the stiffness tensor in the material frame.

Let $\underline{\mathbf{R}}$ the fourth order tensor such that:

$$\left\{ \begin{array}{l} \underline{\varepsilon} = \underline{\mathbf{R}} : \underline{\varepsilon}^* \\ \underline{\sigma} = \underline{\mathbf{R}} : \underline{\sigma}^* \end{array} \right. \quad (19)$$

Then, the Constitutive Equation [17](#) can be rewritten as follows:

$$\underline{\sigma} = \left(\underline{\mathbf{R}} \right)^{-1} \cdot \underline{\mathbf{C}}^* \cdot \underline{\mathbf{R}} : \left(\underline{\varepsilon} - \underline{\varepsilon}_{hyg} \right) \quad (20)$$

or, equivalently:

$$\underline{\sigma} = \underline{\mathbf{C}} : \left(\underline{\varepsilon} - \underline{\varepsilon}_{hyg} \right) \quad (21)$$

$$\text{With } \underline{\mathbf{C}} = \left(\underline{\mathbf{R}} \right)^{-1} \cdot \underline{\mathbf{C}}^* \cdot \underline{\mathbf{R}} \quad (22)$$

MFront provides the mandatory functions to build $\underline{\varepsilon}_{hyg}$ and from the two rotation matrices corresponding to composition of the rotation in the cylindrical frame and to material frame.

Annex 2

In its most widely used configuration, the DK basically consists of (a) two metal columns secured in a minimally invasive manner on the back face of a painted panel in such a way that they stand perpendicular to the wood surface, and (b) two displacement transducers (that constitute the Upper and Lower Measurement Line), whose opposite ends are hinged on the two columns, measuring the distance between them at fixed distances from the wood surface (Fig. 1). The outputs from the transducers are sampled at chosen time intervals, and the resulting data are stored in the memory of a data-logger for further analysis. The line connecting the points in which the axes of the two columns intersect the back face of the panel, should be as perpendicular as possible to the direction of the wood grain. As the panel deforms (for any reason, including environmental variations and applied bending moments) the two columns move and rotate relative to each other, and the centres of the spherical hinges connecting each transducer to the columns move closer together or further apart. The more the deformation of the panel approximates pure cupping without twisting and the rings in the cross-section under the measurement lines are not inclined with respect to the longitudinal direction of the board, the more the two columns remain in the same plane. So that the variations in distance measured by the transducers allow the exact reconstruction, instant by instant, of the cupping angle (i.e. the angle formed by the axes of the columns), based on the geometry of the panel-transducers-columns system (Fig. 1).

Declarations

Data are available from the corresponding author [P.M.] upon reasonable request and with permission of the Superintendence that owns the panel paintings.

The authors declare that they have no known competing financial interests or personal relationships that could have appeared to influence the work reported in this paper.

This research received specific grant from Tuscan Region, Italy (PREMUDE Project—POR-FSE 2014–2020. Modelli innovativi per la conservazione PREventiva in ambienti MUseali e DEpositi temporanei post-emergenza).

Authors' contributions:

L.Riparbelli conceived and discussed the theoretical approach, the methods implemented and the numerical procedures applied, did every step of the modelling, analysed the models and extracted the conclusions, developed the experimental investigations, wrote and revised the paper.

P.M. developed the experimental investigations, discussed the results and revised the paper.

C.M. developed the experimental investigations, revised the paper.

L. U. developed the experimental investigations, revised the paper.

L. Ricciardi, S.R., A. S. and C. C. chose and provide the six historical panel paintings, participated in designing the tests and revised the paper.

J.G. discussed the methods implemented and the numerical procedures applied, reviewed and discussed the numerical results and revised the paper.

M.F. conceived and discussed the theoretical approach, discussed the methods implemented and the numerical procedures applied, reviewed and discussed the results, wrote and revised the paper, coordinated the project.

References

- [1] C. Cennini, *Il libro dell'arte*, Neri Pozza. Frezzato F., 2009. The art book, in Italian,
- [2] L. Uzielli, Historical overview of panel-making techniques in central Italy, in *Proceedings of a Symposium at the J. Paul Getty Museum 24-28 April 1995*. The Getty Conservation Institute, US 1998; 110–135.
- [3] J. Wadum, Historical overview of panel-making techniques in northern countries, in *Proceedings of a Symposium at the J. Paul Getty Museum 24-28 April 1995*. The Getty Conservation Institute, US 1998; 149–177.
- [4] J. Gril, D. Jullien, D. Hunt, Compression set and cupping of painted wooden panels, in *Analysis and Characterisation of Wooden Cultural Heritage by Scientific Engineering Methods*, Halle (Saale), Germany, April 2016. <https://hal.archives-ouvertes.fr/hal-01452161>, last checked December 2022.
- [5] M. Mecklenburg, C. Tumosa, D. Erhardt, Structural response of painted wood surfaces to changes in ambient relative humidity, in *Painted Wood: History and Conservation*. The Getty Conservation Institute, US 1998; 464–483.
- [6] O. Allegretti, M. De Vincenzi, L. Uzielli, P. Dionisi-Vici, Long-term hygromechanical monitoring of Wooden Objects of Art (WOA): A tool for preventive conservation, *J. Cult. Herit.*, 2013; 14 (3):e161–e164. doi: 10.1016/j.culher.2012.10.022.
- [7] J.-C. Dupre et al., Experimental study of the hygromechanical behaviour of a historic painting on wooden panel: devices and measurement techniques, *J. Cult. Herit.*, 2020; 46: 165–175. doi: 10.1016/j.culher.2020.09.003.
- [8] J. Colmars et al., Hygromechanical response of a panel painting in a church, monitoring and computer modeling, in *International conference on wooden cultural heritage, Evaluation of deterioration and management of change*, Hamburg, Germany, 2009., p. 9. <https://hal.archives-ouvertes.fr/hal-00795990>, last checked Decemnbere 2022
- [9] C. Gauvin, *Etude expérimentale et numérique du comportement hygromécanique d'un panneau de bois : application à la conservation des tableaux peints sur bois du patrimoine*, PhD Thesis, LMGC - Laboratoire de Mécanique et Génie Civil, Université de Montpellier 2, 2015. Experimental study and numerical modelling of the hygromechanical behaviour of wood applied to the conservation of panel paintings, in French.
- [10] P. Mazzanti, M. Togni, L. Uzielli, Drying shrinkage and mechanical properties of Poplar wood (*Populus alba* L.) across the grain, *J. Cult. Herit.*, 2012; 13 (3): S85–S89.
- [11] P. Mazzanti et al., A hygro-mechanical analysis of poplar wood along the tangential direction by restrained swelling test, *Wood Sci. Technol.*, 2014; 48: 673–687. doi: 10.1007/s00226-014-0633-4.
- [12] D. Hunt, L. Uzielli, P. Mazzanti, Strains in gesso on painted wood panels during humidity changes and cupping, *J. Cult. Herit.*, 2017; 25: 163–169.
- [13] O. Allegretti, F. Raffaelli, Barrier effect to water vapour of early European painting materials on wood panels, *Stud. Conserv.*, 2008; 53 (3): 187-197. doi: 10.1179/sic.2008.53.3.187.

- [14] J. Stöcklein et al., Hygro-mechanical short-term behaviour of selected coatings: experiments and material modelling on vapour permeability and mechanical properties, *Herit. Sci.*, 2022; 10 (1):141-. doi: 10.1186/s40494-022-00768-5.
- [15] A. Janas et al., Shrinkage and mechanical properties of drying oil paints, *Herit. Sci.*, 2022; 10 (1): 181. doi: 10.1186/s40494-022-00814-2.
- [16] L. Riparbelli et al., Hygromechanical behaviour of wooden panel paintings: Classification of their deformation tendencies based on numerical modelling and experimental results, *Herit. Sci.*, 2023; 11 (25). <https://doi.org/10.1186/s40494-022-00843-x>.
- [17] J. Froidevaux, Wood and paint layers aging and risk analysis of ancient panel painting, PhD Thesis, Université Montpellier 2, 2012.
- [18] D. Dureisseix, B. Marcon, A partitioning strategy for the coupled hygromechanical analysis with application to wood structures of cultural heritage, *Int. J. Numer. Methods Eng.*, 2011; 88(3): 228–256.
- [19] C. Gebhardt, D. Konopka, A. Börner, M. Mäder, M. Kaliske, Hygro-mechanical numerical investigations of a wooden panel painting from “Katharinenaltar” by Lucas Cranach the Elder, *J. Cult. Herit.*, 2018; 29:1–9.
- [20] S. Saft, M. Kaliske, Numerical simulation of the ductile failure of mechanically and moisture loaded wooden structures, *Computers&Structures*, 2011; 89(23–24): 2460–2470. doi: <https://doi.org/10.1016/j.compstruc.2011.06.004>.
- [21] B. Rachwał, Ł. Bratasz, L. Krzemień, M. Łukomski, R. Kozłowski, Fatigue Damage of the Gesso Layer in Panel Paintings Subjected to Changing Climate Conditions, *Strain*, 2012; 48(6): 474–481. doi: <https://doi.org/10.1111/j.1475-1305.2012.00844.x>.
- [22] B. Rachwał, Ł. Bratasz, M. Łukomski, R. Kozłowski, Response of Wood Supports in Panel Paintings Subjected to Changing Climate Conditions, *Strain*, 2012; 48(5): 366–374. doi: 10.1111/j.1475-1305.2011.00832.x.
- [23] A. Kupczak et al., HERIE: A Web-Based Decision-Supporting Tool for Assessing Risk of Physical Damage Using Various Failure Criteria, *Stud. Conserv.*, 2018; 63 (1):151–155. doi: 10.1080/00393630.2018.1504447.
- [24] P. Dionisi-Vici, P. Mazzanti, L. Uzielli, Mechanical response of wooden boards subjected to humidity step variations: climatic chamber measurements and fitted mathematical models, *J. Cult. Herit.*, 2006; 7(1): 37–48.
- [25] O. Allegretti, J. Bontadi, P. Dionisi-Vici, Climate induced deformation of Panel Paintings: experimental observations on interaction between paint layers and thin wooden supports, *Int. Conf. Florence Heri-Tech Future Herit. Sci. Technol.*, 2020. doi.org/10.1088/1757-899X/949/1/012018.
- [26] L. Krzemień, M. Łukomski, Ł. Bratasz, R. Kozłowski, M. F. Mecklenburg, Mechanism of craquelure pattern formation on panel paintings, *Stud. Conserv.*, 2016; 61(6): 324–330. doi: 10.1080/00393630.2016.1140428.
- [27] B. Marcon, G. Goli, M. Fioravanti, Modelling wooden cultural heritage. The need to consider each artefact as unique as illustrated by the Cannone violin, *Herit. Sci.*, 2020; 8(1):24. doi: 10.1186/s40494-020-00368-1.

- [28] EN 15757:2010 - Conservation of Cultural Property - Specifications for temperature and relative. <https://standards.iteh.ai/catalog/standards/cen/ad03d50b-22dc-4c57-b198-2321863f3870/en-15757-2010>.
- [29] L. Uzielli, L. Cocchi, P. Mazzanti, M. Togni, D. Julien, P. Dionisi-Vici, The Deformometric Kit: A method and an apparatus for monitoring the deformation of wooden panels, *J. Cult. Herit.*, 2012;13(3): 94–101.
- [30] P. Dionisi-Vici, I. Bucciardini, M. Fioravanti, L. Uzielli, Monitoring climate and deformation of panel paintings in San Marco (Florence) and other Museums, COST IE0601 International Conference on Wood Science for Conservation of Cultural Heritage, Florence, Italy, 2009; 193–199.
- [31] P. Dionisi-Vici, M. Formosa, J. Schiro, L. Uzielli, Local deformation reactivity of panel paintings in an environment with random microclimate variations: the Maltese Maestro Alberto's Nativity case-study, COST IE0601 International Conference on Wood Science for Conservation of Cultural Heritage, Braga (PT), 2008.
- [32] L. Cocchi, G. Goli, P. Mazzanti, B. Marcon, L. Uzielli, The Lapidazione di Santo Stefano by Giorgio Vasari: the study of the wooden support's deformations as a contribution to restoration and future conservation, in *Proceedings of ESRARC 2014 6th European Symposium on Religious Art, Restoration & Conservation*, Florence (Italy), 2014.
- [33] L. Cocchi et al., Verifying the operation of an elastic crossbar system applied to a panel painting: the Deposition from the Cross by an anonymous artist from Abruzzo, sixteenth century, *Stud. Conserv.*, 2017; 62(3): 150–161. doi: 10.1080/00393630.2015.1137426.
- [34] I. Bremaud, J. Gril, Transient destabilisation in anisotropic vibrational properties of wood when changing humidity, *Holzforschung*, 2021; 75 (4): 328:344. doi: 10.1515_hf-2020-0029
- [35] S. Fortino, F. Mirianon, T. Toratti, A 3D moisture-stress FEM analysis for time dependent problems in timber structures, *Mech. Time-Depend. Mater.*, 2009; 13:333 doi: <https://doi.org/10.1007/s11043-009-9103-z>.
- [36] E. Choong, Diffusion coefficients of softwoods by steady-state and theoretical methods_Choong1965, *Diffus. Coeff. Softwoods Steady-State Theor. Methods*, 1965; 15(1): 21–27.
- [37] C. Skaar, *Wood-water relations*. Berlin: Springer-Verlag, 1988.
- [38] G. Christensen, The rate of sorption of water vapour by wood and pulp, *Appita J*, 1959; 13: 112–123.
- [39] J. Bodig, B. A. Jayne, *Mechanics of Wood and Wood Composites*. Van Nostrand Reinhold Publ., New York US 1982.
- [40] EDF - Électricité De France, *Finite element Code_Aster: Analyse des Structures et Thermo-mécanique pour des Etudes et des Recherches*. 2022.
- [41] T. Helfer, B. Michel, J.-M. Proix, M. Salvo, J. Sercombe, M. Casella, Introducing the open-source mfront code generator: Application to mechanical behaviours and material knowledge management within the PLEIADES fuel element modelling platform, *Comput. Math. Appl.*, 2015; 70(5): 994–1023. doi: <https://doi.org/10.1016/j.camwa.2015.06.027>.

- [42] M. Varnier, L. Ulmet, F. Dubois, N. Sauvat, Characterization and modeling of wood species sorption isotherms for use in civil engineering structures monitoring, In Review, preprint, 2022. doi: 10.21203/rs.3.rs-2113454/v1.
- [43] S. Merakeb, F. Dubois, C. Petit, Modeling of the sorption hysteresis for wood, *Wood Sci. Technol.*, 2009; 43(7): pp. 575–589. doi: 10.1007/s00226-009-0249-2.
- [44] H. L. Frandsen, Selected constitutive models for simulating the hygromechanical response of wood, Ph.D. thesis, Aalborg University, 2007.
- [45] H. Assimi, A. Jamali, A hybrid algorithm coupling genetic programming and Nelder–Mead for topology and size optimization of trusses with static and dynamic constraints, *Expert Syst. Appl.*, 2018; 95: 127–141. doi: 10.1016/j.eswa.2017.11.035.
- [46] N. E. Mastorakis, On the solution of ill-conditioned systems of linear and non-linear equations via genetic algorithms (GAs) and Nelder-Mead simplex search, in *Proceedings of the 6th WSEAS international conference on Evolutionary computing*, Stevens Point, Wisconsin, USA, 2005; pp. 29–35.
- [47] N. E. Mastorakis, Solving non-linear equations via genetic algorithms, *Proceedings of the 6th WSEAS Int. Conf. on EVOLUTIONARY COMPUTING*, Lisbon, Portugal, June 16-18, 2005. <https://citeseerx.ist.psu.edu/document?repid=rep1&type=pdf&doi=cc57ed0b649647f04da29af1e57fc6d2b435644f>, last checked December 2022.
- [48] M. Baudin et al., The graphical user interface of OpenTURNS, a UQ software in simulation, in *Proceedings of the 2nd International Conference on Uncertainty Quantification in Computational Sciences and Engineering (UNCECOMP 2017)*, Rhodes Island, Greece, 2017, pp. 238–257. doi: 10.7712/120217.5366.17143.
- [49] M. Baudin, A. Dutfoy, B. Iooss, A.-L. Popelin, OpenTURNS: An Industrial Software for Uncertainty Quantification in Simulation, *Handbook of Uncertainty Quantification*, 2017; 2001–2038. doi: 10.1007/978-3-319-12385-1_64.
- [50] Z. Kala, J. Kala, T. E. Simos, G. Psihoyios, Ch. Tsitouras, Z. Anastassi, Sensitivity Analysis of Stability Problems of Steel Structures using Shell Finite Elements and Nonlinear Computation Methods, *NUMERICAL ANALYSIS AND APPLIED MATHEMATICS ICNAAM 2011: International Conference on Numerical Analysis and Applied Mathematics*, Halkidiki, (Greece), 2011; 1865–1868. doi: 10.1063/1.3636974.
- [51] T. Cartailier, A. Ghaus, A. Janon, H. Monod, C. Prieur, N. Saint-Geours, Sensitivity analysis and uncertainty quantification for environmental models, *ESAIM Proc.*, 2014; 44: 300–321, doi: 10.1051/proc/201444019.
- [52] W. Du, S. Li, Y. Luo, Implementation of Sobol’s sensitivity analysis to cyclic plasticity model with parameter uncertainty, *Int. J. Fatigue*, 2021; 155: 106578. doi: 10.1016/j.ijfatigue.2021.106578.
- [53] X. Zhang, M. Trame, L. Lesko, S. Schmidt, Sobol Sensitivity Analysis: A Tool to Guide the Development and Evaluation of Systems Pharmacology Models, *CPT Pharmacomet. Syst. Pharmacol.*, 2015; 4(2): 69–79. doi: 10.1002/psp4.6.
- [54] A. Brandao, P. Perré, “The Flying Wood” – A quick test to characterise the drying behaviour of tropical woods, In: *Proceedings of the 5th International IUFRO wood drying conference*, Eds. Cloutier A., Fortin Y., Gosselin R., Quebec City, Canada 1996; 315–324.

Coupling numerical and experimental methods to characterise the mechanical behaviour of the *Mona Lisa*: a method to enhance the conservation of panel paintings

L. Riparbelli¹, P. Dionisi-Vici¹, P. Mazzanti^{1*}, F. Brémand², J.C. Dupré², M. Fioravanti¹, G. Goli¹, T. Helfer³, F. Hesser², D. Jullien⁴, P. Mandron⁵, E. Ravaud⁶, M. Togni¹, L. Uzielli¹, E. Badel⁷, J. Gril^{7,8}

¹ DAGRI, Università di Firenze, Florence, Italy

² Institut Pprime, Université de Poitiers, CNRS, Poitiers, France

³ CEA, DES, IRESNE, DEC, Cadarache F-13108 Saint-Paul-Lez-Durance, France

⁴ LMGC, Univ. Montpellier, CNRS, Montpellier, France

⁵ Ateliers d'Enghien, 12 rue d'Enghien 75010 Paris, France

⁶ C2RMF, Paris, France

⁷ Université Clermont Auvergne, INRAE, PIAF, Clermont-Ferrand, France

⁸ Université Clermont Auvergne, CNRS, Institut Pascal, Clermont-Ferrand, France

* Corresponding author. Email: paola.mazzanti@unifi.it

Highlights

- Integrating innovative numerical analysis and non-invasive experimental tests
- Numerical tool to optimize the conservation conditions of *Mona Lisa*'s wooden panel
- Analysing the internal stress state, and its safe limits, of the panel painting
- FEM numerical modelling for the mechanical characterisation of the artwork
- Assessment of the conservation *status* of panel paintings

Keywords: *Mona Lisa*, FEM modelling, numerical simulation, conservation of panel paintings, non-invasive experimental measurements.

Abstract

This paper presents the method through which a numerical FEM (Finite Elements Method) model was implemented in order to accurately represent the mechanical state and the response to climatic fluctuations of the panel of the *Mona Lisa*, as it is conserved in its exhibition case, and constrained in its auxiliary frame. The model is based on the integration of advanced numerical analysis and various experimental examinations carried out non-invasively on the artwork by the authors during over 15 years. This includes visual, microscopic and X-ray observations together with technological analyses. The latter were mechanical measurements and monitoring of both the deformations the panel undergoes and the constraining external forces acting on the panel itself.

Such integration made it possible (a) to characterise with totally non-invasive techniques the mechanical properties of the panel, and (b) to build a FEM model that reliably evaluate the strains and stresses that are generated in the real wooden panel following the various actions it experiences. The paper consists of the following parts: (i) a short summary of the experimental measurements and other observations, (ii) a detailed description of the FEM numerical model, of the hypotheses it is based on, and of its advantages and limits, (iii) the main results obtained by running the model. This includes the identification of local strains and stresses, the location of most critical areas, an evaluation of the risk that the existing ancient crack may propagate, and an evaluation of safe ranges for the forces acting on the wooden panel, (iv) the validation criteria for such results, and (v) a discussion about the significance of the mechanical model.

1. Introduction

In this section a very brief historical overview is presented, showing how the subject of this paper can be seen as the latest evolution of the integration process between sciences and technologies in the fields of wood, conservation, and engineering, applied to the conservation of panel paintings; bibliographic references having the function of exemplification, not of exhaustive listing.

Until the end of the 19th century (and even quite later) the conservation of the wooden supports was typically entrusted to the competence of more or less skilled cabinet makers. In few particular cases, some ingenious restoration solution was developed, based on the experience and intuition of the restorer artisans. Then, there is the risk that it could be imitated and applied in completely different contexts, with sometimes very negative long-term results.

Progressively, the studies on construction techniques were distinguished from the description of the restoration interventions, which, however, in general, inevitably constitute the starting point. A representative example of these different approaches is given by the 1995 Symposium on "The structural conservation of panel paintings", held in Los Angeles at The Getty Conservation Institute, [1].

Based on their own experience some restorers also worked to scientifically interpret their work and their observations (e.g., [2, 3]), or to propose solutions referring implicitly to engineering criteria (e.g. Part 4 of [1]).

Also, wide and in-depth studies of the engineering properties of the art materials (e.g. [4,5,6]) and on the influence of the surrounding micro-environment on the conservation of works of art (e.g. [7, 8, 9]) have been published worldwide, resulting in important guidelines and standards (e.g. [10, 11]) .

In recent decades several studies have been published, concerning mathematical models based on rational simplifications (including schematization of structures, homogeneity and known laws of behaviour of materials, published data on their properties) (e.g. [6, 12, 13, 14, 15, 16, 17, 18, 19, 20]), and on laboratory tests on mock-models, i.e. simplified physical models built *ad hoc* (e.g. [21, 22, 23]).

However, based on the above-mentioned works, the need of direct measurements of the behaviour of the real artworks has gradually emerged in order to better define and understand this behaviour, to directly derive the properties of the materials, and to validate the numerical models. Among these, the following may be cited by way of examples: some described the development of an *ad hoc* equipment aimed at monitoring deformation responses of real panel paintings to the environmental temperature (T) and relative humidity (RH) fluctuations (e.g.[21, 22]), others reported the results of this kind of medium-term or long-term monitoring activities [26, 27, 28, 29, 30].

Within this frame, since 2004, the wooden panel on which Leonardo da Vinci painted his *Mona Lisa* has been studied by an international research team under the request of the curators of the Louvre Museum. Several experimental campaigns have been carried out to observe, measure, monitor and understand its mechanical, hygroscopic and shape characteristics and behaviour, to evaluate its present state of conservation, and to provide related suggestions. The team, mainly formed by specialists in wood science and technology from Clermont-Ferrand (F), Florence (I) and Montpellier(F), and in optical measurements from Poitiers (F), closely interacted with the curators of the Louvre Museum, associated scientists and restorers taking care of the artwork.

The work of the team was developed according to the following main tightly intertwining topics:

- i. studying the artwork by direct observation and measurements (typically once a year, during the few hours when the *Mona Lisa* panel is out of its climate-controlled display case, for the routine inspection of its conservation conditions, or for the execution of specific studies or measurements) [31];
- ii. monitoring the mechanical behaviour (namely forces and deformations) of the panel during its permanence in the exhibition case, by special ad-hoc equipment, conceived and implemented specifically for this task [31];
- iii. developing, calibrating and validating numerical models based on the first two points observations, to characterise, reproduce and deeply understand the original artwork's behaviour, as consequence of external hygroscopic and/or mechanical actions that might (actually or hypothetically) occur.

The third topic, namely the methods for the development of an innovative numerical model, is the main subject of this paper. The two first topics will also be recalled in the following, since they are an indispensable basis for understanding.

The methodological approach we propose for the numerical analysis of a real panel painting takes into account the following directly observed characteristics in order to reflect the actual behaviour of the artwork:

- analysis of the construction techniques of the artwork, different for periods, schools and workshops in which it was assembled;
- knowledge of the current conservation techniques and methods;
- assessing of the actual shape of the painting;
- technological study of the panel: identification of the wood species and the cut of the board;
- observation of the damages (such as the crack) that occurred in the past and their consequences on the artwork;
- study of the dynamics of contact between the artwork and any stiffening elements such as frames and crossbeams, to name a few;
- study of the reaction of the panel to applied forces and solicitations in general.

A fundamental aspect is the importance of the mechanical characterisation of an artwork. However, destructive or invasive tests are unacceptable. Thus, innovative methods are required to mechanically characterise the different components such as the wood, the ground and the paint layers.

In this paper, the numerical analysis is focused only on the mechanics in order to answer the question of its current state of conservation. The study of the hygro-mechanical behaviour of the artwork will be discussed in a future publication.

The first results of such work have been published in [31, 32, 33, 34, 35, 36, 37], showing the relevance of integrating innovative computational tools with experimental data directly obtained from the original artwork being studied.

This approach, which has been gaining ground in recent years, has necessarily required mutual trust and collaboration among scientists, conservators and restorers, and can be considered as an important step towards fully integrating this kind of research for the in-depth knowledge and conservation of the physical structure of the wooden artworks.

In such framework, the considerable difficulties found in fully interpreting the results of the experimental observations and measurements have highlighted the complexity of the phenomena observed, and the variability from case to case of the observed behaviours. On one hand, these difficulties have confirmed the uniqueness (i.e. non-generalizability) of each artworks also from the material and behavioural point of view (see e.g.[38]) . On the other hand, it appears that this

complexity can be optimally addressed not in a preconceived way, but rather by integrating in an innovative way (as in this paper) the experimental results and adequate computational tools.

2. Aims

This paper describes an innovative method developed in the framework of a project lasting for over 15 years, originated by the curators of the Louvre Museum, aiming to improve the knowledge and optimize the conservation conditions of the *Mona Lisa* wooden panel.

The method is based on the integration between advanced numerical analysis and several experimental examinations carried out non-invasively on the artwork during the project. This paper briefly summarises such examinations, provides details of the numerical model, its validation by means of the experimental data, and its actual or potential developments. The main aims are a) to provide a tool capable to characterise a real panel painting and b) to evaluate the internal stress state of the wooden support, and its safe ranges, deriving from applied forces or climatic variations; so that well-motivated decisions for optimizing its conservation conditions can be made.

Among other beneficial outcomes, the numerical model has already provided valuable technical guidelines for the design of a mechanism (recently implemented in the *Mona Lisa*'s auxiliary frame) to automatically limit the forces acting on the wooden support within safe ranges.

3. Materials and Methods

In this section, all the specificities of a real panel painting are analysed, specifically by observing and measuring them directly, in a non-invasive manner, associating them with the numerical modelling tools.

3.1 Short recall of *Mona Lisa*'s wooden structure and measurement equipment

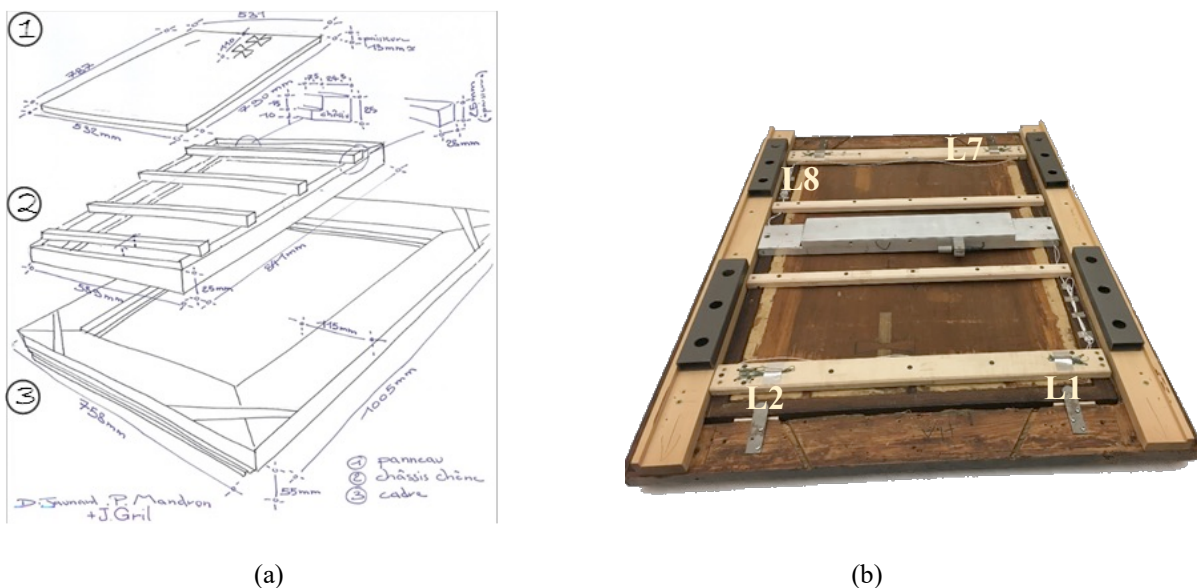


Figure 1 (a,b) - (a) Exploded view and metric survey by the Restorers D. Jaunard and P. Mandron in 2004, later modified by J. Gril [31], showing the various elements which made up the *Mona Lisa* assembly before 2005: (1) Panel, on which

the crack, the “butterflies”, and the convexity are shown; (2) auxiliary frame (*châssis-cadre*) formed by battens with L-shaped section, and four crossbeams, only the top and bottom ones forcing against the Panel because of its out-of-plane distortion; (3) carved and gilded frame (*cadre*), fully visible from the front. (b) Overall view of the back of the assembled system in 2019. Top and bottom crossbeams are equipped with the four miniature load cells installed in 2013 in the four contact locations L1 - L2 - L7 - L8. The aluminium case housing the deflection transducers and the electronic equipment is also shown.

The *Mona Lisa*, painted approximately in the years 1503-1506, is almost unaltered and well preserved despite the several accidents that occurred to throughout its centuries-old existence [32].

The paint layers are applied on the “external” face (that is, the face away from the pith of the trunk from which the board was obtained) of a flat-sawn poplar (*Populus alba* L.) panel, measuring 794 x 534 x 13 mm. The panel is curved both longitudinally and transversally, with the convexity towards the front face. It is pressed against the rim (*feuillure*) of the intermediate auxiliary frame (*châssis-cadre*, see Figure 1a) by two crossbars screwed onto the auxiliary frame itself. The auxiliary frame, with the panel inside, is in turn hosted and pressed by metal brackets in a carved and gilded external wooden frame. An ancient radial-longitudinal crack runs through the wood thickness from the top edge of the panel down to the Lady’s forehead. Two wooden “butterflies” have been inlaid, possibly during the 19th century, into the panel’s thickness to prevent any longitudinal propagation of the crack, one of them now missing and being replaced by a glued canvas strip.

Figure 1b shows an overall view of the back of panel with the four maple wood crossbeams and the aluminium case as it was in 2019. The *Mona Lisa* was equipped to monitor both the deformations that the panel undergoes (mainly produced by the inevitable small climatic fluctuations within the display case) and the constraining forces acting on the panel itself. Such equipment includes load cells hosted in the top and bottom crossbeams and further instrumentation (transducers, data-logger, and further electronics) housed in a closed and robust aluminium case fixed on the auxiliary frame at mid-height, facing but not touching the back of the panel. Case and crossbeams were re-designed and replaced several times according to the evolution of the instrumentation, and the measurement methods are in-depth described in [31].

3.2 Optical Measures

The shape to be used to create the geometrical model was determined by the method of fringe pattern profilometry (FFP, Figure 2). This technique [39, 40] consists in projecting a series of parallel sinusoidal lines on the panel, recording the fringes by a camera, analysing how the panel itself deforms the fringes. An ad hoc developed method permits to obtain accurate measure, with an accuracy of nearly 0.03 mm for a resolution of 0.45 mm/pixel. From this method, two-point clouds have been created, which are the front and the back of the panel. As both were elaborated in the same reference system, it was possible to reconstruct the whole 3D shape, including the right variable thickness.

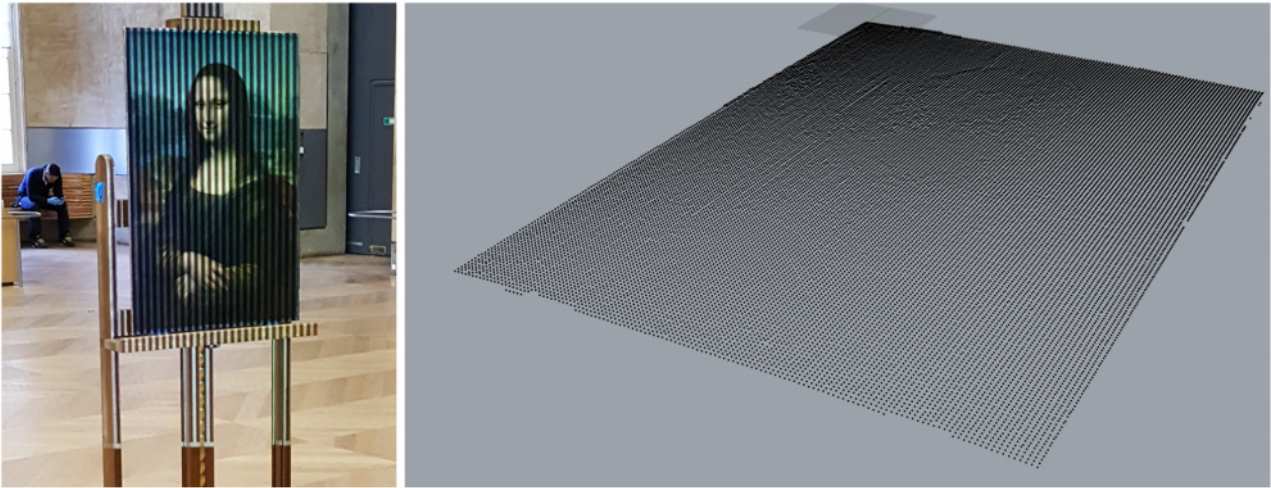


Figure 2 Optical Measurement of the shape (left) and point cloud of the surface (right).

3.3 Force and Displacement Measures

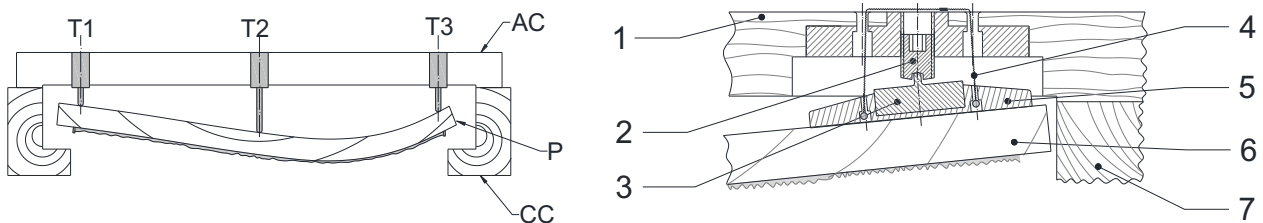


Figure 3 On the left the system to measure the deflection of the wooden panel (P) by means of 3 potentiometric linear transducers (T1, T2 and T3). AC is the aluminium case hosting the measurement system and CC is the auxiliary frame (*châssis-cadre*). On the right the system to measure the forces exerted between the panel and the restraining system: 1 wooden crossbeam, 2 steel grub screw, 3 load cell, 4 string, 5 presser, 6 wooden panel, 7 auxiliary frame (*châssis-cadre*). [31]

In order to produce the numerical model, more detailed information was necessary about the mechanical behaviour of the panel. A force-deformation test was performed during a “*Journée Joconde*”, to observe the elastic behaviour of the panel from which the stiffness properties can be derived. Since the forces were already measured by four load cells mounted on the ends of the “upper” and “lower” crossbeams [31], a slight variation of forces was produced by screwing or unscrewing the grub screw there inserted (element 2 in Figure 3). With the lifting, or lowering, of the grub screw and its precise measuring, it is possible to correlate them to the force variations and hence a force-deformation behaviour could be determined. In order to carry out such test, a specific measuring device was planned at DAGRI (University of Florence), named *Jocondometer* [31]. This made-on-purpose device measures the lifting or lowering of the grub screw that pushes on the load cell in which it is inserted [31].

Before carrying out the tests, two aspects were considered not to affect the reliability of the results: a) possible parasite contacts between the auxiliary frame and the borders of panel and b) the mechanical interaction between the panel and the auxiliary frame. The possible contacts between the auxiliary frame and the panel edges were checked all around the panel by inserting a feeler gauge of 0.1 mm and no contacts were observed. The other question was to exclude the mechanical contribution of the auxiliary frame to the test, so it was stiffened by fastening on it a 20 mm thick MDF panel. Finally, the experimental test was carried out through screwing or unscrewing the grub head screw by 0.25 mm on one load cell at a time, while the other three remained unchanged. Each

step variation of force was recorded with an acquisition rate of 1 sec [31]. When the test was completed for one measuring point, the load cell was repositioned to the value of the display condition and the same experimental procedure was applied to the other measuring points.

3.4 Contact zones identification

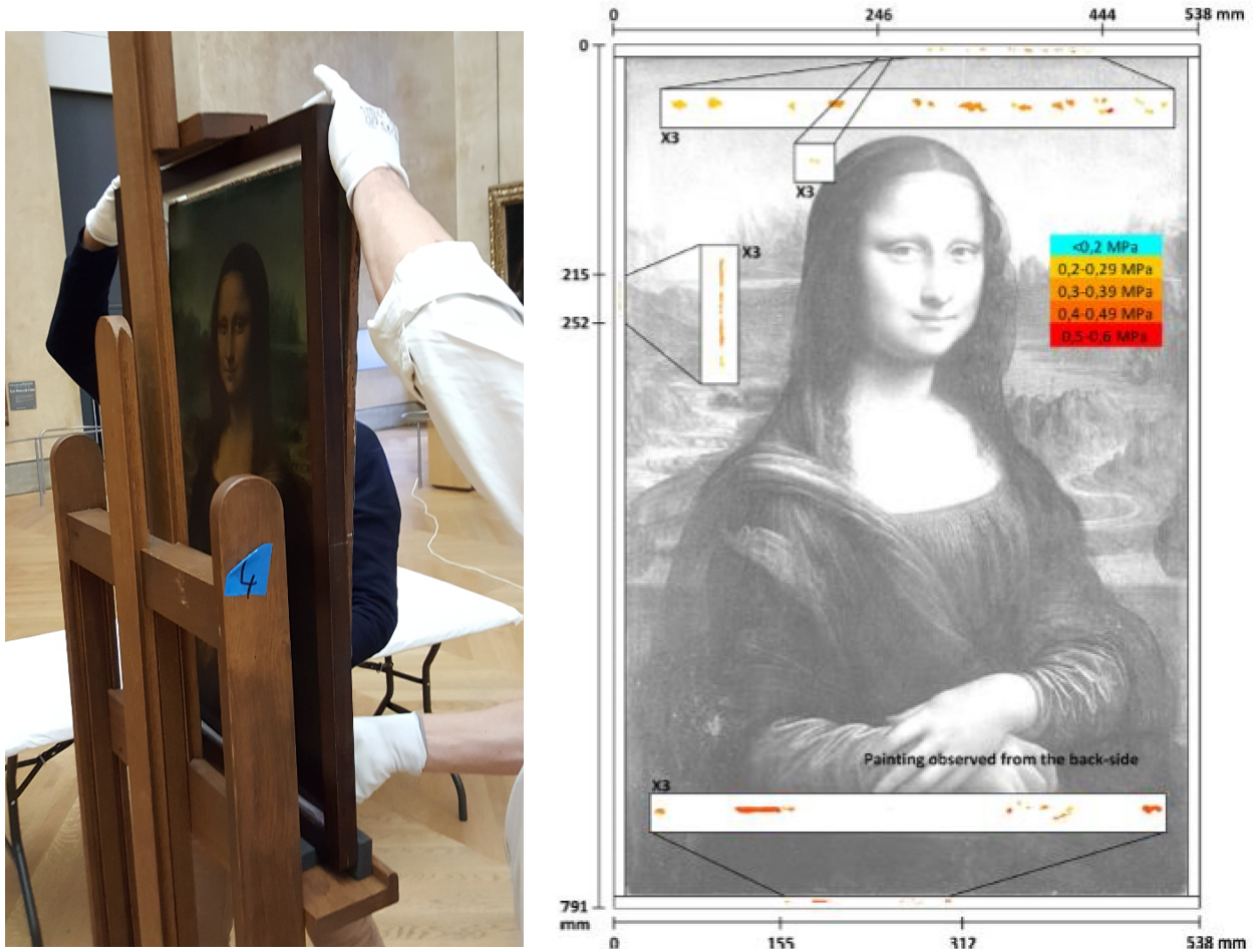


Figure 4 Pressure sensitive film experimental campaign (left) and contact zone detected (right) [41].

In 2012 a specific campaign described in [41] was made to assess the contact zones and pressures of the panel when inside the auxiliary frame. The measurements were made using a Pressure-Sensitive Film (Prescale®). The film is made of two strips, one with colour micro-spheres and the other with a developing material. In brief, thanks to the fact that the two films are interposed inside a mechanical coupling, they show a colour map of the contact zones with a red scale indicating point-by-point the scalar value of the pressure, in a non-invasive way.

Figure 4 shows the results; three main contact zones are present, that confirm the convexity of the panel toward the front.

3.5 Observation of the anatomy of the panel and its modelling

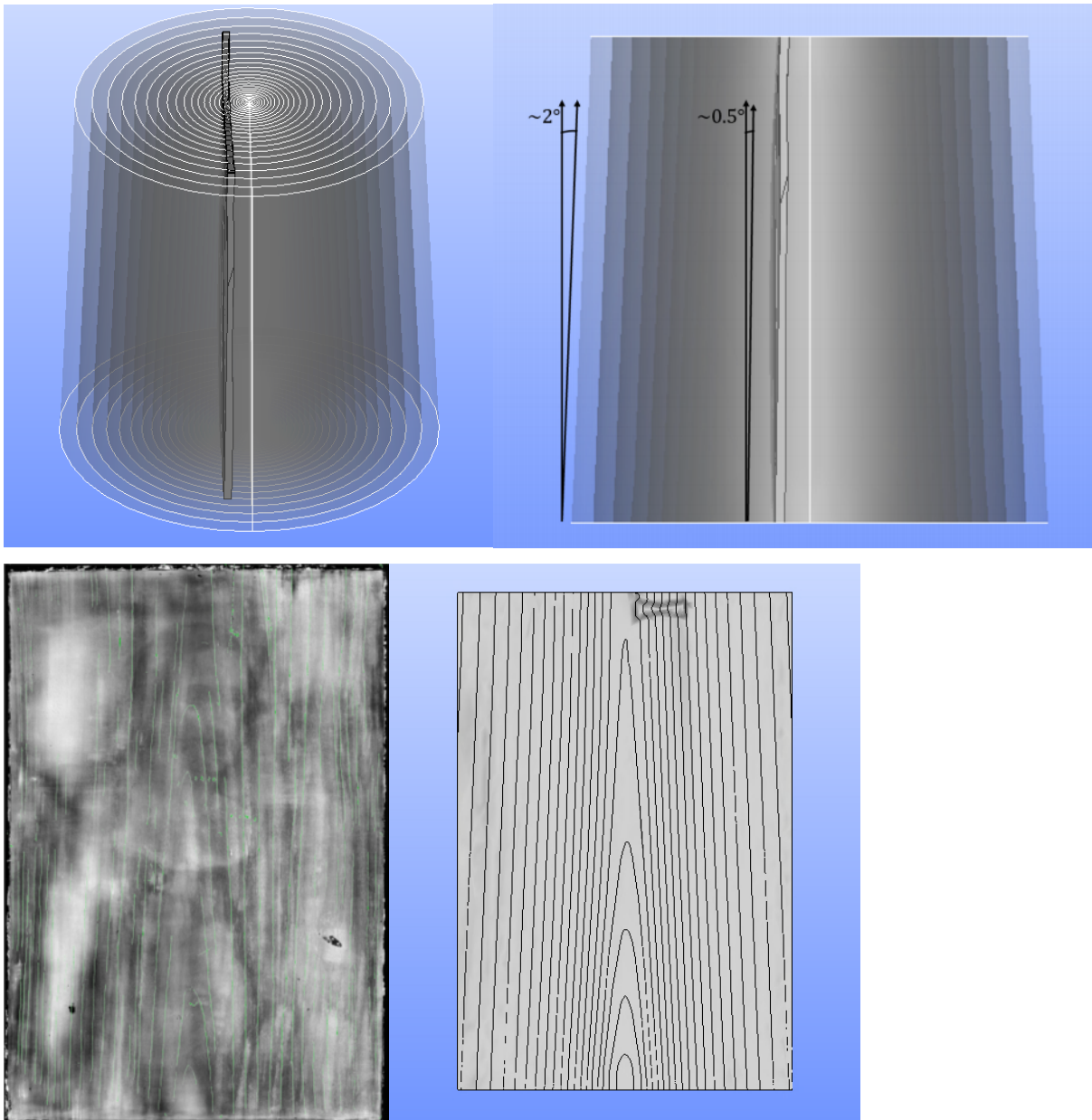


Figure 5 Trace of the annual rings on the surface (down) and identification of the position of the plank inside the original trunk (up), confirmed by the RX image and the drawing based on.

It is well known that wood shows a strongly anisotropic behaviour for mechanical and hygroscopic properties [42, 43]. This is always a challenge and an aspect of paramount importance in modelling. Thus, it is of great importance to study the tree orientation of the panel. The localization within the trunk was carried out through an optimization process based on the experimental measurements of the growth rings visible on the edges, and of the X-ray images [35]. Two variables were associated with this experimental evidence: the possible angle of inclination of the panel with respect to the pith axis and the angle of development of the conical surfaces of the growth rings in the plant height. This geometric optimisation, carried out using the open source 3D modelling software SalomeMeca, developed by Electricité de France [44], made it possible to visually identify a best match for a 4% (2 sexagesimal degrees) inclination of the conical surfaces of the growth rings and a 1% (0.5 sexagesimal degrees) inclination of the panel with respect to the pith axis, i.e. the cutting angle. A

value of 8% of the original tree taper was therefore identified, a plausible value for the lower part of a large poplar tree grown in isolation.

To consider the correct anatomical directions of the panel, we decided to represent the elasticity of the solid in a cylindrical reference, proceeding to a point-by-point definition of the compliance matrix based on the cylindrical coordinates centred in the pith of the trunk that generated the panel. Taking into consideration an orthonormal reference system consisting of the three axes x_1 , x_2 , x_3 , which in the case of the anatomy of the wood and the construction of this model were identified respectively as radial, tangential and longitudinal, for each point of the continuum a θ angle of reference based on the observed position of the pith was defined.

The mechanical behaviour of the wooden panel was assumed hereafter to follow an orthotropic elastic behaviour characterised by 9 elastic coefficients that were identified by an inverse approach in Section 3.8.

This behaviour has been implemented using the MFront open-source code generator [MFrontA, MFrontB] [45, 46] as described in Appendix A.

Thus, each material point of the continuum saw its elasticity, intended as the fourth-order compliance tensor, rotated in the RT plane according to its position with respect to the pith to represent radial and tangential anisotropy, and in the LR plane to represent the conicity of evolution along the height of the growth rings

3.6 Geometrical shape and discretization

The surfaces of the front and back have been reconstructed starting from the point clouds inside Rhinoceros [47] and then exported to the open-source 3D modelling platform Salome-Meca, from which the 3D body has been built. Through Boolean operations and partitions the body was enriched with the contact surfaces described in Section 3.4, the fracture and the butterfly described in Section 3.1. The model of the panel was then positioned with respect to the origin of the axes according to the observations in Section 3.2 and an additional body was inserted consisting of the front part of the *châssis-cadre*. In the geometric model, a surface layer of 0.2 mm was considered to represent the ground layer of the *Mona Lisa*, such value being an approximation obtained from direct observation. To such surface layer, specific mechanical characteristics were added, different from the wood panel ones.

The numerical model was built by meshing this body with a Netgen algorithm, computed within Salome-Meca. The following criteria were adopted for the construction of the mesh:

- Maximum Aspect Ratio: 5
- Minimum Angle: 4 degrees
- Maximum Warping: 4 degrees
- Minimum Transition Factor: 0.4

Additionally, refinements of the discretization were required for the internal surfaces of the fracture, for the contact surfaces between the butterfly and the panel painting, for the auxiliary frame and the panel painting contact areas, and finally for the areas that showed accentuated curvatures such as the edges or imperfections of the back.

The mesh was refined close to the contact zones with the load cells at the back.

The resulting mesh was composed of 441999 second-order 10 nodes-tetrahedrons.

The ground and paint layers were modelled with two-dimensional elements, in accordance with the Kirchhoff-Love theory, that share their nodes with the nodes of the wood surface elements. The thickness used in the model for these surface elements was 0.2 mm. This parameter is very uncertain and variable inside an artwork, however, in the *Mona Lisa* it was observed that it is thin and made only of *blanc de plomb*. The modelling choice for the ground and paint layers was therefore to consider them as a single layer with homogeneous mechanical characteristics and in the overall mechanical relationship with the wooden support as a composite with perfect adherence of the two surfaces.

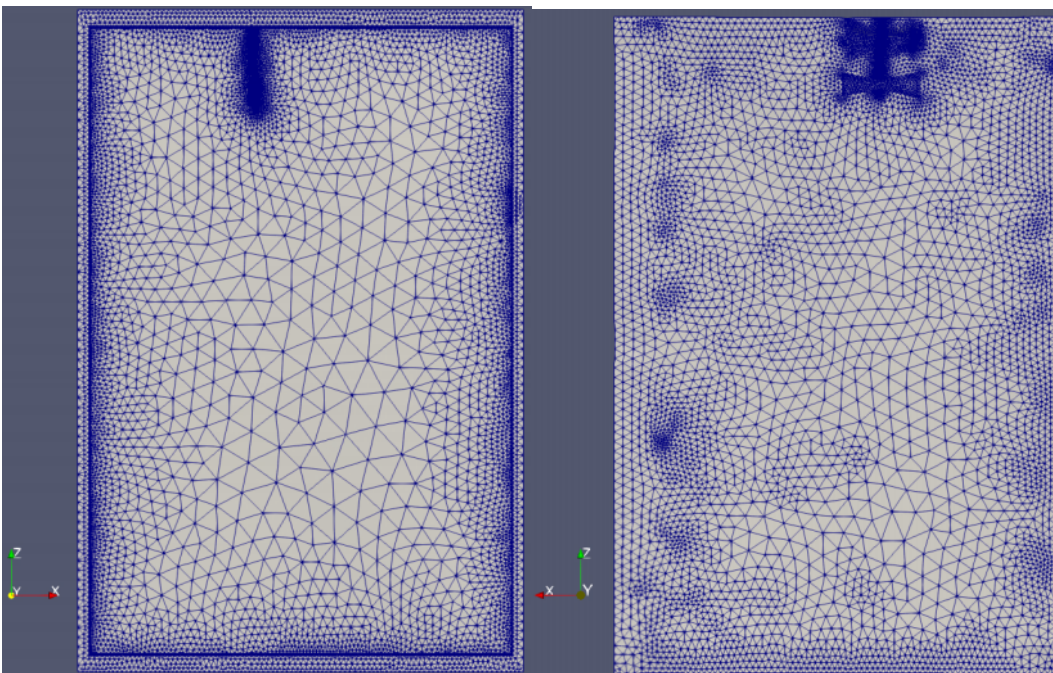


Figure 6 Geometrical discretization of the wooden panel. The refinement of the mesh was increased in the zones that show spatial particularities.

3.7 Nonlinear analysis with contact mechanics

Finite element analyses were performed with the opensource solver code `_aster`, developed by EDF [44]. This tool was used for its high level of industrial validation, the quality of the algorithms in case of mechanical contacts, the possibility to run in parallel allowing to solve large problems in a reasonable time, and above all the fact that it works as a low level programming language allowing integrating directly blocks of code and custom algorithms. Moreover, the opensource licence ensures transparency and replicability of the numerical methods.

To consider the correct behaviour of the panel with the auxiliary frame in which it is inserted, it was decided to carry out analyses that consider nonlinear contact, with friction.

The numerical treatment of the contact-friction phenomenon was dealt with a Stabilized Lagrangian formulation [48] following the law of Signorini-Coulomb, which from the operational point of view provides two defined surfaces in correspondence of the contact zone, commonly called master and slave, at which to enforce the contact condition means to prevent the slave nodes to penetrate the

master surfaces. In the light of this assumption, in order to ensure a solid and rapid convergence of the non-linear solution, the following logic was considered for the choice of contact surfaces [49]: the one that presented the lower rigidity in the direction normal to contact, the one with the lower area, or the one with a less fine mesh compared to the other, was chosen as the slave surface between the two in contact (result in Figure 7). The contact areas detected by the pressure sensitive film (Section 3.4) were then inserted as slave contact areas, leaving the upper edge of the auxiliary frame as the master surface.

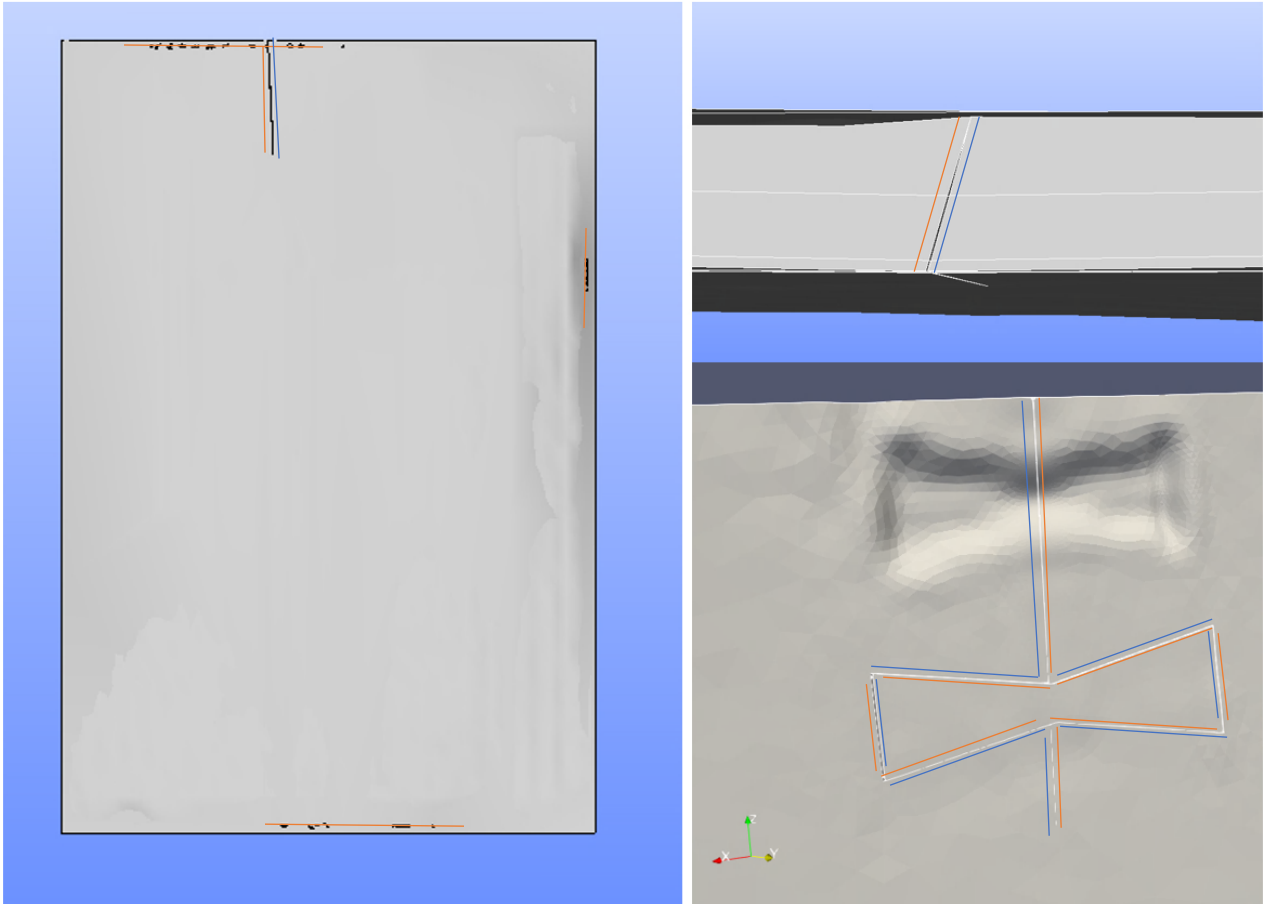


Figure 7 Contact zones: in red the slave surfaces, in blue the master surfaces

3.8 The optimization scheme

To determine the mechanical characteristics of the panel and of the ground and paint layers an iterative optimization technique was used.

A cost functional J is introduced, dependent on c , vector of the n parameters to be identified:

$$J(c) = \|d - d_{exp}\| \quad (1)$$

where d are the numerically calculated reactions in the position of the load cells, d_{exp} are the corresponding mechanical reactions experimentally determined and $\|\cdot\|$ is a norm on L , space of the observable values.

Substantially the inverse identification is a minimization of the cost functional $J(c)$ where we want to find $c^* \in O$, closed convex of \mathbb{R}^n .

$$J(c^*) = \min_{c \in O} J(C) \quad (2)$$

Minimisation was performed by means of a technical solution [50] based on the succession of a genetic algorithm followed by a Nelder Mead-type [32,33] minimisation scheme. This proves to be a very effective method [51] for finding solutions where, in general, a small variation in the coefficients objects of the minimization, generates considerable variations in the results.

The wood part is assumed to behave elastically according to cylindrical orthotropy, with a compliance matrix expressed in the following way:

$$\underline{\underline{S}}_{ij}^* = \begin{pmatrix} aS_{11}^0 & \sqrt{ab}S_{12}^0 & \sqrt{ac}S_{13}^0 & 0 & 0 & 0 \\ \sqrt{ab}S_{12}^0 & bS_{22}^0 & \sqrt{bc}S_{23}^0 & 0 & 0 & 0 \\ \sqrt{ac}S_{13}^0 & \sqrt{bc}S_{23}^0 & cS_{33}^0 & 0 & 0 & 0 \\ 0 & 0 & 0 & \sqrt{bc}S_{44}^0 & 0 & 0 \\ 0 & 0 & 0 & 0 & \sqrt{ac}S_{55}^0 & 0 \\ 0 & 0 & 0 & 0 & 0 & \sqrt{ab}S_{66}^0 \end{pmatrix} \quad (3)$$

where $\underline{\underline{S}}_{ij}^*$ is the optimized compliance tensor, S_{ij}^0 components of the compliance matrix estimated based on the actual mean density of around 450 kg/m³ [43], and a, b, c are constant coefficients affected by the optimization. The preparation layer behaves according to isotropic elasticity, with a Young's modulus $E_{GROUND} = d$ GPa, where d is coefficient also subjected to optimization, and a Poisson's ration ν_{GROUND} set to a fixed value of 0.2.

A sensitivity preliminary test, that we omit, has been conducted to assure the significance of the choice of the variables for this specific mechanical numerical problem, with positive result.

4. Results and validation

The iterative optimization process led to identify the values of rigidity of the main anatomical wood directions (longitudinal, radial and tangential) and rigidity of the ground+paint layer (Table 1)

Table 1 Initial and optimized value of rigidities.

Rigidity	Initial values	Optimized values
$E_L = \frac{1}{S_{11}^0}$	10.06 [GPa]	9.60 [GPa]
$E_R = \frac{1}{S_{22}^0}$	1.19 [GPa]	1.02 [GPa]
$E_T = \frac{1}{S_{33}^0}$	0.58 [GPa]	0.73 [GPa]
$\frac{E_L}{\nu_{LR}} = \frac{E_R}{\nu_{RL}} = \frac{1}{S_{12}^0}$	28.25 [GPa]	31.33 [GPa]

$\frac{E_T}{\nu_{TL}} = \frac{E_L}{\nu_{LT}} = \frac{1}{S_{13}^0}$	21.40[GPa]	19.70 [GPa]
$\frac{E_R}{\nu_{RT}} = \frac{E_T}{\nu_{TR}} = \frac{1}{S_{13}^0}$	1.69 [GPa]	1.76 [GPa]
$G_{RT} = \frac{1}{S_{44}^0}$	0.2 [GPa]	0.21 [GPa]
$G_{LR} = \frac{1}{S_{55}^0}$	0.64 [GPa]	0.59 [GPa]
$G_{LR} = \frac{1}{S_{66}^0}$	0.86 [GPa]	0.95 [GPa]
E_{GROUND}	1. [GPa]	1.96 [GPa]
ν_{GROUND}	0.2	Not subjected to optimization

For the ground and paint layers an isotropic Young modulus of 1.96 GPa was identified, value that is consistent with [52].

A process of evaluation of these results was made to ensure the consistency of the numerical model with the experimental evidence.

Table 2 shows the comparison between the experimental reading and the numerical result on the numerical model (Section 3.3) of the reactions generated on each load cell for an increment of vertical displacement of 0.25 mm, with a good matching, with a notable difference only on L8.

Table 2 The experimental (Section 3.3) and numerical values of the rigidity of the panel are reported, together with their difference.

Load Cell	Experimental values [N]	Numerical values [N]	Difference [N]
L1	8.58	8.61	0.03
L2	5.37	5.49	0.02
L7	6.46	6.42	-0.04
L8	7.94	7.53	-0.41

The validation of the predictive model was done by comparing the measurements of the central transducer with the computations, in the same points, of the displacements perpendicular to the plane of the panel. For an increment of force of 5 N on the load cell L2, the vertical displacement in the transducer T3 was measured and computed, then the process was repeated applying the same increment in L8 and reading the displacement again in T3.

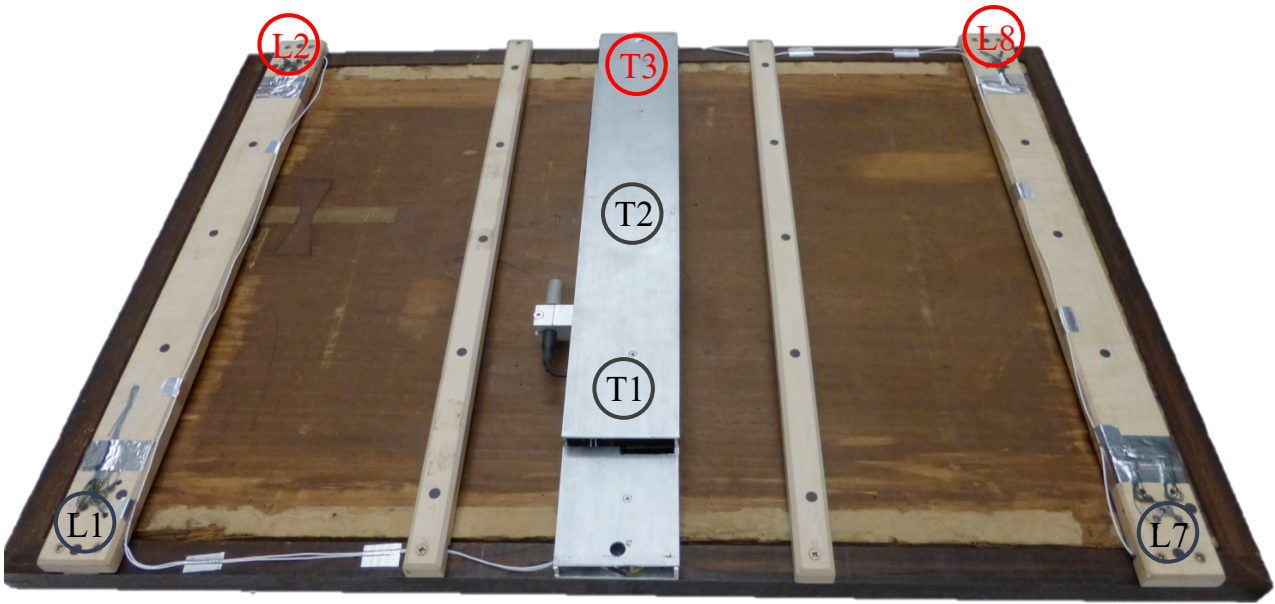


Figure 8 Position of load cells (L1-L8) and transducers (T1-T3). L2, L8 and T3 are the locations used for the FEM model validation.

Table 3 and Table 4 show the results of this procedure with a good matching.

Table 3 The vertical displacement measured and computed in T3, a force variation was applied in L2.

Force variation L2 [N]	Experimental displacement T3 [mm]	Numerical displacement T3 [mm]
5	0.077	0.070

Table 4 The vertical displacement measured and computed in T3, a force variation was applied in L8.

Force variation L8 [N]	Experimental displacement T3 [mm]	Numerical displacement T3 [mm]
5	0.053	0.049

A further evaluation of the accuracy of the model was carried out from optical measurements. However, the comparison can only be made qualitatively, considering that the deformations obtained are conditioned by an albeit slight deformability of the contact zones due to the bending and torsional distortion of the *châssis-cadre*. The effect of this difference is easily seen in the lateral contact areas:

while in the model they are at a constant and equal height to the other contacts, in the optical shots they change their mutual height depending on the stiffness of the *châssis-cadre*.

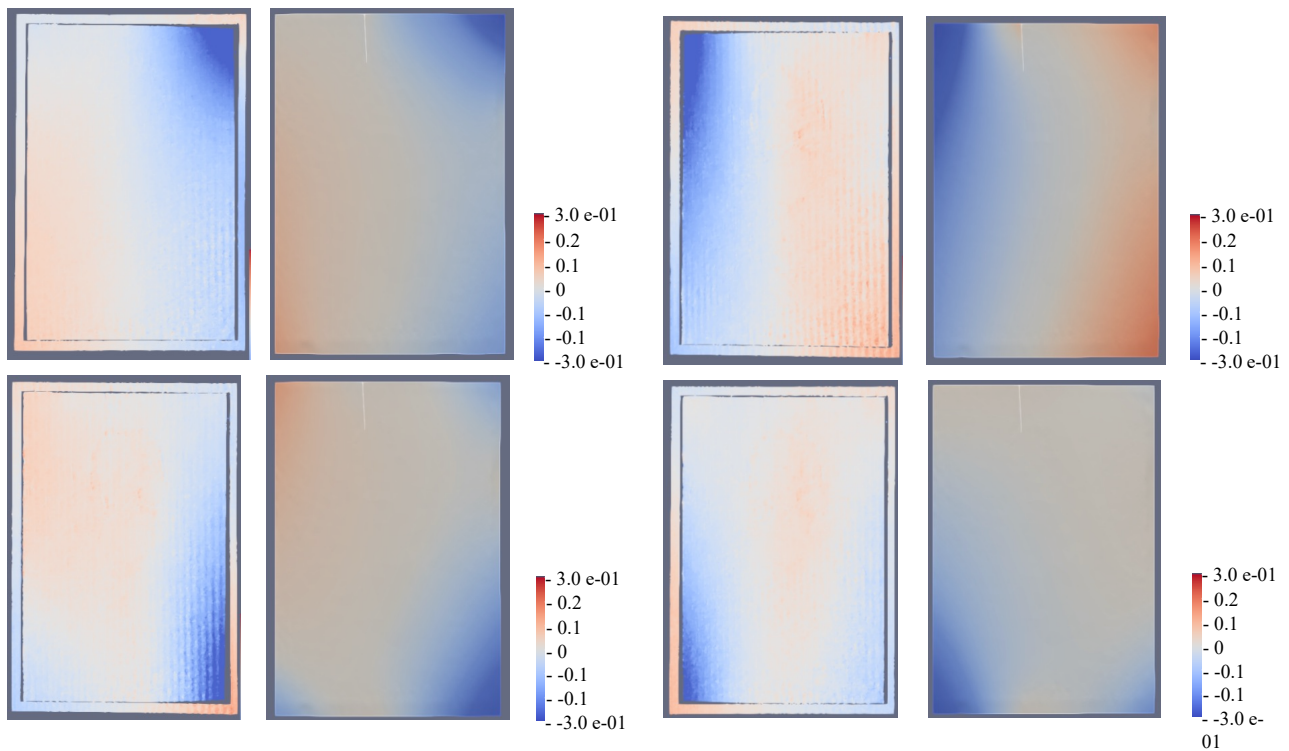


Figure 9 - Comparison between optical measurements and numerical model. For each couple of images it is displayed the out-of-plane displacement [mm], on the left the optical measurement results and on the right the numerical model results. The images are front view; thus, the auxiliary frame is clearly visible on the optical measurements. Four cases are presented characterised by a specific boundary condition each one (clockwise) given by decrements of 9.48 N for position 1 (top left), 5.54 N for position 2 (top right), 8.17 N for position 7 (bottom left), 7.48 N for position 8 (bottom right), respectively.

The four cases shown in Figure 9 represent four different boundary conditions given by decrements of 9.48 N for position 1 (Figure 9a), 5.54 N for position 2 (Figure 9b), 8.17 N for position 7 (Figure 9b), 7.48 N for position 8 (Figure 9b), respectively.

Despite the limitations of the comparison discussed above, we can see that the behaviour of the panel is extremely close between optical imaging and numerical modelling. Again, it allows us to consider the elaborated model to be very close to the physical reality of the *Mona Lisa* support.

5. Discussion

The model presented in this study does not consider the hygroscopic and moisture-dependent behaviour of the panel, but despite this, as the climatized display case of the *Mona Lisa* at the Louvre Museum keeps the humidity and temperature values extremely constant, the developed model can be used to understand directly the tensional and deformation states of the panel painting in its standard conservation conditions.

It should be emphasised that a panel left free of stiffening tends to develop a permanent curvature due to the hygroscopic oscillations to which it is invariably subjected in its storage environment, and that this phenomenon is known in the industry as compression set [53, 54]. To avoid permanent deformations typically induced by compression set phenomena, forces are normally applied to the panel by the restraining system, in our case the *châssis-cadre*. Such forces are considered as the boundary condition for the numerical models presented in this Section.

Table 5 The forces applied by the restraining system to the *Mona Lisa* measured by the load cells.

Location	L1	L2	L7	L8
Measured forces [N]	7	15	17	11

A first level of results to be discussed are the main directions of deformation at the interface between wood and preparation. In Figure 10 the principal deformations are recalling briefly that these represent the directions in which the wood is subjected to simple contraction or extension (without shear deformations) and that the deformations have a maximum value in these directions. It should be clarified that at the interface between pictorial layers and wood, deformations, considering a principle of perfect adherence between the two layers and material coherence, present the same values; the same cannot be said for stresses, which in general do not present the same values at the interface, the two materials having different constitutive models (isotropic pictorial layers, orthotropic wood).

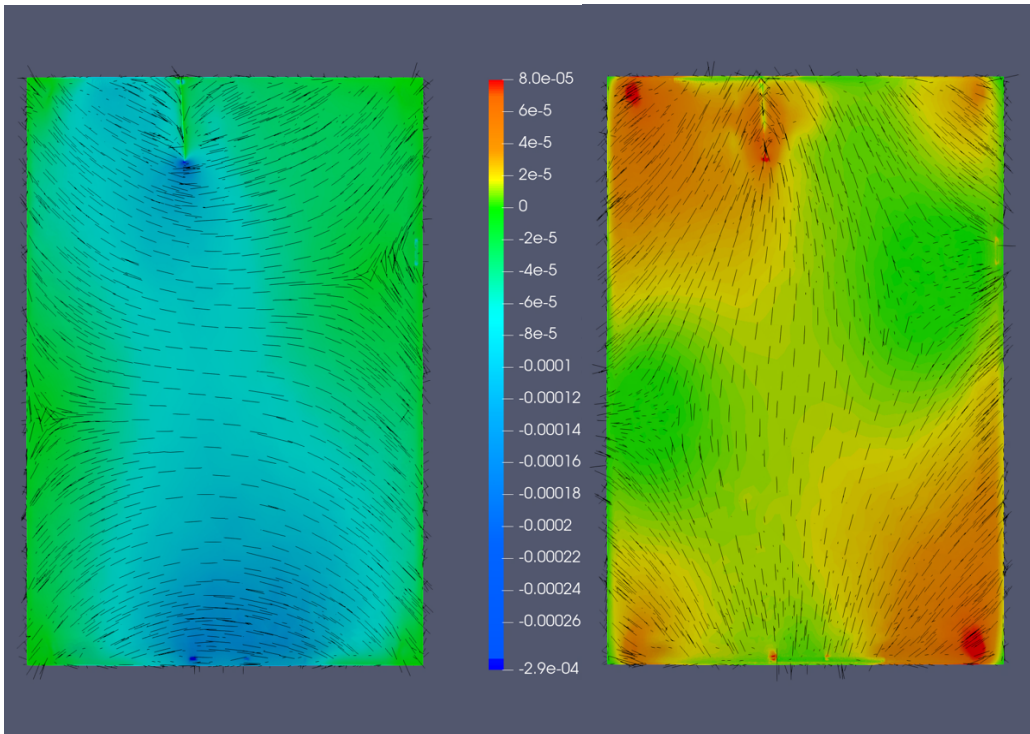


Figure 10 Principal strains directions and related values at the interface between wood and pictorial layers. In blue the contraction strains, in red the extension strains.

These values are much lower than the values identified in the literature [55] for the damage of the ground layer, and therefore it confirms the efficiency of the current conservation method at the Louvre Museum. Moreover, the isostatic deformations show a verifiable analogy with the direction of the painting's craquelure detected [34] and it is shown in Figure 11.

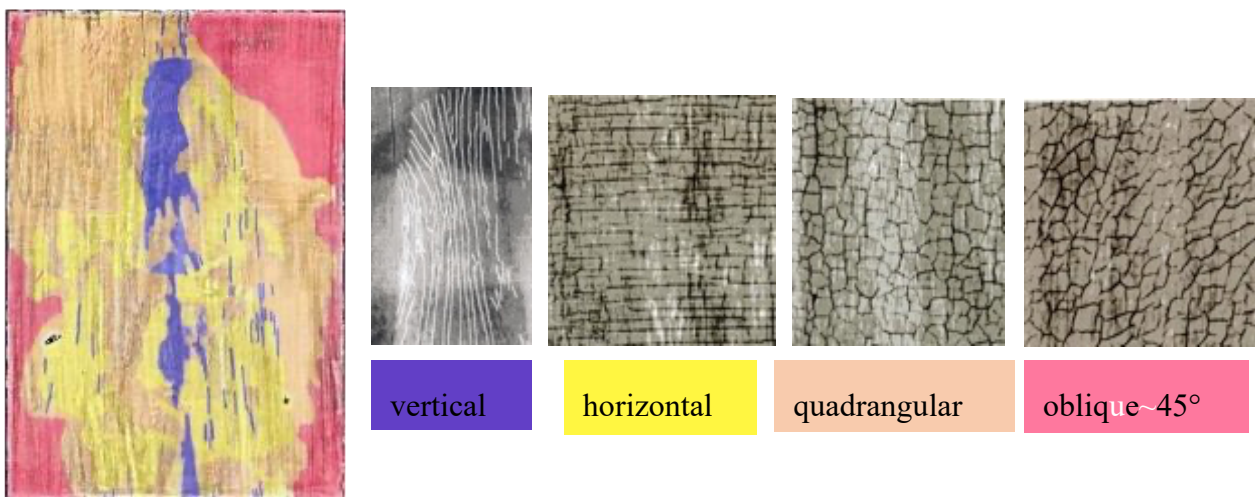


Figure 11 Distribution of the craquelure and pattern observed in the panel.

Regarding the fracture, it occurred in the first decades of the artwork's life [35]. The main directions of deformation in the area of the fracture, which also have a pattern compatible with the craquelure, confirm that the fracture occurred before the formation of the craquelure itself.

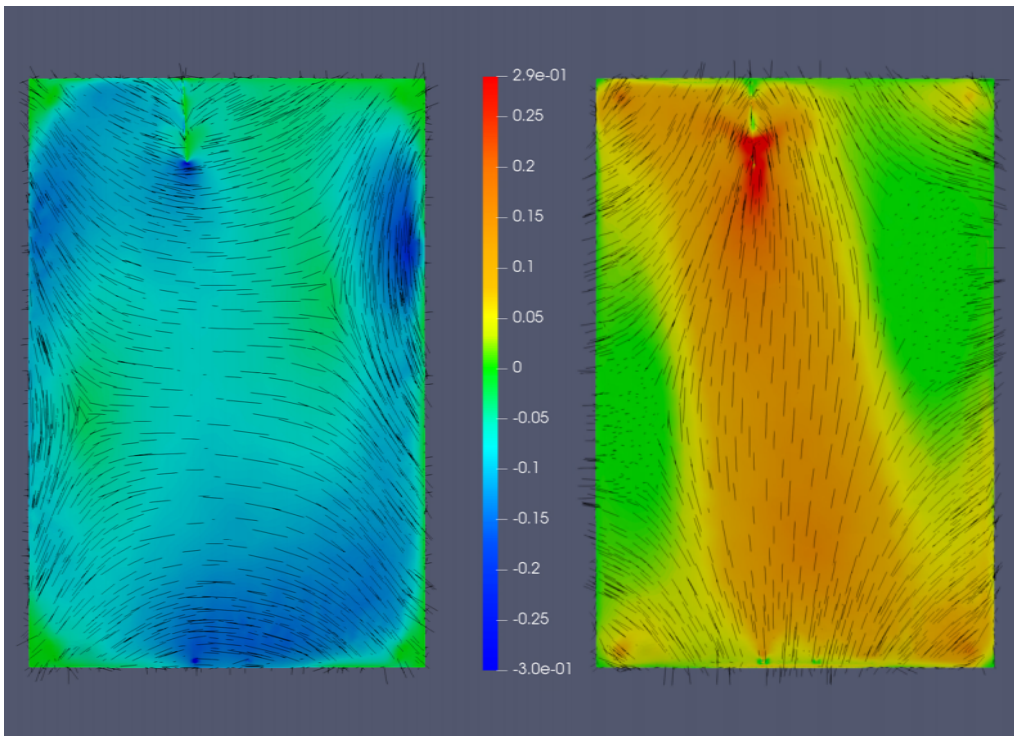


Figure 12 Principal stresses [MPa] calculated in the plane of the panel, extracted in the wood below the ground layer. On the left are the compression states and on the right the tension ones. The maximum compression values are localized on the contact area between the panel and the auxiliary frame and the maximum tension stresses are localized near the fracture.

In Figure 12, the main stresses to which the panel painting is subjected in its display condition can be observed. The tension stresses perpendicular to the grain are generally low, calculated between 0 and 0.015 MPa, even if concentrations occur immediately below the fracture, where the stress increases up to 0.29 MPa. The compression states perpendicular to the grain are very low, as well, calculated between 0 and - 0.015 MPa; they decrease up to - 0.03 MPa on the underside near the contact zones between the panel and the auxiliary frame. The values of possible damage in transversal direction of poplar wood as reported in [56] are one order of magnitude higher than those found in the typical display condition of the *Mona Lisa*. As a consequence, even if the forces applied by the restraining system, and the related stresses calculated, are not negligible to avoid compression set phenomena, they are in any case very far from values that may induce compression plasticization of the wood due to panel bending. The values showed in Figure 12 are close to 10 % of the transversal wood strength [56], while a 20 % is considered as a threshold between the viscoelastic and viscoplastic behaviour of the wood in compression perpendicular to the grain [56]. Remaining below this value, that is approximately with forces acting on the panel two times bigger in modulus than the current display condition, ensures that no long-term permanent deformations due to mechanical bending occur [31]. Moreover, there is no danger of damage for these values when any forces of that magnitude are applied for short time (transitory state).

Subsequently, the volume density of elastic deformation energy both for the panel and the ground plus paint layers was calculated. That is the energy stored by the panel painting and its components upon application of the forces (Table 5). Therefore, it is always present in the panel painting under its usual display conditions. While the lower part of the panel painting is affected by an increase in the central zone of the energy due to the concomitance in that zone of bending moment and normal contact forces, the upper part is characterised by a concentration near the fracture only (Figure 13).

Considering that the value of the deformations at the interface is the same for painting and wood layers, the difference seen in Figure 13 is mainly due to the difference in stiffness that exists between the two materials, considered primarily in the direction of the main bending moment acting on the painting and witnessed by the main deformations in Figure 10.

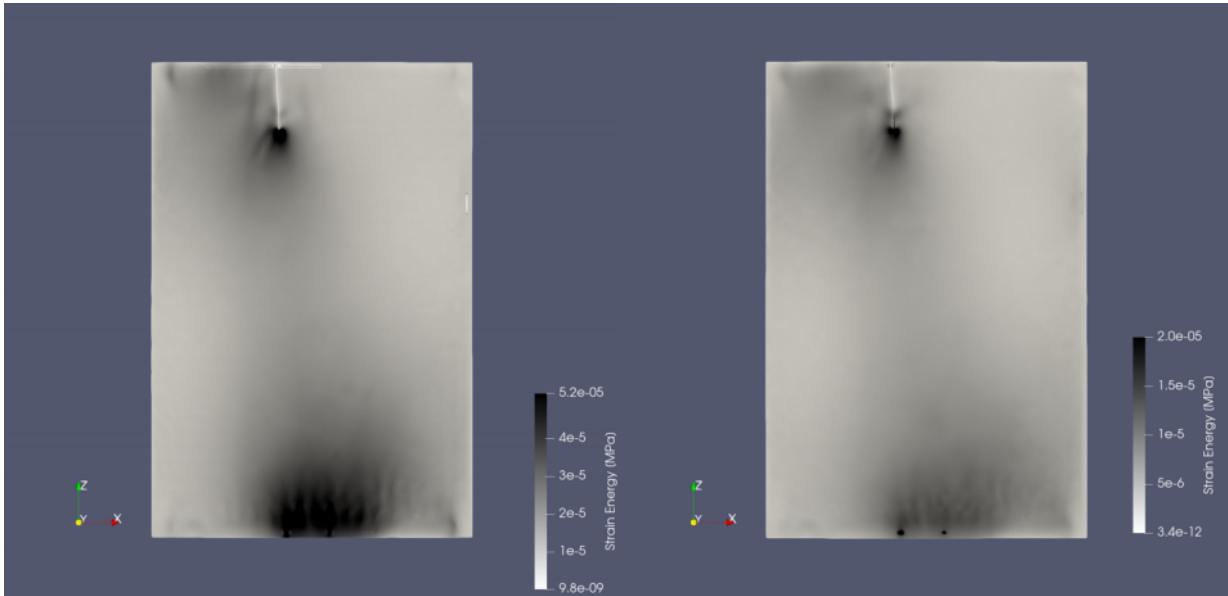


Figure 13 Strain energy in the ground and paint layer (on the left) and in the wood below the ground layer (on the right).

In general, the same operating logic also applies to the reverse side where, in addition (Figure 14), peaks can be seen in the specific zones of the butterflies, both the one missing and the one present. Taking a closer look at Figure 13, regarding the butterfly, one can observe a trace on the slot just above its tip due to its mechanical effect.

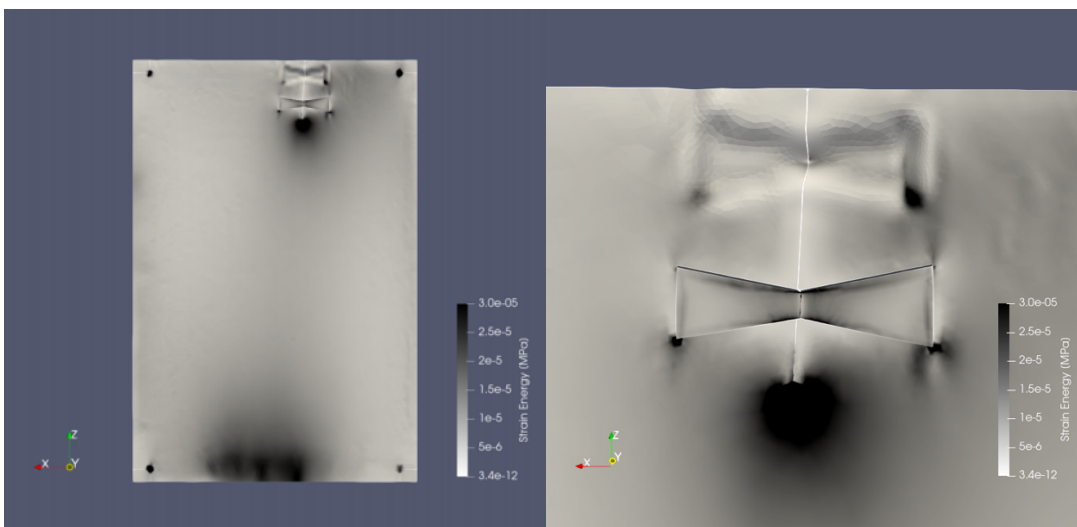


Figure 14 Strain energy on the back of the panel and particularly on the zone of the butterfly

This model was used to calculate the difference in elastic energy between the reference configuration (display condition) and other possible configurations obtained by adding up 5 N on one of each 4 locations of application of the forces at a time. It allowed to evaluate the zones of influence for each point of force application and to determine which have the greatest impact on the overall deformation behaviour of the panel painting, with reference to the fracture (Figure 15).

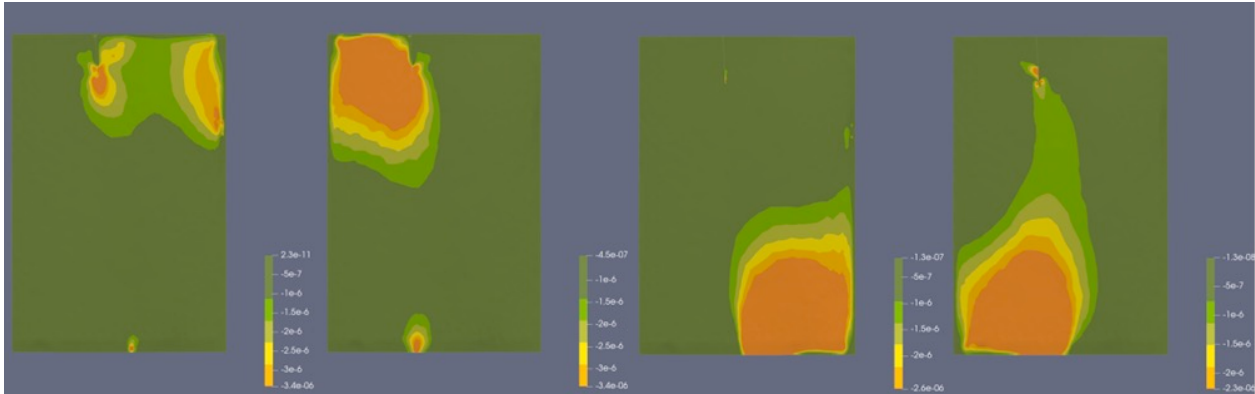


Figure 15 The difference in elastic energy between the reference configuration (display condition) and other possible configurations obtained by adding up 5 N on one of each 4 locations of application of the forces. From left to right +5 N were applied on L1, L2, L7 and L8 location, from the front.

The behaviour of the panel is essentially independent in its two vertical halves, due to the fracture and the distribution of the contacts. Location 2 is undoubtedly the most influential area with respect to the energy embedded in the fracture zone. In this regard, it can be observed that a substantial part of the energy of location 1 is discharged on a lateral contact privileged in terms of force transmission by being aligned in the longitudinal direction of the wood with respect to the point of application of the forces. Finally, location 8, although it mainly affects the lower part of the panel painting (as location 7) showed the greatest global value, even affecting the area close to the fracture.

6. Conclusions

With a sophisticated coupling between a systematic experimental study of the panel of the *Mona Lisa*, and a complex numerical procedure, it was possible to estimate the actual mechanical characteristics of the panel. This numerical model cannot catch the whole complexity of the real artwork, but it can represent consistently the displacements that the panel exhibit when subjected to external forces. Moreover, the model permits to assess the stresses and strains that may occur for a change in the loads or in general in boundary conditions.

Underlining the intrinsic limitations of this procedure, which can be briefly schematized in a great dependence of the results on the boundary conditions, on the geometry of the continuum and in general on the modelling choices, as well as the great request of computational resources, this method allows to "ask" directly to the object what are its stiffness characteristics in a non-invasive way and respecting its real historicized boundary conditions.

This study was developed only in the mechanical field, specifically not time-dependent nor moisture-dependent. Further studies, starting from this, in the hygro-mechanical field are in a finalizing stage.

Declarations

This research did not receive any specific grant from funding agencies in the public, commercial, or not-for-profit sectors.

Appendix A: Description of the implementation of the elastic orthotropic behavior of the wooden panel in MFront

This appendix describes how the of the elastic orthotropic behavior of the wooden panel has been implemented using the open source-code generator MFront co-developed under strict assurance quality constraints by CEA, EDF and Framatome in the context of a numerical platform dedicated to the simulation of the nuclear fuel elements named PLEIADES. MFront is distributed as part of the Salomé-Méca platform and is tightly integrated with code_aster.

Notations used

Symbol	Description
ε	Total strain in the reference system
ε^*	Total strain in the material frame
σ	Stress in the reference system
σ^*	Stress in the material frame
\mathbf{C}	Stiffness tensor in the reference system
\mathbf{C}^*	Stiffness tensor in the material frame

In the material frame, the orthotropic elastic behaviour amounts to the following relationship between the total strain ε^* and the stress σ^* :

$$\sigma^* = \mathbf{C}^* : \varepsilon^* \tag{4}$$

where \mathbf{C}^* denotes the stiffness tensor in the material frame.

Let \mathbf{R} the fourth order tensor such that:

$$\begin{cases} \varepsilon = \mathbf{R} : \varepsilon^* \\ \sigma = \mathbf{R} : \sigma^* \end{cases} \tag{5}$$

Then, the Constitutive Equation [1](#) can be rewritten as follows:

$$\sigma = \left(\mathbf{R} \right)^{-1} \cdot \mathbf{C}^* \cdot \mathbf{R} : \varepsilon \tag{6}$$

or, equivalently:

$$\sigma = \mathbf{C} : \varepsilon \tag{7}$$

With

$$\mathbf{C} = \begin{pmatrix} \mathbf{R} \\ \vdots \\ \vdots \end{pmatrix}^{-1} \cdot \mathbf{C}^* \cdot \mathbf{R} \quad (8)$$

MFront provides the mandatory functions to build the \mathbf{C} from the two rotation matrices corresponding to composition of the rotation in the cylindrical frame and to material frame (See Section).

In a sense, usage of MFront in this paper is mostly a matter of convenience, as performing those operations in code_aster would have been much more cumbersome. However, usage of MFront paved the way for ongoing works, such as including the effect of moisture.

Author's contributions and roles

LR conceived the methods implemented and the numerical procedures applied, did every step of the modelling, analysed the models and extracted the conclusions, wrote the paper. LR,PDV,LU,PMaz,JG,GG, MT,ER conceived and developed the experimental investigations. PMaz and LU revised the paper. TH and LR developed the law of behaviour for conical elasticity. FB, JCD and FH did and elaborated the optical measurements. LR, MF and JG discussed in depth the methodological approach. LR, JG, DJ, MF, EB discussed the modelling specifications. PMan took care of the manipulation of the artwork in the experimentation. LR and JG discussed and analysed the conclusions. JG coordinated and directed the project. All authors discussed the research outcome, as well as developed the manuscript. All authors read and approved the final manuscript.

References

- [1] K. Dardes, A. Rothe, eds., The structural conservation of panel paintings: Proceedings of a Symposium at the J. Paul Getty Museum 24-28 April 1995, in: The Getty Conservation Institute, Los Angeles, 1998.
- [2] R.D. Buck, Some applications of mechanics to the treatment of panel paintings, in: Recent Advances in Conservation, International Institute for the Conservation of Historic and Artistic Works (IIC), G. Thomson, London, 1963: pp. 156–162.
- [3] R.D. Buck, Some applications of rheology to the treatment of panel paintings, *Studies in Conservation*. 17 (1972) 1–11.
- [4] M. Mecklenburg, C. Tumosa, D. Erhardt, Structural response of painted wood surfaces to changes in ambient relative humidity, in: *Painted Wood: History and Conservation*, The Getty Conservation Institute, Dorge V. and Howlett FC, US, 1998: pp. 464–483.
- [5] M. Richard, Factors Affecting the Dimensional Responses of Wood, *Studies in Conservation*. 23 (1978) 131–135. <https://doi.org/10.1179/sic.1978.s030>.
- [6] B. Rachwał, Ł. Bratasz, M. Łukomski, R. Kozłowski, Response of Wood Supports in Panel Paintings Subjected to Changing Climate Conditions, *Strain*. 48 (2012) 366–374. <https://doi.org/10.1111/j.1475-1305.2011.00832.x>.
- [7] D. Camuffo, *Microclimate for Cultural Heritage*, Third Edition, Elsevier, 2019.
- [8] D. Camuffo, C. Bertolin, Unfavorable microclimate conditions in exhibition rooms: early detection, risk identification, and preventive conservation measures. *journal of paleontological techniques, JPT*. 15 (2016) 144–161.
- [9] J. Wadum, Microclimate boxes for panel paintings, in: Undefined, 1998. <https://www.semanticscholar.org/paper/AN-ECONOMICAL-DESIGN-FOR-A-MICROCLIMATE-VITRINE-FOR-Sozzani/6d17abe84483091d4df21ed3a21d0ce51bc41515> (accessed December 7, 2022).

- [10] ASHRAE [American Society of Heating, Refrigerating, and Air-Conditioning Engineers]., Museums, Galleries, Archives, and Libraries. Chap 24 in ASHRAE Handbook—HVAC Applications, ASHRAE [American Society of Heating, Refrigerating, and Air-Conditioning Engineers]., Atlanta, USA, 2019. <https://www.ashrae.org/> (accessed December 7, 2022).
- [11] EN 15757:2010 - Conservation of Cultural Property - Specifications for temperature and relative, (n.d.). <https://standards.iteh.ai/catalog/standards/cen/ad03d50b-22dc-4c57-b198-2321863f3870/en-15757-2010> (accessed October 5, 2022).
- [12] O. Allegretti, M. Fioravanti, P. Dionisi-Vici, L. Uzielli, The influence of dovetailed cross beams on the dimensional stability of a panel painting from the Middle Ages, *Studies in Conservation*. 59 (2014) 233–240.
- [13] D. Konopka, C. Gebhardt, M. Kaliske, Numerical modelling of wooden structures, *Journal of Cultural Heritage*. 27 (2017) S93–S102. <https://doi.org/10.1016/j.culher.2015.09.008>.
- [14] C. Gebhardt, D. Konopka, A. Börner, M. Mäder, M. Kaliske, Hygro-mechanical numerical investigations of a wooden panel painting from “Katharinenaltar” by Lucas Cranach the Elder, *Journal of Cultural Heritage*. 29 (2018) 1–9.
- [15] D. Konopka, M. Kaliske, Transient multi-FICKian hygro-mechanical analysis of wood, 197 (n.d.) 12–27.
- [16] Ł. Bratasz, M.R. Vaziri Sereshk, Crack Saturation as a Mechanism of Acclimatization of Panel Paintings to Unstable Environments, *Studies in Conservation*. 63 (2018) 22–27. <https://doi.org/10.1080/00393630.2018.1504433>.
- [17] A. Kupczak, M. Jędrychowski, Ł. Bratasz, M. Łukomski, R. Kozłowski, Processing relative humidity data using discrete Fourier transform to control strain in art objects, *Strain*. 55 (2019) e12311. <https://doi.org/10.1111/str.12311>.
- [18] A. Janas, M.F. Mecklenburg, L. Fuster-López, R. Kozłowski, P. Kékicheff, D. Favier, C.K. Andersen, M. Scharff, Ł. Bratasz, Shrinkage and mechanical properties of drying oil paints, *Herit Sci*. 10 (2022) 181. <https://doi.org/10.1186/s40494-022-00814-2>.
- [19] O. Allegretti, J. Bontadi, P. Dionisi-Vici, Climate induced deformation of Panel Paintings: experimental observations on interaction between paint layers and thin wooden supports, *International Conference Florence Heri-Tech: The Future of Heritage Science and Technologies*. 949 (2020).
- [20] J. Stöcklein, D. Konopka, G. Grajcarek, O. Tietze, S. Oertel, A. Schulze, M. Kaliske, Hygro-mechanical short-term behaviour of selected coatings: experiments and material modelling on vapour permeability and mechanical properties, *Herit Sci*. 10 (2022) 141. <https://doi.org/10.1186/s40494-022-00768-5>.
- [21] P. Dionisi-Vici, P. Mazzanti, L. Uzielli, Mechanical response of wooden boards subjected to humidity step variations: climatic chamber measurements and fitted mathematical models, *Journal of Cultural Heritage*. 7 (2006) 37–48.
- [22] Ł. Bratasz, Allowable microclimatic variations for painted wood, *Studies in Conservation*. 58 (2013) 65–79. <https://doi.org/10.1179/2047058412Y.0000000061>.
- [23] M. Łukomski, Painted wood. What makes the paint crack?, *Journal of Cultural Heritage*. 13 (2012) S90–S93. <https://doi.org/10.1016/j.culher.2012.01.007>.

- [24] L. Uzielli, L. Cocchi, P. Mazzanti, M. Togni, D. Julien, P. Dionisi-Vici, The Deformometric Kit: A method and an apparatus for monitoring the deformation of wooden panels, *Journal of Cultural Heritage*. 13 (2012) 94–101.
- [25] L. Cocchi, B. Marcon, G. Goli, P. Mazzanti, C. Castelli, A. Santacesaria, L. Uzielli, Verifying the operation of an elastic crossbar system applied to a panel painting: the *Deposition from the Cross* by an anonymous artist from Abruzzo, sixteenth century, *Studies in Conservation*. 3630 (2016) 1–12. <https://doi.org/10.1080/00393630.2015.1137426>.
- [26] P. Dionisi-Vici, I. Bucciardini, M. Fioravanti, L. Uzielli, Monitoring climate and deformation of panel paintings in San Marco (Florence) and other Museums, in: 2009: pp. 193–199.
- [27] J. Colmars, B. Marcon, E. Maurin, R. Remond, F. Morestin, P. Mazzanti, J. Gril, Hygromechanical response of a panel painting in a church, monitoring and computer modeling, in: *International Conference on Wooden Cultural Heritage, Evaluation of Deterioration and Management of Change*, Hamburg, Germany, 2009: p. 9. <https://hal.archives-ouvertes.fr/hal-00795990> (accessed December 7, 2022).
- [28] P. Dionisi-Vici, M. Formosa, J. Schiro, L. Uzielli, Local deformation reactivity of panel paintings in an environment with random microclimate variations: the Maltese Maestro Alberto’s Nativity case-study, in: 2008.
- [29] L. Uzielli, E. Cardinali, P. Dionisi-Vici, M. Fioravanti, N. Salvioli, Structure, mock-up model and environment-induced deformations of Italian laminated wood parade shields from the 16th century, in: n.d.
- [30] J.C. Dupre, D. Jullien, L. Uzielli, F. Hesser, L. Riparbelli, C. Gauvin, P. Mazzanti, J. Gril, G. Tournillon, D. Amoroso, P.H. Massieux, P. Stepanoff, M. Bousvarou, Experimental study of the hygromechanical behaviour of a historic painting on wooden panel: devices and measurement techniques, *Journal of Cultural Heritage*. 46 (2020) 165–175. <https://doi.org/10.1016/j.culher.2020.09.003>.
- [31] L. Uzielli, P. Dionisi-Vici, P. Mazzanti, L. Riparbelli, G. Goli, P. Mandron, M. Togni, J. Gril, A method to assess the hygro-mechanical behaviour of original panel paintings, through in situ non-invasive continuous monitoring, to improve their conservation: a long-term study on the Mona Lisa, *Journal of Cultural Heritage*. 58 (2022) 146–155. <https://doi.org/10.1016/j.culher.2022.10.002>.
- [32] N. Volle, G. Aitken, D. Jaunard, B. Lauwick, P. Mandron, J.P. RIOUX, Early Restorations to the Painting, in: J.P. Mohen, M. Menu, B. Mottin (Eds.), *Mona Lisa, inside the Painting*, Abrams, New York, 2006: p. 18.21.
- [33] D. Dureisseix, O. Arnould, Mechanical Modeling of the Activity of the Flexible Frame, in: J.P. Mohen, M. Menu, B. Mottin (Eds.), *Mona Lisa, inside the Painting*, Abrams, New York, 2006: pp. 52–53.
- [34] E. Ravaud, The Complex System of Fine Cracks, in: J.P. Mohen, M. Menu, B. Mottin (Eds.), *Mona Lisa, inside the Painting*, Abrams, New York, 2006: pp. 38–42.
- [35] E. Ravaud, The Mona Lisa’s Wooden Support, in: J.P. Mohen, M. Menu, B. Mottin (Eds.), *Mona Lisa, inside the Painting*, Abrams, New York, 2006: pp. 32–37.
- [36] P. Perré, R. Remond, J. Gril, Simulation of the Effects of Ambient Variations, in: J.P. Mohen, M. Menu, B. Mottin (Eds.), *Mona Lisa, inside the Painting*, Abrams, New York, 2006: pp. 50–51.

- [37] J. Gril, E. Ravaud, J.C. Dupré, P. Perré, D. Dureisseix, O. Arnould, P. Dionisi Vici, D. Jaunard, P. Mandron, Mona Lisa saved by the Griffith theory: assessing the crack propagation risk in the wooden support of a panel painting, in: M. Fioravanti, N. Macchioni (Eds.), International Conference on Integrated Approach to Wood Structure, Behaviour and Application, Joint Meeting of ESWM and COST Action E35, Florence, 2006: pp. 99–104.
- [38] B. Marcon, G. Goli, M. Fioravanti, Modelling wooden cultural heritage. The need to consider each artefact as unique as illustrated by the Cannone violin, *Heritage Science*. 8 (2020) 24. <https://doi.org/10.1186/s40494-020-00368-1>.
- [39] F. Brémand, P. Doumalin, J.C. Dupré, F. Hesser, V. Valle, Measuring the Relief of the Panel Support without Contact, in: J.P. Mohen, M. Menu, B. Mottin (Eds.), *Mona Lisa, inside the Painting*, Abrams, New York, 2006: pp. 43–47.
- [40] F. Brémand, M. Cottron, P. Doumalin, J.-C. Dupré, A. Germaneau, V. Valle, Mesures en mécanique par méthodes optiques, *Techniques de l'Ingénieur. hand* (2011). <https://www.techniques-ingenieur.fr/base-documentaire/mesures-analyses-th1/grandeurs-mecaniques-42407210/mesures-en-mecanique-par-methodes-optiques-r1850/> (accessed December 7, 2022).
- [41] G. Goli, P. Dionisi Vici, L. Uzielli, Locating contact areas and estimating contact forces between the Mona Lisa wooden panel and its frame, *Journal of Cultural Heritage*. 15 (2013) 391–402.
- [42] J. Langer, *Wood Handbook. - Wood as Engineering Material*, 1969. <http://scholar.google.com/scholar?hl=en&btnG=Search&q=intitle:No+Title#0>.
- [43] D. Guitard, *Mécanique du matériau bois et composites*, Cepadues Editions, 1987.
- [44] EDF - Électricité De France, *Finite element Code_Aster: Analyse des Structures et Thermo-mécanique pour des Etudes et des Recherches*, (2022).
- [45] T. Helfer, B. Michel, J.-M. Proix, M. Salvo, J. Sercombe, M. Casella, Introducing the open-source mfront code generator: Application to mechanical behaviours and material knowledge management within the PLEIADES fuel element modelling platform, *Computers & Mathematics with Applications*. 70 (2015) 994–1023. <https://doi.org/10.1016/j.camwa.2015.06.027>.
- [46] <https://thelfer.github.io/tfel/web/index.html>, (2022).
- [47] <https://www.rhino3d.com/mcneel/about/>, (2022).
- [48] EDF, *Éléments de contact dérivés d'une formulation hybride continue*, (2019). https://code-aster.org/V2/doc/default/fr/man_r/r5/r5.03.52.pdf.
- [49] EDF, *Notice d'utilisation du contact dans Code_Aster*, (n.d.). https://code-aster.org/V2/doc/v11/fr/man_u/u2/u2.04.04.pdf.
- [50] H. Assimi, A. Jamali, A hybrid algorithm coupling genetic programming and Nelder–Mead for topology and size optimization of trusses with static and dynamic constraints, *Expert Systems with Applications*. 95 (2018) 127–141. <https://doi.org/10.1016/j.eswa.2017.11.035>.
- [51] N.E. Mastorakis, On the solution of ill-conditioned systems of linear and non-linear equations via genetic algorithms (GAs) and Nelder-Mead simplex search, in: *Proceedings of the 6th WSEAS International Conference on Evolutionary Computing*, World Scientific and Engineering Academy and Society (WSEAS), Stevens Point, Wisconsin, USA, 2005: pp. 29–35.

- [52] J. Sanahuja, L. Dormieux, S. Meille, C. Hellmich, A. Fritsch, Micromechanical Explanation of Elasticity and Strength of Gypsum: From Elongated Anisotropic Crystals to Isotropic Porous Polycrystals, *Journal of Engineering Mechanics*. 136 (2010) 239–253. [https://doi.org/10.1061/\(ASCE\)EM.1943-7889.0000072](https://doi.org/10.1061/(ASCE)EM.1943-7889.0000072).
- [53] J. Gril, D. Jullien, D. Hunt, Compression set and cupping of painted wooden panels, in: *Analysis and Characterisation of Wooden Cultural Heritage by Scientific Engineering Methods*, Halle (Saale), Germany, 2016. <https://hal.archives-ouvertes.fr/hal-01452161> (accessed December 13, 2022).
- [54] P. Mazzanti, J. Colmars, D. Hunt, L. Uzielli, A hygro-mechanical analysis of poplar wood along the tangential direction by restrained swelling test, *Wood Science and Technology Volume*. 48 (2014) 673–687. <https://doi.org/10.1007/s00226-014-0633-4>.
- [55] A. Kupczak, M. Jędrychowski, M. Strojecki, L. Krzemień, Ł. Bratasz, M. Łukowski, R. Kozłowski, HERIE: A Web-Based Decision-Supporting Tool for Assessing Risk of Physical Damage Using Various Failure Criteria, *Studies in Conservation*. 63 (2018) 151–155. <https://doi.org/10.1080/00393630.2018.1504447>.
- [56] P. Mazzanti, M. Togni, L. Uzielli, Drying shrinkage and mechanical properties of poplar wood (*Populus alba* L.) across the grain, *Journal of Cultural Heritage*. 13 (2012) S85–S89. <https://doi.org/10.1016/j.culher.2012.03.015>.

Conclusions

A first significant achievement of the work is the technical feasibility of implementing specific and more generalized experimental methods that simultaneously allow the monitoring of the artworks and the non-invasive characterization of their hygro-mechanical properties using numerical techniques. This allowed the calibration of reliable models and the calculation of reference hygro-mechanical properties for each artwork. Moreover, this study represents the first attempt to characterize original works of art and provide experimental values for the material properties in a significant number of paintings. The derived calibrated model also allows, as exemplified by the Mona Lisa case study, a comprehensive investigation of the conservation conditions of an artwork in relation to both the mechanics of its containment and display system and the microclimate to which it is exposed. In addition, a calibrated model facilitates the exploration of substantial changes in mechanical scenarios and risk assessments. From an analytical point of view, the methods and equipment developed for the continuous monitoring of the morphological and mechanical state of an original painting in a museum exhibition setting have proved to be potentially very effective for achieving preservation's goals. The uniqueness of such art works, which are immensely valuable, vulnerable and constantly on public display, requires a thorough technological analysis of the panel and its assembly. Furthermore, it has been shown that monitoring in accordance with these principles is effective in providing a comprehensive understanding of the artifact and its behavior, as well as the data necessary for the calibration of numerical models capable of describing the hygro-mechanical behavior of the work of art. This approach, as demonstrated by the specific case of the Mona Lisa, can be applied to other panels to obtain monitoring of forces and deformations and measure their stiffness characteristics; however, it is important to note that methods must be designed and adapted to the unique characteristics and constraints of each work. Well designed and structured monitoring must provide data on (i) force-displacement relationships in static conditions, (ii) force-displacement relationships influenced by the climate over significant periods of time. The interpretation of these data will ultimately allow a deeper understanding of the characteristics and their evolution over time, which is crucial for the preservation of the panel painting.

To sum up, the experimental part of a study shall take into account the specificities of each art work in order to help curators and restorers to assess their state of conservation.

For the analysis part, the initial phase of the study is of epistemological nature and involves the identification of the fundamental parameters that exert an influence on the deformation tendencies of an original work of art. This investigation, has shown that, among the many variables involved, three are high correlated and particularly decisive in determining how a wooden painting deforms. These variables are the emissivity and stiffness of the paint layers and the anatomical cut of the board. The subsequent phase of the study aims to provide experimental support for this assumption and to experimentally decouple the behavior of these variables in order to measure their individual contributions in a non-invasive manner. It is important to note that the anatomical cut of the panel is not a variable that requires experimental or analytical determination, as it is easily observable. To support this thesis, we have developed an innovative experimental method based on measuring the cupping of the panel, resulting from two step changes in humidity, with the first configuration involving the waterproofing of the front and the second, being left in the normal condition. These two configurations allow the experimental isolation of the emissivity from the stiffness, thus the experimental

identification of their deformation contributions. By combining these results with numerical modeling elements and a sensitivity study, we were able to reconstruct three reference macro-categories, and position the six original paintings within them. In addition, it was observed through the waterproofing that the front surface of the panel painting resulted in a non-negligible moisture flow, which had a clear effect on the deformation; this method makes it possible to evaluate the deformation effect of the stiffness of the paint layers, as well as that of the emissivity, and to group the paintings into deformation families accordingly.

The analysis suggests that the effect of the three variables considered, and their reciprocal interactions, can produce a highly articulated hypothetical field of variation, here referred to as the "domain of existence," which has been confirmed by experimental observations. If all material properties and boundary conditions are specifically determined through direct experimentation on real works of art, as in the methodology introduced in this work, the results of numerical simulations can be accurate and correspond to the actual behavior of the artworks. Numerical simulations are useful for classifying real objects and explaining observed phenomena, so numerical methods should be used to extend the knowledge provided by experimental results.

By cross-referencing numerical results with experimental evidence, it was possible to classify the original paintings under experiment into 3 main groups, revealing different physical behavior and therefore different modes of deformation:

1. Panel paintings that do not present flying wood (FW, non-monotonous curvature change) in both configurations.
2. Panel paintings that do not have FW behavior under normal conditions but do show FW behavior with the waterproofing of the painted face.
3. Panel paintings with FW in both configurations.

Based on this experimental phase, a more in-depth analytical analysis was developed to identify (i) some of the infinite variables that are dimensioning for the physical phenomenon of the deformation tendency of WPPs, (ii) understand the weight of the variables within the phenomenon, and finally (iii) quantitatively analyze reference values. The variables we have identified consist of:

1. Wood diffusion coefficient
2. Painting front emissivity
3. Painting rear emissivity
4. A correction coefficient for hygroscopic deformation in wood
5. A correction coefficient for wood stiffness

An extensive sensitivity analysis, based on variance, has shown that each of the selected variables is significant in terms of deformation tendency and that variations of each individual variable result in different variations of cupping deformations over time.

Sobol's analysis was used to confirm the high level of complexity of the system under study by demonstrating the significant variations in the indices over time for each variable, and also to provide a hierarchy of the influence of the variables on the deformation tendency of the board. The analysis of the system at different time intervals, 3-days, 6-days, and 9-days, showed that the first-order index and the total index are approximately coincident for the 3-day analysis. However, in the 6-day and 9-day analyses, there is a significant deviation between the total index and the first-order index. (This deviation indicates the existence of an interaction between the input variables, i.e., the extent to which the distribution of one variable is influenced by the variation in the distribution of another variable; in simple terms, two inputs have an interaction

if their combined effect on the output is greater than the sum of their individual effects). This highlights the importance of evaluating variables in their actual physical interactions rather than isolated. In addition, this deviation also indicates the presence of strong system effects, which, together with the observation that small variations in the input variables lead to large variations in the kinetic configuration of the system, is indicative of a system with a high degree of complexity.

Sensitivity analysis is also a widely used method for assessing the impact of uncertainties in input variables on the response of a model. In this respect, it is possible to examine how the use of material properties that have not been specifically calibrated for the given study, but are derived from literature values or simulations, can lead to significant variations in the outcome. With regard to the results obtained from the optimization process, it is important to note that the iterative nature of the methodology produces numerical results that are in close agreement with the experimental data, with a majority of the results showing a determination coefficient (R^2) always over 0.9; this serves as evidence that the physical system and that numerical models can be successfully calibrated.

The primary objective of this part of the study was to construct a model that is sufficiently descriptive, to calibrate using experimental datasets, and to ensure its alignment with the experimental evidences. As a result, the input parameters of the model can be representative of those that are associated with the actual phenomenon. However, it is important to recognize that these parameters are subject to uncertainties due to constitutive and modelling assumptions, as well as the assumption of material homogeneity.

By applying this methodological approach to the real case of the Mona Lisa, it has been possible to identify its stiffness characteristics, characterize the panel, and evaluate the conservation conditions applied.

The main objectives of this part of the research were twofold: firstly, to develop a tool that is capable of characterizing a real panel painting, and secondly, to evaluate the internal stress state of the wooden support, including its safe ranges, as a result of applied forces or climatic variations. This will allow for well-informed decisions to be made regarding to the optimization of conservation conditions. In addition, the numerical model has already provided valuable technical guidelines for the design of a mechanism (recently implemented in the Mona Lisa's auxiliary frame) that automatically limits the forces acting on the wooden support within safe ranges.

The characterization of the panel has allowed the construction of a numerical model that behaves similarly to that of the real panel and can therefore provide us with extremely valuable information from a conservation point of view. In fact, it has allowed us to assess that the deformation behavior of the work under the exhibition conditions is perfectly compatible with its well-being, being well below the values identified in the literature as the damage limit; moreover, the deformation isostatics show an impressive analogy with the craquelure observable in the panel, confirming the hypothesis that the crack present in the panel developed prior to the appearance of the craquelure. With regard to the stress states in the wood, it can be observed that they are in range that is well below the values that could induce viscoplasticization phenomena, but sufficient to counteract compression set phenomena. Finally, the analysis of the variation of deformation energy allowed us to understand which internal energy variations are associated with variations in the applied forces in the boundary conditions.

A combination of experimental study and numerical modelling has been used to determine the mechanical characteristics of the panel of the Mona Lisa. In addition, the model makes it possible to evaluate the stresses and strains that may occur under varying in loads or boundary

conditions. Despite the limitations of this approach, such as the dependence on boundary conditions, geometric assumptions, modelling choices, and the high computational demands, this method allows for the non-invasive and contextually accurate determination of stiffness characteristics of the panel.

In summary, the present research takes an innovative methodological approach, treating WPPs as complex systems; this approach recognizes that the behavior of complex systems can often only be measured and therefore develops an object-learning logic. It is based on established hygro-mechanical models and aims to calibrate their characteristics through non-destructive experimental tests conducted on individual artworks. This approach avoids preconceived notions about the components and instead represents all physical entities with characteristics that, when interacting, provide a model that behaves similarly to the original when subjected to experimental characterization tests. Numerical analysis then becomes a way of extracting advanced information from experimental evidence that does not provide it directly. In addition, this approach emphasizes the importance of direct analysis on the object to avoid obtaining results that are unrelated to reality. The proposed strategy is based on methods and tools familiar to the research group and is open to evolution and improvement. Ultimately, the key principle is "learning from objects".

In this approach, It is essential to start by inquiring about the deformation tendencies of the object through experimental studies; numerical analyses serve as a complementary method, developed in parallel with the experiments, to increase knowledge and extraction of as much information as possible. From restoration point of view in example, the deformation tendency of the panel plays a crucial role in determining the choice and dimensioning of any restraining systems, such as crossbeams and frames, as well as the design of any climate control system. The complex nature of these systems, as demonstrated by this study, highlights the need to treat each panel as a unique object and to characterized its condition before implementing any conservation treatment or preventive conservation and climate control plan. The parameters that characterize these artworks, such as the hygroscopicity of the paint layers, mechanical stiffness, anatomical cutting, and the conservation environments, constitute a set of interconnected and interacting physical subsystems. The temporal evolution of these subsystems, which is not random, is highly dependent on knowledge of the initial conditions, boundary conditions, and internal structural mechanics characterization; as small differences in these conditions can lead to very different characteristics and behavior of the system, WPPs may not be predictable, even if the variables and equations governing them are known.

As with other complex systems, the behavior of WPP can only be determined by measurement, rather than prediction. The methodology presented in this thesis involves the direct determination of material properties and boundary conditions through experimentation on real works of art. This allows for numerical simulations to provide accurate representations of the actual behavior of the WPP. Furthermore, numerical simulations are useful for classifying and interpreting observed phenomena, and can be used to enhance the understanding gained from experimental results.

Summarizing, the main innovations of this research are as follows:

1. Six original paintings representative of different construction methods and ages were tested.
2. The strongly coupled interaction between the emissivity of paint layers, the generalized rigidity of paint layers, and the anatomical reaction of the panel, determines the deformation mode of an original panel painting

3. The use of an insulation of the paint layers was employed to experimentally determine the stiffness and emissivity of paint layers.
4. Macro families for the deformation tendencies of WPPs were identified.
5. An analytical estimation of the hygro-mechanical characteristics of WPPs was determined.
6. A strategy was identified to apply effective experimentation to characterize an original painting in exhibition, using the case of the Mona Lisa as an example.
7. A calibrated model of the artwork was created and useful information for conservators/curators was extracted.

Methodologically, the innovation lies in the development of methods to directly use experimental readings to understand the intrinsic complexity of panel paintings and, as a result, their deformation tendencies.

It is necessary to reflect on the role that experimental and simulation experience have played in this research and how their interaction has been essential both in achieving the desired results and in developing an effective method for approaching WPPs. Often in the scientific world, without wishing to generalize and aware that there are exceptions of enormous success, the experimentalist and modeler positions are separated and tend to see the other as strictly functional to their own. The modeler tends to use modelling in general to validate his own model or to feed it with new laws whose material characterization is essential. The experimentalist needs models that make his tests intelligible and that explain an observed behavior. The approach pursued here represents a third way in which the two approaches are parallel: to accompany the experiment from its inception through the simulation of the experiment, and at the same time to understand how to improve the experiment to obtain the results that the model could have given us by elaborating the experiment. Both in the case of the 6 panels and in the case of the Mona Lisa, different experimental setups were simulated to understand which one was then the most effective in terms of simulation; in addition, in the case of the 6 paintings, the idea of using the waterproofing of the front was dictated by the need, which emerged from the model, of additional parameters to characterize its hygro-mechanical behavior. As well as the enormous biodiversity of the deformation modes of WPP, both for entities and for shapes, that emerged from the experimental tests, led us to want to define a range of plausible deformability, which turned out to be much wider than initially thought. We could say, then, that a fundamental aspect of this research and its approach was the link between these two worlds, which allowed us to extract from tests that were complex in terms of implementation but simple in terms of output, calibrated models capable of answering to deep conservative questions.

The main developments of this research are of two types, immediately applicable and developable, assuming that the third, the evaluation of the state of conservation of an artwork, has already been sufficiently treated with the Mona Lisa.

The first is the scientific support to the restoration project or, alternatively, the scientific dimensioning of the stiffening systems; in this case, a calibrated model of the panel can be restored with various different reinforcement solutions and, within each of these, different dimensions. The various solutions, which will represent different levels of containment of the panel on the one hand, and the different levels of stresses and deformations in the wood and paint layers on the other, will allow conservators and curators to make knowledgeable choices about the solutions to be implemented.

The second is the analysis of the response of a painting in a real climate, with its fluctuations; this aspect takes on even greater importance in an era such as ours, where particular attention

to energy consumption shall be paid. In fact, understanding the acceptable variations for a given painting or for a collection can make it possible to adjust the climate control system to optimize the consumption; if, on the other hand, some works prove to be critical or of particular importance, special settings could be implemented.

As a conclusion to the perspectives of this study, I believe it is necessary to discuss how it relates to innovative methods and techniques that are emerging in today's times. First, I believe it is important to emphasize how the present study is absolutely compatible with full-field analysis of paintings subject to deformations. With minimal technical modifications and an important methodological study, it is possible in my opinion to have a more extensive characterization that is not strongly dependent on a punctual measurement. Various questions arise here that only a more in-depth study of the specific problem can try to clarify, which are the following:

- Use additional data to enrich the characterization or to consider variability within the panel?
- Divide the continuum into sub-domains or seek descriptive functions of the variability of characteristics, such as wood near the pith and at distances?
- Which of the above options is technically feasible?

Another issue of interest could be the study of simplified parameters, such as characteristic times associated with the deformation phenomenon from which it is possible to estimate the reactivity of the panel. Based on the studies conducted so far, it is highly unlikely, given the complexity of the system and how strongly its components are interconnected. It can perhaps help to narrow down the existence domain of deformation in some way but cannot lead to the construction of descriptive models or models that can justify or assist conservative choices.

An absolutely open question in this study is whether and how an application of uncertainty propagation methods starting from it makes sense and is legitimate. I would like to divide more cases in this regard:

- Reconstruct the behavior of a painting based solely on physical observation without support of tests performed on the painting. This solution, while the most desirable in the conservation sector, appears to me to be ill-posed and generally superficial. It would mean, in a first approximation, evaluating the deformation tendency or some derived parameter (such as stresses, energy, etc.) in a manner similar to how the deformability domain was determined in this study; it does not have representativeness on the individual case as it contemplates changes in deformation state (flying wood - non-flying wood) that determine different physical reactions of the panel. And all this behind the assumption of having, assuming they exist, statistically reliable and representative distributions of material characteristics, that seems not realistic.
- Alongside careful characterization, use uncertainty propagation to insert into the model what cannot be directly measured; this specific method seems to me the most promising. Indeed, some material characteristics require destructive analysis to be determined and therefore lend themselves to being simulated as uncertain quantities. Within this context, I also believe that the study of any reduced models or metamodelling, that can make computational analysis extremely fast, has a lot of sense.
- An approach like the previous one can be successfully extend to the design of ad hoc conservation devices so that they are compatible with complex works.

Clearly, the application of these methods can enable the creation of digital mechanical twins of works of art; that is, engineering simulations of their hygro-mechanical behavior and

deformation tendency, excluding directly, of course, any implication of their replica for display. This can provide real-time knowledge of their deformation conditions and stresses, mixing simulations and experimental data on the fly in real time.

The entire treatment of this study has been carried out in a deeply didactic way, using open-source tools, free and available to everyone, so that these applications can really be within the reach of other researchers to be applied, replicated and, I hope, improved!

Acknowledgments

In this journey, I had the fortune and honor to collaborate with some of the best restorers, conservators and scientists in the field. Working with the best is a blessing that illuminates your life.

I first thank the Opificio delle Pietre Dure as an institution that understood and actively supported this research: in particular, the teachings of Ciro Castelli, Andrea Santacesaria and Luciano Ricciardi opened and illuminated this path with the wisdom of those who deeply understand and never settle, always wanting to improve. I tried with all my strength to translate your enormous experience and wisdom into technical-scientific terms.

A huge thanks to the Louvre Museum, specifically to Vincent Delieuvin, Sebastien Allard, for allowing access to the Mona Lisa and supporting its study. The excellence that shines through in every approach was illuminating.

I want to thank my French colleagues who welcomed me with friendship and generosity: Delphine Jullien, Eric Badel, Jean-Christophe Duprè, Cecilia Gauvin, Rostand Moutou-Pitti, Arthur Bontemps, Phan Nhat Tung.

Thanks to my Florentine colleagues Giacomo Goli, Marco Togni, Chiara Manfredi; your generosity and continued support is a memory that will always accompany me. A special thanks to Paola Mazzanti, for always being helpful and kind.

Two people who played a fundamental role in my training need to be mentioned. Luca Uzielli taught me what wood is and wood technology, how to approach experimentation, and introduced me to the Mona Lisa project; if you had not conveyed your seriousness, intellectual honesty, and especially your passion for paintings, I would never have embarked on this journey and therefore would never have lived the unforgettable moments in front of the paintings. Ioannis Christovasilis taught me what numerical modeling and finite elements are, and above all how to approach unconventional models; your friendship is one of the best gifts life has given me.

Joseph Gril: Thank you so much! You made my stay in Clermont Ferrand a fun and incredibly productive learning experience. I will treasure everything you generously taught me and will try in every way to use, and especially imitate, your extraordinary analytical approach in the future. Your hospitality and continued support will remain one of the best memories of this experience.

Marco Fioravanti: I find it difficult to express my gratitude. You were the best possible PhD advisor. Thank you for the trust and friendship you placed in me. But thank you even more for the decision and timeliness with which you corrected and directed me when there was a risk of not reaching the goals. You taught me in the best way, by example and not with words, how a scientist should behave. You made this PhD period one of the most fun and fulfilling moments of my life, and that obviously has no price.

Special thanks to my family, my wife Valentina and my beautiful little girl Cora, my beloved parents who unfortunately could not hear how beautiful and satisfying this journey was, and my adoptive family, Valentina's family (Damaris, Italo, Annalisa), who always supported me. Thanks to my two elective brothers Lorenzo and Niccolò (and their families) for always being there for me in both calm and stormy seas.